UNIVERSITAT DE BARCELONA

Evoked and induced activity in the auditory nervous system: deviance detection and brainwave entrainment

Francisco José López Caballero

EVOKED AND INDUCED ACTIVITY IN THE AUDITORY NERVOUS SYSTEM: DEVIANCE DETECTION AND BRAINWAVE ENTRAINMENT

Francisco José López Caballero

PhD Thesis

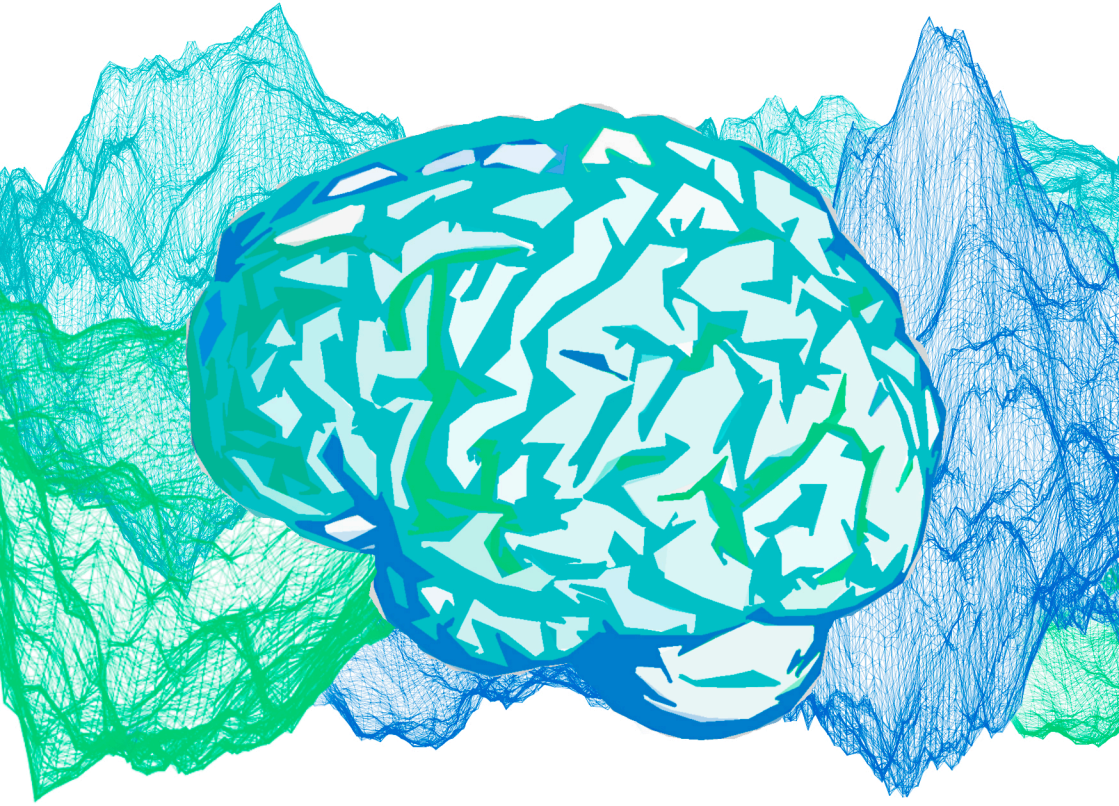

BrainLab - Grup de Recerca en Neurociència Cognitiva
Departament de Psicologia Clínica i Psicobiologia (secció Psicobiologia)
Facultat de Psicologia
Universitat de Barcelona

Evoked and induced activity in the auditory nervous system: deviance detection and brainwave entrainment

Thesis presented by

Francisco José López Caballero

To obtain the

Grau de Doctor per la Universitat de Barcelona

In accordance with the requirements for the

International PhD Diploma

Programa de Doctorat en Biomedicina

Supervised by **Dr. Carles Escera**

Barcelona, May 2019

Agradecimientos

No he redactado unos agradecimientos en mi vida, de modo que no sé muy bien qué decir. Pero me encanta tener la oportunidad, por primera vez, de dejar plasmado en un papel lo mucho que quiero a tantas personas y cuán agradecido estoy de haberlas conocido. Quizás normalmente no lo demuestre por ser una persona de carácter más bien tímido, así que mejor aprovechad y leer bien estas líneas porque en la vida real me dará vergüenza repetirlo :)

Bueno, una excepción a esa regla es mi madre Teresa, a ella no me cuesta expresarle lo mucho que significa para mí, pero a veces ni aun así es consciente del valor enorme que tiene. Una trabajadora incansable pese a todas las adversidades. Ella me ha inculcado lo que significa tener fuerza de voluntad y no quejarse. Nada de lo que escriba aquí definiría del todo hasta qué punto es única, pero si hay alguien que ha permitido que yo sea lo que soy hoy es ella. A mi abuelo Fermín y mi abuela Corazón, que tan orgullosos se sentían de mí y tan felices estarían de ver dónde he llegado. Agradezco a mis tías en Madrid, especialmente a la tía Luisa que tan pendiente ha estado siempre de mis logros, a mi hermano al que sé que en el fondo le gusta presumir de mí, y a todos mis primos, en especial a Lorenzo y Mireia, que siempre me han mandado fuerzas y ánimos.

También a Meri por su comprensión y apoyo cuando mi ambición quiso sobrepasar sin éxito mis capacidades, a Toni, un amigo como pocos con quien tanto me he desfogado y que siempre ha estado ahí para escucharme, a Joan, el único que entiende de qué van mis artículos, a Oriol, el chico listo, guapo y rico de medicina (pero no pijo!) y, como no, a Héctor, el friki más friki del mundo y mi mejor amigo. No se me olvida mencionar a los orgullosos integrantes del Betis Florida, al Christian, el Jose y sus ánimos, el Nico, el Juanan y su clase, el Dani y su mala leche, y todos esos genios del barrio que tanto echaré de menos.

Del BrainLab qué puedo decir... Pese a ser todavía ignorante en la mayoría de las cosas, miro tres años atrás y no me creo lo mucho que he aprendido de mi estancia aquí, y no solo en lo académico. Cuando llegué no sabía lo que era trabajar en equipo de verdad, no había ido en mi vida a un congreso, no me atrevía a hablar en público y prácticamente nunca había viajado al extranjero. Aquí he vivido tantas experiencias y conocido a tanta gente que me llevo unos recuerdos imborrables y, sobre todo, muchos amigos. Me da una pena terrible marcharme y espero algún día volver, gracias por haber proporcionado siempre ese ambiente tan lleno de alegría y cariño.

Quisiera dar las gracias a tantas personas que no sé ni por quién empezar. Pero bueno esto no es un ranking. Tere, cuántas cosas nos hemos contado desde que llegaste y cuanto nos hemos apoyado el uno al otro. Muchas gracias por preocuparte siempre por mí y por tantos momentos divertidos. Ten fe en ti porque vales muchísimo más de lo que crees. A Natàlia, con quien tantos viajes y experiencias he vivido, mi compi del lab desde que entré y la persona con quien siempre se puede contar, te deseo lo mejor decidas lo que decidas en tu futuro. A Paco, por alegrarme los días y enseñarme tantas cosas, eres un tío brillante con el que he aprendido muchísimo, además de un friki/deportista de los buenos. Gracias por defenderme aquel día cuando tiré el petardo en la playa, pero el policía se fue directo hacia ti. Y bueno fuiste un poco cobarde de no participar en mi experimento de TMS pero se te perdona porque eres un crack. A Jordi ¿cómo se puede saber tanto y que no se te suba a la cabeza? disfrutas aprendiendo y enseñando y eres llano y accesible como pocos, he aprendido y me he reído muchísimo contigo, gracias por todo lo que me has enseñado y por tu amabilidad. Me hubiese gustado pasar horas enteras hablando contigo de ciencia. Mil gracias también a Vittoria, la risueña violinista del lab que tanto me ha ayudado, siempre podrás contar conmigo, a Kasia, el ángel que me guió en mis primeros pasos en el BrainLab. Gracias por ser tan dulce y paciente. Ojalá hubieses estado más tiempo para que estuvieras orgullosa de mí. Te admiraré siempre. A Cristina, me encanta verla por las mañanas con esa alegría que trae, y a Marta Turró, una madre para todos los del laboratorio y una de las personas que más quiero del lab.

Me acuerdo también de Lenka, Miriam y Marc Recasens, a quienes conocí en mis primeros días como estudiante de máster y que tan bien me acogieron. A Marius, Mariuuuusss, you have to go back to Spain one day, forget about Germany. I am proud to have such an awesome friend. To Tin, thanks for making me laugh so much, I had a lot of fun while we shared the office. Thanks for worrying about me and I'm sure I'll see you again soon. Also, thanks to Mary-Jo, Òscar, Maria Giovanna, Marta Ortega, and all the visitors we had who made the lab so lively.

También quiero agradecer en especial a los malakes por hacerme la vida más amena en estos meses de amargura redactando la tesis. A Nadia, talento puro y gusto por lo que hace, es un placer hablar contigo de ciencia y de todo en general. Eres maravillosa. A Jonatan, un genio de la MRI estructural, te preguntaré muchas cosas cuando esté en Pittsburgh. A Sonia, la alegría hecha carne y una chica encantadora, ojalá hubieras llegado antes al lab. A María y Montse, por preocuparos por mí y organizar estas quedadas tan chulas. Pese a veros poco os he cogido cariño en estos pocos meses. A Marta Font y su tranquilidad infinita, fuiste

mi compi de mesa, ¿recuerdas? Te echaré mucho de menos también. Y a los nuevos, Giannina, gracias por tus ánimos con la escritura. Al no tan nuevo Jose, por ser un tío tan sencillo y grande a la vez. Te pediré consejos cuando escriba mi novela de fantasía. Ah! Y no se me olvida mi alumno de prácticas más motivado, Jordi Tobajas, tu pasión por la ciencia no tiene límites.

Muchas gracias a Carles, un jefe severo, pero de gran corazón que busca siempre lo mejor para sus doctorandos y del que he aprendido tanto. Si Marta Turró era la madre, Carles es el padre de todos. Me siento orgulloso allá donde voy de poder decir que lo tuve de supervisor. Gracias también a Iria San Miguel, la mujer más inteligente que he conocido en mi vida, y aun así tan llena de paciencia, humildad y cariño. Pura bondad. También a mi colegui Marc Via, otra perfecta combinación de sabiduría y sencillez que me ha hecho más alegres tantos días con sus chistes malos. Gracias por escucharme cuando tenía dudas y por dar tan buenos consejos. A Xavi le doy solo gracias escuetamente por ser tan culé, pero lo quiero igual. Gracias también a MJ Corral, Ana Adán y Juanjo por su increíble organización de las clases y por ponérmelo tan fácil, si me ha encantado hacer docencia estos años es todo gracias a vosotros. Y a Imma, que ha actuado como una madre para mi desde que entré en la carrera de psicología y me inspiró a dedicarme a la neurociencia.

Gracias a los miembros del Brain Stimulation Lab, a Lídia, Kilian, Anna y en especial a Pablo, con quien he aprendido mucho pero también me lo he pasado genial. Y a David Bartrés por su amabilidad y acogida en el laboratorio, me sentí como uno más del grupo. También a Manolo Malmierca, Guillermo, Gloria y Catalina, que tan bien me acogieron cuando visité Salamanca y con quienes tan buenos ratos pasamos en el workshop de Escaló.

Finally, I also want to thank Gavin Bidelman for taking his time to teach me so many things in just three months, along with his team and all the amazing people I met during my stay in Memphis. Thanks to Jonathan Rogers, my Spanish connection while I was there, for organizing so many activities and being on board for all the fun plans we made with the group. Thanks also to Jessica, always busy, Holly, awesome gym partner, Caitlin, Lipika, Helen, Kara, Gwyneth, Daniel and my buddy Bhanu, I'll always remember you. Also to Laís, my Brazilian neighbor who helped me so much at the beginning, and to Kelsey, remember what you said, "we will be old like the big fish in the science world, will meet each other at congresses and will remember how we used to play racquetball when we were doing PhD".

Index

Abstract 9
Resumen 11
Resum 13
Foreword 15
List of original publications 16
Abbreviations 17
General introduction 19
The auditory system 19
Physics and transduction of sound 20
Neural basis of the auditory nervous system 21
Study of the auditory nervous system with EEG 22
Evoked activity: deviance detection and the Frequency-Following Response 24
Induced activity: brainwave entrainment with binaural beats 28
Aims 31
STUDY I 33
STUDY II 45
STUDY III 79
Summary of results 93
General discussion 95
Hierarchical organization of deviance detection under predictive coding theory 95
Neural generators of the FFR 99
Brain rhythms: induced activity with binaural beats 101
Conclusions 105
References 107

Abstract

The auditory system is a crucial element in our interaction with the environment, linked with several cognitive functions such as attention, memory and language. Further characterizing the neural mechanisms explaining auditory processing may help to understand better these connections, and ultimately improve our knowledge on numerous clinical conditions associated with abnormal auditory processes, including language impairment, schizophrenia or autism spectrum disorder. With the present thesis, we aimed to contribute to the characterization of two different mechanisms of brain function within the auditory domain, as measured with electroencephalography (EEG). On the one hand, evoked activity, reflecting subjacent cognitive process time-locked to the processing of the stimulus. On the other hand, induced brain oscillations, referring to brain rhythms which self-emerge, related with several cognitive functions, and are modulable by acoustic input. Within the first mechanism, two studies are included. In the first study, we focused on deviance detection, a defining feature of the auditory system consisting on the detection of stimuli breaking a previously encoded acoustic regularity. Here, we measured middle latency and long latency responses, two evoked potentials reflecting activity from different hierarchical levels of auditory processing, and demonstrated a functional dissociation between them in the encoding of deviant probability. In the second study, we focused on the Frequency-following response (FFR), an evoked potential following the periodical features of the acoustic stimulus, aiming to disentangle its cortical contributions as a function of stimulus frequency. By combining EEG with an inhibitory transcranial magnetic stimulation (the continuous Theta Burst Stimulation, cTBS) paradigm, we aimed to transiently inactivate auditory cortex and compare FFR recorded before and after this inactivation. However, our results suggested cTBS did not affect the auditory evoked potentials recorded, and it may be ineffective to produce inhibitory effects in the auditory cortex. Concerning the second mechanism of brain function studied, induced oscillations, in the third study we aimed to disentangle whether binaural beats, an auditory illusion produced by the dichotic presentation of two pure tones with slightly different frequencies, would modulate ongoing oscillatory activity in the brain at different frequency bands. Using strict control and baseline-treatment-washout sessions, our results suggest no modulation of brain rhythms in any of the frequency bands measured occurs during or after binaural beat stimulation, as compared to baseline. Overall, with the findings of these three studies, we hope to have

contributed to the better understanding of the neurophysiological basis of auditory function.

Resumen

El sistema auditivo es un elemento crucial en nuestra interacción con el entorno, vinculado a varias funciones cognitivas, como la atención, la memoria y el lenguaje. Una mejor caracterización de los mecanismos neuronales que explican el procesamiento auditivo puede ayudar a comprender mejor estas conexiones y, en última instancia, mejorar nuestro conocimiento sobre numerosas afecciones asociadas con procesos auditivos anormales, como trastornos del lenguaje, esquizofrenia o trastornos del espectro autista. Con la presente tesis, nuestro objetivo fue contribuir a la caracterización de dos mecanismos diferentes de la función cerebral dentro del dominio auditivo, medidos con electroencefalografía (EEG). Por un lado, la actividad evocada, reflejando procesos cognitivos subyacentes asociados en el tiempo al procesamiento del estímulo. Por otro lado, las oscilaciones cerebrales inducidas, refiriéndose a los ritmos cerebrales que emergen por sí mismos, en relación con varias funciones cognitivas, y son modulables por los estímulos acústicos. Dentro del primer mecanismo, se incluyen dos estudios. En el primer estudio, nos centramos en la detección de desviaciones, una característica definitoria del sistema auditivo que consiste en la detección de estímulos que rompen una regularidad acústica previamente codificada. Aquí, medimos las respuestas de latencia media y larga, dos potenciales evocados que reflejan la actividad de diferentes niveles jerárquicos de procesamiento auditivo, y demostramos una disociación funcional entre ellos en la codificación de la probabilidad de la desviación. En el segundo estudio, nos enfocamos en la respuesta de seguimiento de frecuencia (*Frequency-Following Response*, FFR), un potencial evocado que sigue las características periódicas del estímulo auditivo, con el objetivo de averiguar sus contribuciones corticales en función de la frecuencia del estímulo. Combinando EEG con un paradigma de estimulación magnética transcraneal inhibitoria (*continuous Theta Burst Stimulation*, cTBS), nuestro objetivo fue inhibir transitoriamente la corteza auditiva y comparar la FFR registrada antes y después de esta inhibición. Sin embargo, nuestros resultados sugirieron que la cTBS no afectó los potenciales evocados auditivos registrados, y puede ser ineficaz para producir efectos inhibitorios en la corteza auditiva. Con respecto al segundo mecanismo de la función cerebral estudiado, las oscilaciones inducidas, en el tercer estudio intentamos diferenciar si los pulsos binaurales, una ilusión auditiva producida por la presentación dicótica de dos tonos puros con frecuencias ligeramente diferentes, modularían la actividad oscilatoria en curso en el cerebro en diferentes bandas de frecuencia. Usando un controles estrictos y sesiones con línea base, tratamiento y post-tratamiento, nuestros resultados

sugieren que los ritmos cerebrales en curso no se modularon en ninguna de las bandas de frecuencia medidas durante o después de la estimulación con pulsos binaurales, en comparación con la línea de base. En general, con los hallazgos de estos tres estudios, esperamos haber contribuido a una mejor comprensión de las bases neurofisiológicas de la función auditiva.

Resum

El sistema auditiu és un element crucial en la nostra interacció amb l'entorn, vinculat a diverses funcions cognitives, com l'atenció, la memòria i el llenguatge. Una millor caracterització dels mecanismes neuronals que expliquen el processament auditiu pot ajudar a comprendre millor aquestes connexions i, en última instància, millorar el nostre coneixement sobre nombroses afeccions associades amb processos auditius anormals, com trastorns del llenguatge, esquizofrènia o trastorns de l'espectre autista. Amb la present tesi, el nostre objectiu va ser contribuir a la caracterització de dos mecanismes diferents de la funció cerebral dins el domini auditiu, mesurats amb electroencefalografia (EEG). D'una banda, l'activitat evocada, reflectint processos cognitius subjacents associats en el temps al processament de l'estímul. D'altra banda, les oscil·lacions cerebrals induïdes, referint-se als ritmes cerebrals que emergeixen per si mateixos, en relació amb diverses funcions cognitives, i són modulables pels estímuls acústics. Dins el primer mecanisme, s'inclouen dos estudis. En el primer estudi, ens centrem en la detecció de desviacions, una característica definitòria del sistema auditiu que consisteix en la detecció d'estímuls que trenquen una regularitat acústica prèviament codificada. Aquí, mesurem les respostes de latència mitjana i llarga, dos potencials evocats que reflecteixen l'activitat de diferents nivells jeràrquics de processament auditiu, i demostrem una dissociació funcional entre ells en la codificació de la probabilitat de la desviació. En el segon estudi, ens enfoquem en la resposta de seguiment de freqüència (*Frequency-Following Response*, FFR), un potencial evocat que segueix les característiques periòdiques de l'estímul auditiu, amb l'objectiu d'esbrinar les seves contribucions corticals en funció de la freqüència de l'estímul. Combinant EEG amb un paradigma d'estimulació magnètica transcranial inhibitòria (*continuous Theta Burst Stimulation*, cTBS), el nostre objectiu va ser inhibir transitòriament l'escorça auditiva i comparar la FFR registrada abans i després d'aquesta inhibició. No obstant això, els nostres resultats van suggerir que la cTBS no va afectar els potencials evocats auditius registrats, i pot ser ineficaç per produir efectes inhibitoris en l'escorça auditiva. Pel que fa al segon mecanisme de la funció cerebral estudiat, les oscil·lacions induïdes, en el tercer estudi vam intentar diferenciar si els polsos binaurals, una il·lusió auditiva produïda per la presentació dicòtica de dos tons purs amb freqüències lleugerament diferents, modularien l'activitat oscil·latòria en curs a el cervell en diferents bandes de freqüència. Emprant controls estrictes i sessions amb línia base, tractament i post-tractament, els nostres resultats suggereixen que els ritmes cerebrals en curs no es van

modular en cap de les bandes de freqüència mesurades durant o després de l'estimulació amb polsos binaurals, en comparació amb la línia de base. En general, amb les troballes d'aquests tres estudis, esperem haver contribuït a una millor comprensió de les bases neurofisiològiques de la funció auditiva.

Foreword

This thesis is presented to obtain the Degree of Doctor by the University of Barcelona, with the International doctor mention, and is the result of the work carried out at the BrainLab Cognitive Neuroscience Research Group (Centre of Excellence established by the Generalitat de Catalunya SGR 2014-177) at the department of Clinical Psychology and Psychobiology, Faculty of Psychology, University of Barcelona, led by Dr. Carles Escera, and partially at the Brain-Stimulation Lab, Faculty of Medicine, University of Barcelona, led by David-Bartrés Faz.

This work was supported by the Spanish Ministry of Economy and Knowledge (PSI2012-37174; PSI2015-63664-P), the Catalan Government (SGR2014-177; SGR2017-974) and the ICREA Academia Distinguished Professorship awarded to Carles Escera. It also supported by a Spanish Ministry of Economy and Competitiveness (MINECO) 35 grant to David Bartrés-Faz [grant number PSI2015-64227-R], and a PhD and a travel grant from the University of Barcelona to Fran López-Caballero (Ajuts de personal investigador en formació, APIF-UB).

List of original publications

Study I

López-Caballero, F., Zarnowiec, K., & Escera, C. (2016). Differential deviant probability effects on two hierarchical levels of the auditory novelty system. Biological psychology, 120, 1-9.

Study II

López-Caballero, F., Martín-Trias, P. Ribas-Prats, T., Gorina-Careta, N., Bartrés-Faz, D & Escera, C. (2019). The effects of cTBS on the Frequency-Following Response and other auditory evoked potentials. *In preparation*

Study III

López-Caballero, F., & Escera, C. (2017). Binaural beat: A failure to enhance EEG power and emotional arousal. Frontiers in human neuroscience, 11, 557.

Abbreviations

ABR Auditory Brainstem Response

AEP Auditory Evoked Potential

CN Cochlear Nerve

cTBS continuous Theta Burst Stimulation

EEG Electroencephalography

FFR Frequency-Following Response

fMRI functional Magnetic Resonance Imaging

IC Inferior Colliculus

LLR Long Latency Response

MEG Magnetoencephalography

MLR Middle Latency Response

MMN Mismatch Negativity

TMS Transcranial Magnetic Stimulation

General introduction

The auditory system

The auditory system plays a pivotal role in our understanding of and the interaction with our environment. It allows us to explore and experience our surroundings by transducing soundwaves into bioelectrical signals, which are further processed giving rise to auditory perceptions (Recanzone and Sutter, 2008). The auditory system is responsible for the processing of the many different features of the sounds, such as frequency, intensity and timing, with which we can create a faithful representation of the auditory scene (Long, Wan, Roberts, Corfas et al., 2018). Thanks to these abilities, we are able to accomplish feats such as identify thousands of different sounds, from the engine of a car or the falling rain to a slamming door or different types of footsteps, localize their sources in space, segregate sounds from one another, extract information from objects or follow a musical melody (Schunpp, Nelken and King, 2011; Litovsky, 2015). More importantly, the processing of sounds in the auditory system is the base for human communication and language, facilitating learning, supporting the exchange of information with others, and ultimately leading to the development of social skills, allowing us to stablish relationships with others and adapt to the social world (Kraus, Anderson and White-Schwoch, 2017).

The importance of the auditory system also lays on its multiple interactions with cognitive domains such as attention, memory, language or executive function, and it constitutes a window to further study and characterizing them (Machado, Teixeira and Costa, 2018). In fact, auditory information is one of the first sensorial inputs our brain is exposed to, even before birth. While a newborn can barely see a few months after birth, auditory experience is already present at very early stages of brain maturation. Therefore, as a process that requires the interaction with the environment, cognitive development is inherently linked with the auditory system (Litovsky, 2015). The understanding of the links between audition and cognition becomes more complex as we try to disentangle its neural underpinnings in the central nervous system, and the field of auditory neuroscience, in which the present thesis is developed, serves this purpose.

Studying the neural basis of the auditory system also becomes relevant when considering the numerous clinical conditions associated with abnormal auditory processes. This includes hearing loss (5% of the world's population according to WHO, 2015), auditory processing disorders, as well as communication disorders

with more subtle connections with the auditory domain, such as language impairment (Rocha-Muniz et al., 2012). Moreover, developmental disorders such as autism spectrum disorder or mental disorders such as schizophrenia also have clinical symptoms associated with abnormalities in the processing of sounds, including auditory hypersensitivity or auditory hallucinations, respectively. In this regard, a better understanding of the functionality of the auditory nervous system in the healthy brain would help improve our knowledge on how these functions are altered in pathologies.

When discussing auditory processing phenomena in the following pages, we will be referring to terms related with the physical properties of sound and the auditory nervous system. Therefore, it deems necessary to briefly describe the physics of sound, the transduction of auditory information into the nervous system and how that information travels along the auditory pathway.

Physics and transduction of sound

Sound can be defined as a pressure wave that travels longitudinally through a compressible medium, generating regions with high and low pressure (compression and rarefaction regions of the medium, respectively). For example, the initial motion of a loudspeaker diaphragm would create a displacement of air molecules surrounding it, compressing them altogether. When the loudspeaker diaphragm returns to its original position, air molecules would occupy the empty space, therefore rarefying. This would create a pattern of increases and decreases in air pressure that eventually reaches the ear (Goldstein, 2009). Like any other wave, pressure waves that define sound have different characteristics, including amplitude, frequency and phase, and these are related with the perceptual aspects of sound such as intensity, pitch and timing, respectively (Schunpp, et al., 2011). For the physical sound to become a brain signal, a transduction process takes place in the ear, in which the signal travels in different forms: acoustic, mechanical, hydraulic and bioelectrical. The sound vibrations travel through the acoustic canal to reach the eardrum, where they are transformed into a mechanical movement of the middle ear bones. Then, this mechanical movement is transferred into the cochlea, a fluid-filled structure that contains a basilar membrane with ciliate cells sensitive to vibrations. Afterwards, such cells transduce the vibrations into bioelectrical activity that travels through the auditory nerve fibers to access the central nervous system (Goldstein, 2009).

Notably, within the cochlea starts one of the best characterized aspects of sound processing, and that is the codification of the sound frequency. The base and apex parts of the basilar membrane have different sensitivities to slow and fast oscillations (low and high frequencies, respectively), due to slow oscillations traveling faster through the liquid, and faster ones doing so trough the solid structure of the basilar membrane, which is stiffer at the base. Therefore, ciliate cells at the base respond mainly to vibrations of higher frequencies whereas cells at the apex do the same to low frequencies (Culler et al., 1943), conforming a tonotopic representation. This phenomenon gave rise to Békésy's place theory, which states that the representation of frequency in the auditory nervous system is based on the location of the fibers responding. Furthermore, information of frequency is also carried by the specific firing rate of nerve impulses (temporal coding theory, August Seebeck, 1841), that is, ciliate cells within the cochlea respond in synchrony with the pressure oscillations of sound, faster for higher frequencies and slower for lower frequencies. However, because of the limitations of the firing capacities of neural cells, giving their refractory periods (phase locking limit, see Joris, Schreiner and Rees, 2004), timing information is only informative for frequencies below ~4000 Hz. Overall, both place and timing of neural responses contribute to frequency coding in the auditory nervous system (Goldstein, 2009).

Neural basis of the auditory nervous system

Once the acoustic information reaches the central nervous system, it is further processed at different stages along the auditory pathway (Purves et al., 2004; Jürgen K. Mai and George Paxinos, 2012; Aminof, Boller and Swaab, 2015). Electrical activity from the auditory nerve first reaches the cochlear nuclei (CN) of the brainstem, from where it ascends to the superior olive of the mid-pons. This nuclei contains neurons acting as coincidence detectors and participates in the integration of auditory information from each ear, detecting interaural time delays which support sound localization. Moreover, superior olive is also a key element in the perception of the auditory illusions called binaural beats (Draganova, Ross, Wollbrink and Pantev, 2007), a phenomenon studied in the present thesis. Fiber projections from the CN also innervate the nucleus of the lateral leminiscus, important in the signaling of the sound onset and duration. From these nuclei, the CN and the superior olive, main projections ascend to the Inferior Colliculus (IC), where they are integrated. IC contains information from neurons responding

mainly to frequency-modulated sounds and is crucial for the processing of complex sounds, including those of speech (Purves, et al., 2004).

Upper in the auditory pathway we find the medial geniculate nucleus of the thalamus and the auditory cortex (Purves et al., 2004; Winer and Schreiner, 2011). The auditory thalamus receives main projections from the IC and, in turn, projects fibers to the Heschl's gyri of the superior temporal plane, which contains the primary auditory cortex. All projections going to the auditory cortex have a neural relay in the thalamus and, among others, the role of the medial geniculate nucleus has been related with the direction of auditory attention (Bartlett, 2013). Once signal reaches primary auditory cortex, as well as secondary auditory cortical areas, a more higher-order processing of the information takes place, especially of complex acoustic signals, such as music and sounds used for communication. Furthermore, auditory cortex is crucial for the processing of temporal sequences of sound, such as phonetic sequences forming syllables and words (Wernicke's area). Notably, auditory cortex is not sufficient but necessary for the perception of auditory signals (Heffner and Heffner 1990; Winer and Schreiner, 2011).

Despite the schematic description of the auditory pathway depicted here, it must be noted that the projections from the different neural relays described are far more complex than a linear up-ward pathway. In fact, feed-forward connections between nuclei exist at every stage. Overall, while subcortical structures encode temporal, spectral or intensity aspects of the auditory input, as the information ascends along the auditory pathway, ultimately reaching the cortex, more complex patterns of these aspects are extracted, until reaching meaningful percepts such as speech and music (Litovsky, 2015).

Study of the auditory nervous system with EEG

Beyond the structural organization, the objectives of the present thesis are set to further characterize how different functions of auditory processing occur along the auditory pathway. Given the importance of the auditory system discussed above, a further understanding of the neurophysiological bases of auditory processing is deems necessary. Specifically, little is known about the cognitive aspects of acoustic information processing, or how different hierarchical levels along the auditory pathway interact to reach higher-order processing of sounds, such as that of speech. To this regard, human electroencephalography (EEG) studies have long addressed these questions and offer different ways to assess human auditory cognition. Above other neuroscience techniques, EEG's high

temporal resolution is especially helpful when studying the auditory nervous system, as one defining feature of this system is its remarkable temporal precision (Kraus et al, 2017; Long, et al., 2018).

By means of EEG, the analysis of different temporal and spectral aspects of the signal allows the study of different mechanisms of brain function. On one hand, evoked activity, or event-related potentials (Galambos, 1992; Tallon-Baudry and Bertrand, 1999; see Luck, 2012), can inform us about stereotyped brain responses to a particular acoustic stimulus or a subjacent cognitive process time-locked to the processing of the stimulus. On the other hand, the analysis of induced brain oscillations, or brain rhythms, refers to high-order processes of information transfer (Singer and Gray, 1995) by means of ongoing synchronous activity of large neuronal assemblies (Varela, 1995; David, Kilner and Friston, 2006), which self-emerges in the brain even after the acoustic input inducing it is no longer present.

With the three studies of the present thesis, we aim to contribute to the knowledge on both evoked activity and induced oscillations within auditory brain function, as reflected in its two different aspects of EEG activity (evoked and induced). In the first two studies we try to characterize the roles of different hierarchical levels of auditory processing along the auditory pathway, from the cortex to the brainstem, by measuring event-related potentials reflecting activity from each of them. Specifically, the first study (López-Caballero, Zarnowiec, Escera, 2016) concerns the hierarchical organization of deviance detection responses along the auditory system, and how two different cortical levels of the auditory pathway are sensitive to different aspects of the acoustic predictable patterns. In the second study (López-Caballero, Martin-Trias, Ribas-Prats, Gorina-Careta, Bartrés-Faz, Escera, 2019), we move to lower levels of this hierarchy by analyzing the Frequency-Following Response (FFR; Skoe and Kraus, 2010), an auditory evoked response classically conceived to reflect activity from the brainstem, and try to disentangle its recently suggested cortical contribution (Coffey, Herholz, Chepesiuk, Baillet and Zatorre, 2016). Therefore, in the first two studies we assess the processing of acoustic input at different levels of the auditory hierarchy by measuring its evoked activity. In turn, in the third study (López-Caballero and Escera, 2017), induced oscillatory activity is measured instead. There, we aim to describe whether acoustic stimulation with binaural beats, an auditory illusion, would modulate ongoing neural oscillations at frequency bands associated with different cognitive states, given the inconclusive evidence regarding this topic in the literature.

Evoked activity: deviance detection and the Frequency -Following Response

Among event-related potentials, those elicited by acoustic input are referred as Auditory Evoked Potentials (AEP), and can reflect stimulus-elicited activity of different hierarchical levels along the auditory pathway, from lower (brainstem) to higher levels (auditory cortex) (Picton, 2010), thus allowing a non-invasive study of the neurophysiological basis of auditory processing. The first two studies of the thesis are set in this context. Several AEPs can be distinguished according to different aspects such as its neural generators or its onset latencies. Auditory Brainstem Response (ABR; Jewett and Williston, 1971) comprises a series of waveforms with latencies up to 10 ms from sound onset, which are originated by several nuclei along the auditory brainstem, including the cochlear nerve and nucleus, or the superior olive. The FFR is an evoked potential sometimes described as the sustained part of the ABR (Skoe and Kraus, 2010), with hypothetical sources, although controversial, in subcortical levels of the auditory hierarchy (see Bidelman, 2018). The Middle-Latency Response (MLR) ranges from 12 to 50 ms from stimulus onset, and has neural generators including the auditory thalamus and the primary auditory cortex (Picton et al., 1974; Yvert et al., 2005). Finally, Long-Latency Responses (LLR) include several AEP components such as P50 or N1, with onset latencies starting from 50 ms from sound onset, and the context-depending component mismatch negativity (MMN; Näätanen, Gaillard and Mäntysalo, 1978), with described sources in the anterior Heschl's gyrus (Opitz, Schröger, and Von Cramon, 2005) and the superior-temporal gyrus (Schonwiesner et al., 2007).

A particular phenomenon of auditory processing that is distributed along the whole auditory pathway, as reflected in different AEPs, is deviance detection. In other words, brain evoked responses to redundant sounds following a predictable pattern and responses to novel sounds, breaking that pattern, are different. To this regard, deviance detection phenomena have been long described in cortical potentials (LLR), such as in P50 and N1 components. P50 amplitude is attenuated with redundant repetitive stimuli and thought to reveal a neurological process of sensory gating, that is, the filtering of irrelevant information in the brain (Davis, Mast, Yoshie and Zerlin, 1966; Fruhstorfer, Soveri and Jarvilehto, 1970). Also, within the LLR, the most widely studied AEP for deviance detection is MMN (see Näätänen, Paavilainen, Rinne and Alho, 2007). In contrast with P50 or N1, MMN is a context-dependent component obtained by subtracting the evoked response to the predicted sound from the evoked response to the infrequent sound. Often,

experiments measuring MMN or other AEPs reflecting deviance detection phenomena use trains of repeated invariant stimuli (standard) rarely interrupted (e.g., 10% probability) by a stimulus differing from the rest in intensity, frequency, location or inter-stimulus interval, among others (deviant). In the MLR, reflecting activity from thalamus and auditory cortex, amplitude attenuation in regular vs random stimulation patterns (Cornella, et al., 2015) as well as deviance detection responses to different regularity violations (e.g., Grimm, Escera, Slabu and Costa-Faidella, 2011; Cornella, Leung, Grimm and Escera, 2012) were also observed. Moreover, differential responses to deviant and standard stimuli were shown in the FFR (Slabu, Grimm and Escera, 2012; Skoe, Chandrasekaran, Spitzer, Wong and Kraus 2014; Shiga et al., 2015), thought to reflect activity from subcortical sources; supportive evidence of deviance detection in the IC was found using functional Magnetic Resonance Imaging (fMRI) (Cacciaglia et al., 2015). Notably, animal studies using single unit recordings have also observed Stimulus Specific Adaptation (SSA), a parallel phenomenon to deviance detection at the single neuronal level, at different stages of the auditory pathway, such as IC (Pérez-González, Malmierca and Covey, 2005), thalamus (Antunes and Malmierca, 2011) and cortex (Ulanovsky, Las and Nelken, 2003).

Given the described findings, deviance detection appears to be a defining feature of auditory processing and a basic property of the auditory nervous system (Malmierca, 2003; Escera and Malmierca, 2014). Interestingly, the kind of acoustic predictable patterns from which deviance detection responses can be elicited depend upon the stage of the auditory pathway where this response comes from, thus suggesting a hierarchical organization of deviance detection along the auditory pathway (Escera, Leung and Grimm, 2014; Escera and Malmierca, 2014; Malmierca, Sanchez-Vives, Escera, and Bendixen, 2014). To this regard, MMN, of cortical origin, can be elicited to simple regularity violations, such as that of a stimulus differing from a previous train of repeated identical stimuli in intensity, duration or frequency (Näätänen, Pakarinen, Rinne and Takegata, 2004), but also to violations to more complex contingencies between stimuli (for a review, see Paavilainen, 2013). For instance, this includes the direction of pitch change within pairs of stimuli presented in a row (Saarinen et al., 1992). Alternatively, in MLR, deviance detection is observed for simple-feature deviants (e.g., frequency change: Grimm et al., 2011) but not with a frequency-location feature-conjunction paradigm (Althen, Grimm and Escera, 2013). At the subcortical level, to date, only simple regularity violations have proven to modulate FFR (Slabu et al., 2012; Shiga et al., 2015). Evidence for the hierarchical organization of deviance detection along the auditory pathway has also its counterpart in animal single-unit recordings. Progressively larger attenuation of neuronal responses to self-generated

(predictable) sounds in comparison to random (unpredictable) sounds were found in auditory thalamus, auditory cortex and hippocampus, with the larger attenuation found at hippocampus (Rummell et al., 2016). In our first study, we aimed to further characterize this hierarchy by assessing MLR sensitivity to deviance probability (i.e., how often would the regularity be broken), previously shown to modulate MMN.

Several theories have hypothesized the rationale behind deviance detection phenomena (see Heilbron and Chait, 2017). On the one hand, the memory-trace hypothesis (Näätänen et al., 1978; regarding MMN specifically) suggests that a memory template is build over the presentation of a regular pattern of stimuli, and new acoustic input is compared with it, triggering an error signal if a difference is detected. On the other hand, the adaptation hypothesis (May et al., 1999) suggests that the repetitive presentation of a standard stimuli would produce neuronal refractoriness in the population of neurons responding to these stimuli, which would contrast with the activity of another population of neurons responding to the deviant stimulus. As a consequence, responses to deviant stimuli would appear as stronger compared to those elicited to standard stimuli. However, by using proper control conditions such as a many-standards paradigm (Schröger and Wolff, 1996) or a cascade deviant (Ruhnau, Herrmann, and Schröger, 2012), true deviance detection can be separated from simple adaptation (see Carbajal and Malmierca, 2018). In this context, a comprehensive theory in the field of neuroscience sets in between these two approaches to explain deviance detection and helps to understand its hierarchical organization: predictive coding.

Predictive coding theory states that the brain is constantly generating a hierarchical generative model of the world, that is, patterns of activity representing external stimuli, which constitute predictions. Such predictions would be continuously compared with external stimuli, and mismatches would produce prediction error signals (i.e., deviance detection responses in AEPs) which would trigger adjustments in the predictions (Heilbron and Chait, 2017). Predictive coding constitutes a Bayesian perspective of brain function, with a prediction continuously updated from new observations, and covers different sensory modalities, including the auditory domain. In neurophysiological terms (Shipp, 2016), within each hierarchical level (e.g., associative or primary region of the auditory cortex), patterns of activity in neural populations from layers V/VI of the cortex would send "top-down" projections to lower hierarchical units, representing from more complex to simpler features of the prediction. The incoming stimuli would then be compared with the prediction at each hierarchical level by means of "bottom-up" projections from cortical layers I/III, eliciting error signals at a

particular level in case of a mismatch. According to predictive coding theory, deviance-detection signals such as MMN would be partially the result of a comparison between the acoustic input and a prospective prediction rather than a retrospective memory template (Heilbron and Chait, 2017). Results from our first study on the hierarchical organization of deviance detection phenomena, therefore, can be interpreted in the context of this theory.

Within the study of the hierarchical organization of deviance detection, a next step after the study of deviant probability on MLR was to assess whether lower levels of the auditory hierarchy would reveal deviance detection to complex rules, such as the ones described in Saarinen et al. (1992), or the sensitivity to deviant probability, among others. As previously described, deviance detection to simple acoustic deviations had already been shown in subcortical structures with fMRI (Cacciaglia et al., 2015), as well as had been observed in the FFR evoked potential (Slabu et al., 2012; Shiga et al., 2015). However, these effects had not been tested, to the best of our knowledge, with complex rules.

In more detail, FFR reveals phase-locked activity of the auditory nervous system to the spectral and temporal components of the auditory input (Krishnan et al., 2004; Chandrasekaran and Kraus 2010) and, because of its associations with phenomena such as musical training (Bidelman, 2013), bilingualism (Krishnan et al., 2005), or language impairment (Rocha-Muniz, 2012), it is thought to reveal a crucial mechanism in auditory perception and language. As mentioned, the sources of FFR were traditionally attributed to subcortical structures (Sohmer and Pratt, 1977; Langner, 1992; Nelken, 2004; see Bidelman, 2018). To this regard, continuing with the characterization of the auditory hierarchy to deviance detection, FFR, as an indicator of subcortical activity, was our next target to test for complex contingency encoding at the subcortical level. However, at that point, controversy on the actual subcortical origin of this AEP arose due to a study pointing towards a cortical contribution to FFR (Coffey et al., 2016). Therefore, it deemed necessary to first disentangle the sources of this signal, and that was the goal of study two.

Evidence supporting the subcortical generators of the FFR traditionally came from animal studies using single unit recordings in cats. Among their findings, for instance, the cooling of IC reduced drastically the scalp recorded FFR (Smith, Marsh and Brown, 1975), scalp recorded FFRs showed phase correspondence with spike activity in cochlear and superior olivary complex (Marsh, Brown and Smith, 1974), and first spike latencies aligning with FFR onset latency were found in IC (Schreiner and Langner, 1988). Moreover, in human research, no FFR could be recorded from patients with upper brainstem lesions (Sohmer and Pratt, 1977) and

EEG studies applying inverse solution methods to infer the origin of the scalp-recorded signal pointed towards a subcortical origin as well (Bidelman, 2015b).

Despite all the previous evidence, Coffey et al. study (2016) challenged the assumption on FFR being completely subcortical, but also raised a very important question on the FFR field, and that is whether the contribution from the cortex was dependent on the frequency of the stimulus. The rationale behind this was the fact that the encoding of stimulus frequencies in the auditory brain depends partially, as described before, on the specific firing rate of neurons (temporal coding theory), specially for frequencies below ~4000 Hz, and firing rate capacities of neurons vary along different stages of the auditory hierarchy (Joris, et al.,, 2004). Specifically, they are progressively reduced from brainstem to cortical levels and reach a ~100 Hz limit at the cortex. FFR being a signal reflecting neural phase locking to the stimulus frequency, these differences in firing rate capabilities along the auditory pathway must be relevant in our understanding of its neural generators. Therefore, and more precisely, in our second study we aimed not only to disclose the potential contribution from auditory cortex to the FFR, but also test the hypothesis on whether this contribution was dependent on stimulus frequency.

Induced activity: brainwave entrainment with binaural beats

Paralleling the study of evoked activity, induced oscillatory activity in the brain was another topic of interest of the present thesis, as reflected in study three. Ongoing oscillations, sometimes referred as brain rhythms, are thought to reflect a neuronal synchronization process, in which large population of neurons respond in phase producing membrane potential fluctuations in neighboring cells, therefore facilitating information transfer (Varela, 1995; David et al., 2006). Ongoing oscillations have classically constituted a differentiated domain of brain activity in comparison to evoked activity, since they are not stimulus-locked. However, such oscillations can be induced from rhythmic external stimuli, by means of a process known as brainwave entrainment, or oscillatory entrainment (Walter, 1953; for a review, see Herrmann, Strüber, Helfrich and Enge, 2016).

Notably, among brain rhythms measured with EEG, different frequency bands (delta, ~1-3 Hz; theta, ~3-7 Hz; alpha, ~7-13 Hz; beta, ~13-30 Hz; and gamma, ~30-70 Hz) have been associated with several sensory and cognitive processes, as reflected in behavioral performance. For instance, theta band has been related

with working memory (Moran, Campo, Maestu, Reilly, Dolan and Strange, 2010), alpha-band with stimulus detection (Mathewson et al., 2009), beta-band with increased alertness (Kamiński, Brzezicka, Gola and Wróbel, 2012), and gamma-band with selective visual attention (Fries, Reynolds, Rorie and Desimone, 2001). Moreover, within predictive coding theory, gamma activity is hypothesized to reflect bottom-up signal (prediction error) whereas beta and lower bands would reflect top-down (prediction) signals (Bastos, Usrey, Adams, Mangun, Fries, Friston, 2012). Meanwhile, different methods have been used to entrain certain brain rhythms, such as EEG-neurofeedback, repetitive transcranial magnetic stimulation (rTMS), transcranial alternating current stimulation (tACS) and, more importantly for the purposes of this thesis, rhythmic sensory stimulation (Herrmann et al., 2016).

Given the relevance of auditory stimulation for brainwave entrainment and the different perspective that this domain of brain activity offers relative to the AEPs, in the third study of the thesis we aimed to test the potential capacity of a particular type of acoustic stimulation in the modulation of brain rhythms: the binaural beats. Binaural beats are the result of the simultaneous presentation of two pure-tone sinewaves with slightly different frequencies (e.g., 300 and 305 Hz), one to each ear. A periodic amplitude modulated tone with a frequency corresponding to the frequency difference between the two tones (e.g., 5 Hz) is perceived as a "beat", although no physical combination of the original tones occurs outside the auditory system (Dove, 1841). This type of beats, as generated within the auditory system (Draganova, et al., 2007), have been suggested as a brainwave entrainment tool differentiated from other classical acoustic inputs (see Vernon, 2009). However, literature on induced oscillations with binaural beats is controversial, mainly because of the variability in the methodologies used and the lack of proper controlled conditions (e.g., "placebo"). Therefore, in our third study we used strict controls, with treatment versus placebo, and baseline-treatment-washout sessions, to disentangle the potential benefits of this type of stimulation for the enhancement of different brain rhythms (theta, alpha, beta and gamma). Overall, with the third study, we aimed to contribute to the knowledge of induced oscillations with acoustic stimuli and explore a different perspective of the auditory brain function, beyond that of evoked activity.

Aims

With the three studies of this thesis we aimed to further characterize, first, the hierarchical organization of the deviance detection system along the auditory pathway (study one), second, the sources of the scalp-recorded FFR (study two) and, third, the modulation of brain rhythms with a particular acoustic input, the binaural beats (study three). The rationale behind these topics was the study of two classically differentiated domains of brain activity, as measured with EEG. First, evoked activity, time-locked to the presentation of a sound and revealing brain mechanisms related with its processing. Second, induced activity, on-going oscillations in the brain present even in the absence of acoustic stimuli, but induced by them, and classically associated with different sensorial and cognitive phenomena.

Given previous literature on how progressively more complex types of regularities can be encoded from lower to higher levels of the auditory hierarchy, in study one (López-Caballero, Zarnowiec, Escera, 2016) we looked for potential differences on the sensitivity of two different levels to deviant probability, that is, how often a regularity is broken. To test this, we measured two AEPs originating at different hierarchical levels of the auditory system: LLR as generated in primary and secondary auditory cortex, and MLR as having main contributions from thalamus and primary auditory cortex. Since sensitivity to deviant probability was already demonstrated at the level of the LLR, with this study we explored whether MLR would also be modulated by deviant probability.

In the second study, we focused on the FFR, an evoked potential which follows the periodic features of the acoustic input, traditionally associated with subcortical sources. However, the cortical contributions to FFR were recently identified, and therefore we aimed to disentangle whether FFR generators were actually purely subcortical or had cortical contributions. Additionally, we aimed to test whether such contribution would be dependent on stimulus frequency. To this achieve this, in study two (López-Caballero, Martin-Trias, Ribas-Prats, Gorina-Careta, Bartrés-Faz, Escera, 2019), we combined FFR recordings with an inhibitory transcranial magnetic stimulation (TMS) protocol in the auditory cortex.

In the third study (López-Caballero and Escera, 2017), we focused on induced oscillatory activity of the brain, as measured with EEG frequency bands. Specifically, we aimed to assess ongoing oscillations in the brain could be modulated by binaural beats, an auditory illusion produced by the combination in the brainstem of the input from two tones with slightly different frequencies,

presented one to each ear. Such beats have been suggested in the literature as capable of producing brainwave entrainment and induced oscillations, although with inconclusive evidence. Given the associations of different brain rhythms (theta, alpha, beta and gamma) with specific cognitive processes, and the possibility to modulate these by external acoustic stimulation, the study of induced oscillations not only allows for the characterization of this domain of the auditory brain function, but also may be beneficial for the potential enhancement of these cognitive processes.

STUDY I:

Differential deviant probability effects on two hierarchical levels of the auditory novelty system

Biological Psychology 120 (2016) 1–9

Contents lists available at ScienceDirect

Biological Psychology

journal homepage: www.elsevier.com/locate/biopsycho

Differential deviant probability effects on two hierarchical levels of the auditory novelty system

Fran López-Caballero[a,b], Katarzyna Zarnowiec[a,b], Carles Escera[a,b,c,*]

[a] Brainlab-Cognitive Neuroscience Research Group, Department of Clinical Psychology and Psychobiology, University of Barcelona, Passeig de la vall d'Hebron 171, 08035 Barcelona, Catalonia, Spain
[b] Institute Neurosciences, University of Barcelona, Passeig de la Vall d'Hebron 171, 08035 Barcelona, Catalonia, Spain
[c] Institut de Recerca Pediàtrica Hospital Sant Joan de Déu (IRP-HSJD), Esplugues de Llobregat, Barcelona, Spain

ARTICLE INFO

Article history:
Received 6 January 2016
Received in revised form 16 June 2016
Accepted 2 August 2016

Keywords:
Auditory evoked potential
Deviance detection
Deviant probability
Middle-latency response
Mismatch negativity

ABSTRACT

Deviance detection is a key functional property of the auditory system that allows pre-attentive discrimination of incoming stimuli not conforming to a rule extracted from the ongoing constant stimulation, thereby proving that regularities in the auditory scene have been encoded in the auditory system. Using simple-feature stimulus deviations, regularity encoding and deviance detection have been reported in brain responses at multiple latencies of the human Auditory Evoked Potential (AEP), such as the Mismatch Negativity (MMN; peaking at 100–250 ms from stimulus onset) and Middle-Latency Responses (MLR; peaking at 12–50 ms). More complex levels of regularity violations, however, are only indexed by AEPs generated at higher stages of the auditory system, suggesting a hierarchical organization in the encoding of auditory regularities. The aim of the current study is to further characterize the auditory hierarchy of novelty responses, by assessing the sensitivity of MLR components to deviant probability manipulations. MMNs and MLRs were recorded in 24 healthy participants, using an oddball location paradigm with three different deviant probabilities (5%, 10% and 20%), and a reversed-standard (91.5%). We analyzed differences in the MLRs elicited to each of the deviant stimuli and the reversed-standard, as well as within deviant stimuli. Our results confirmed deviance detection at the level of both MLRs and MMN, but significant differences for deviant probabilities were found only for the MMN. These results suggest a functional dissociation between regularity encoding, already present at early stages of auditory processing, and the encoding of the probability with which this regularity is disrupted, which is only processed at higher stages of the auditory hierarchy.

1. Introduction

The ability to automatically detect sounds disrupting acoustic regularities within the auditory scene, that is deviance detection, is a critical functional property of the auditory system (Escera & Malmierca, 2014), which is necessary to reallocate attention pre-attentively towards potentially relevant stimuli (Escera, Alho, Winkler & Näätanen, 1998; Escera & Corral, 2007). Such ability is revealed as a differential electrophysiological response to the same sound when presented in a regular and predictable pattern (as "standard" stimulus) and when it is infrequent and unexpected (as "deviant" stimulus). In order for the deviant stimulus to be detected, the auditory system must extract the relationships between elements of the sound sequence (Winkler, 2007), a process known as regularity encoding.

Regularity encoding and deviance detection have been shown by recording human Auditory Evoked Potentials (AEPs) in the so-called Long-Latency Responses (LLR; i.e., responses peaking at circa 80 ms onwards from stimulus onset). Among them, the classical deviance-related response, the Mismatch Negativity (MMN; Näätänen, Gaillard & Mäntysalo, 1978), is a regularity violation signal peaking around 100–250 ms from stimulus onset, displaying maximum amplitudes at the frontocentral scalp. This scalp distribution is consistent with generator sources located in upper regions of the auditory cortex, such as secondary auditory areas (Opitz, Schröger, & Von Cramon 2005; Schönwiesner et al., 2007), and beyond in prefrontal cortex (Deouell, 2007). However, AEPs generated at shorter latencies and anatomically lower cortical regions than those yielding the MMN can also reflect acoustic regularity

* Corresponding author at: Department of Clinical Psychology and Psychobiology, University of Barcelona, Passeig de la Vall d'Hebron 171, 08035 Barcelona, Catalonia, Spain.
E-mail address: cescera@ub.edu (C. Escera).

http://dx.doi.org/10.1016/j.biopsycho.2016.08.001
0301-0511/

violations, such as by the Middle-Latency Response (MLR; Picton, Hillyard, Krausz & Galambos, 1974). The MLR is a series of waveforms ranging from 12 to 50 ms from stimulus onset, with neural generators distributed from the primary auditory cortex to the superior temporal gyrus (Yvert, Fischer Bertrand & Pernier, 2005). In the MLR range, deviance responses have been observed for frequency deviants in the Pa (Slabu, Escera, Grimm & Costa-Faidella, 2010) and Nb (Alho, Grimm, Mateo-León, Costa-Faidella & Escera 2012; Althen, Grimm & Escera, 2013; Grimm, Escera, Slabu, & Costa-Faidella, 2011; Leung, Cornella, Grimm & Escera, 2012) components; for intensity deviants in Na and Pa components (Althen, Grimm & Escera, 2011); for location deviants in the Na component (Cornella, Leung, Grimm & Escera, 2012; Grimm, Recasens, Althen & Escera, 2012; Sonnadara, Alain & Trainor, 2006b); and for temporal regularity deviants in Nb and Pa components (Leung, Recasens, Grimm & Escera, 2013). Moreover, correlates of deviance detection have also been found in the brainstem by AEP studies recording the Frequency Following Response (FFR; Slabu, Grimm & Escera, 2012), as well as by functional magnetic resonance imaging studies (Cacciaglia et al., 2015).

Paralleling results in human AEPs, animal studies using single-unit recordings support that deviance detection occurs also at lower stages of the auditory pathway than those eliciting MMN. These studies have found that specific neurons in the primary auditory cortex (Ulanovsky, Las & Nelken, 2003), the medial geniculate body (MGB; Anderson, Christianson & Linden, 2009; Antunes, Nelken, Covey & Malmierca, 2010; Richardson, Hancock & Caspary, 2013) and the inferior colliculus (IC; Pérez-González, Malmierca & Covey, 2005; Malmierca, Cristaudo, Pérez-González & Covey 2009; Patel, Redhead, Cervi & Zhang, 2012) show Stimulus Specific Adaptation (SSA) within the first 30 ms from deviant onset (Pérez-González, Malmierca, & Covey, 2005; Von der Behrens, Bäuerle, Kössl & Gaese, 2009). That is to say, these neurons reduce their discharge rate after the repetition of a standard frequent tone, but regain their response when presented with an infrequent different stimulus (Ulanovsky et al., 2003; Ulanovsky, Las, Farkas & Nelken, 2004). SSA was originally postulated as the neuronal correlate of MMN (Nelken & Ulanovsky, 2007). However, because of its latency, neural generators and different relation with the NMDA receptor function (Farley, Quirk, Doherty, & Christian, 2010), SSA has been recently proposed a better correlate of earlier deviance-related AEPs, such as MLR (Escera, Leung & Grimm, 2014; Grimm et al., 2016).

Interestingly, distinct AEP components reflect brain responses playing different roles in regularity encoding and deviance detection, whose functional relationship is still not fully characterized. The MMN can be elicited when the deviant stimuli differ from the standard in various simple features, such as intensity, duration, frequency or location (Näätänen, Pakarinen, Rinne & Takegata, 2004), but also with more complex types of regularity violations, such as changes in phonetic category (Shestakova et al., 2002) or by deviations in abstract rules (Paavilainen, 2013; Saarinen, Paavilainen, Schöger, Tervaniemi, & Näätänen, 1992), like a tone repetition that breaks a previous sequence of alternating tones (Nordby, Roth & Pfefferbaum, 1988). However, at the level of the MLR, the auditory system is sensitive to the physical characteristics of complex stimuli (Cornella, Leung, Grimm & Escera, 2013), but deviance detection can only be observed when using simple-feature stimuli deviations (Cornella et al., 2012), as more complex types of regularity violations are only caught up at later processing stages, by the generator ranges of the MMN. This is the case, for instance, of alternating-tone violations with repetition (Cornella et al., 2012), feature conjunctions (Althen et al., 2013) or global as compared to local rules (Recasens, Grimm, Wollbrink, Pantev & Escera, 2014). This supports the emerging view that the auditory deviance detection system is organized in a hierarchical manner at different levels of the auditory pathway, from brainstem to cortex (Escera et al., 2014; Escera & Malmierca, 2014; Malmierca, Sanchez-Vives, Escera, & Bendixen 2014).

In the present study, we aimed to further characterize the auditory hierarchy of deviance responses by testing the sensitivity of MLR, as an early correlate of deviance detection, to deviant stimulus probability. Deviant probability manipulations have been found to modulate the amplitude of components belonging to the LLR (Näätänen, Sams, Järvilehto & Soininen, 1980; Näätänen & Picton, 1987; Ritter et al., 1992). However, the effects of such contingences of the deviant stimulus have yet to be assessed at shorter latencies. Previous studies have shown that lower probabilities of the deviant stimulus elicit larger MMN responses, an effect confirmed with oddball paradigms using deviations in frequency (Sabri & Campbell, 2001) location (Sonnadara, Alain & Trainor, 2006a), and duration (Evstigneeva & Aleksandrov, 2009), as well as with multi-feature MMN (Fisher, Grant, Smith & Knott, 2011) and roving-standard (Haenschel, Vernon, Dwivedi, Gruzelier & Baldeweg, 2005) paradigms. Likewise, animal studies have demonstrated more robust deviance-related single neuron responses (SSA) when decreasing the probability of the deviant stimulus (Antunes et al., 2010; Malmierca et al., 2009; Patel et al., 2012; Ulanovsky et al., 2003), interestingly, in neural stages postulated to give rise to components with earlier latencies than MMN in the human brain.

The AEP studies mentioned above suggest that high levels of the auditory pathway, giving rise to MMN, can detect the violation of a previous acoustic regularity, but are also sensitive to the probability with which this regularity is disrupted. However, to our knowledge, it remains to be determined whether at lower levels, involved in MLR generation, this contingency of the deviating stimuli is also appraised, as suggested by animal studies. Considering the probability dependence of MMN evoked potential and SSA, proposed as the neuronal correlate of MLR (Grimm et al., 2016), our hypothesis was that deviant probability manipulations would modulate the MLR.

2. Materials and methods

2.1. Participants

Twenty-four participants (five males) were recruited, ranging in age from 20 to 30 years (mean = 23.1; standard deviation = 2.8). Exclusion criteria were history of neurologic or psychiatric condition, as well as abnormal hearing. A pure-tone audiometry was performed for each participant before the experiment started, ensuring mean hearing thresholds below 20 dB SPL. The experimental protocol was approved by the Ethical Committee of the University of Barcelona, and was in accordance with the Code of Ethics of the World Medical Association (Declaration of Helsinki). All participants signed a written informed consent form and were paid for participation.

2.2. Stimuli

The stimulus used in the experiment was an up-chirp (Dau, Wegner, Mellert & Kollmeier 2000; Fig. 1A) (also known as "Don chirp"), with a length of 16.7 ms, presented at 60 dB SPL. It was constructed by summing rising harmonic series of cosine waveforms from 50 to 8000 Hz, in accordance with Elberling, Don, Cebulla, & Stürzebecher study (2007). This stimulus's wideband frequency spectrum is known to stimulate different sections of the basilar membrane simultaneously, and was reported to generate MLR with higher signal to noise ratio and larger amplitude than click or down-chirp stimuli (Dau et al., 2000; Rupp et al., 2002). Moreover, it has been successfully used in recent studies recording

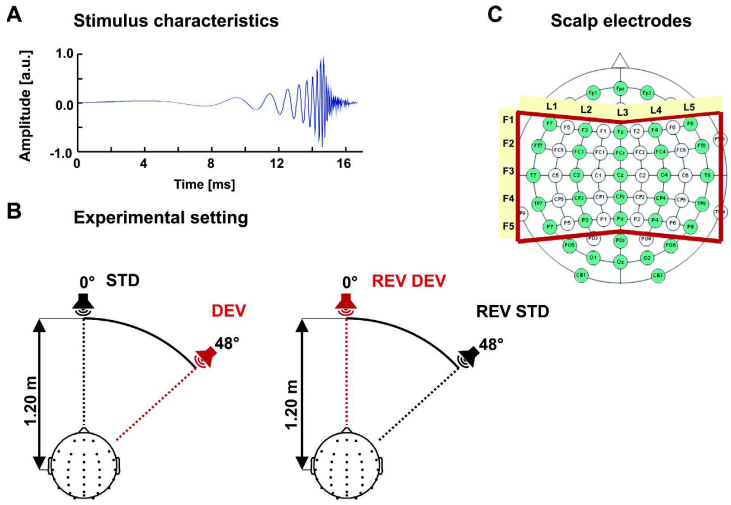

Fig. 1. A) Stimulus characteristics. Up-chirp of 16.7 ms duration composed of rising harmonic series of cosine waveforms from 50 to 8000 Hz. B) Experimental setting. In the oddball condition, standard stimuli (STD) were presented through loudspeakers at 0° from participant's head, whereas the deviant stimuli (DEV) were the same stimuli presented at 48° clockwise. In different oddball blocks, the probability of the deviant was either 5%, 10% or 20%. In the reversed-standard condition, standard (now REV STD) and deviant (now REV DEV) stimuli location were reversed. C) Scalp electrodes used in the EEG recording (in green). The red square shows the 25 electrodes used to study differences in topographical distributions among stimulus probabilities. The F (Frontality) and L (Laterality) labels indicate, respectively, the rows and columns of electrodes within the square that formed the horizontal and vertical electrodes used for the topographical analyses. (for interpretation of the references to colour in this figure legend, the reader is referred to the web version of this article).

deviance-related responses in the MLR and MMN range (Leung et al., 2013; Aghamolaei, Zarnowiec, Grimm & Escera, 2016).

2.3. Procedure and experimental design

During EEG recordings, participants sat comfortably in an electrically shielded and sound-attenuated chamber, while passively listening to the auditory stimuli presented through two cube loudspeakers (BOSE Professional Systems, Framingham, Massachusetts) located 1.20 m from participant's head. Participants were instructed to watch a silent movie of their choice with subtitles, and to ignore the auditory stimuli. Stimuli were created and presented using MATLAB software (The Mathworks, Inc., Natick, MA) and the Psychophysics Toolbox extensions (Brainard, 1997; Pelli, 1997; Kleiner, Brainard & Pelli, 2007), with a stimulus-onset asynchrony (SOA) jittered from 105 to 195 ms (mean 150 ms).

We employed an oddball location paradigm (Fig. 1B), in which deviant and standard stimuli differed in their source location relative to the participant's head. Two different conditions were employed: in the oddball condition, standard frequent stimuli were chirps presented at 0° from the participant's head, while deviants were the same stimuli delivered from 48° clockwise. In the reversed-standard condition, these roles were reversed, allowing us to control for potential effects due to the stimulus specific location on the MLR components. For the oddball condition, the probability of appearance of the deviant stimuli was 5%, 10% or 20%, in separated blocks. In the reversed-standard condition, the reversed-standard probability remained at 91.5%, the weighted probability of the presented standards in all three oddball blocks. The rationale behind the use of location deviants was that neither the frequency nor the duration of the Up-chirp could be modified, as it is defined by the stimulus itself. Thus we could use either intensity or location deviations and, in the pilot experiments, location deviants elicited clearer MMN and more robust MLR responses compared to intensity deviants.

Stimuli were presented in 18 randomly intermixed blocks: eight oddball blocks in which deviant stimuli appeared with a probability of 5%; four blocks with deviant probability of 10%; two blocks with deviant probability of 20%, and four blocks for the reversed-standard condition. For each participant, a total of 1000 trials for each deviant probability, as well as 1000 trials for the reversed-standard stimuli were presented. Before each block, participants were instructed to direct the head to the front loudspeaker. A headband with three infrared LEDs placed on the participant's head, along with an infrared-sensitive camera in the recording room, allowed the experimenter to ensure that the participant's head remained at 0° from the front loudspeaker (see details in Aghamolaei et al., 2016; Grimm et al., 2012).

2.4. Data acquisition

Continuous EEG recordings were carried out from 36 scalp electrodes (FP1, FPz, FP2, F7, F3, Fz, F4, F8, FT7, FC3, FCz, FC4, FT8, T7, C3, Cz, C4, T8, TP7, CP3, CPz, CP4, TP8, P7, P3, Pz, P4, P8, PO5, POz, PO6, O1, Oz, O2, CB1 and CB2) (Fig. 1C) and two electrodes placed on the left and right mastoids (M1 and M2). An electrode on the tip of the nose was used as an online reference. To control for eye movements, the electrooculogram (EOG) was also measured with two bipolar electrodes placed above and below the left eye (VEOG), and two bipolar electrodes placed on the outer canthi of the eyes (HEOG). The scalp electrodes were mounted on an elastic nylon cap (Quickcap, Neuroscan, Compumedics), in accordance with the extended 10–20 system. EEG signals were amplified using SynAmps RT amplifier (NeuroScan, Compumedics, Charlotte,

NC), digitized with a sampling rate of 2 kHz, and online-band-pass filtered from 0.05 to 500 Hz using Neuroscan 4.4 software (NeuroScan, Compumedics, Charlotte, NC). During the acquisition, all electrode impedances were kept below 10 kΩ.

2.5. Data analysis

Data from all the scalp electrodes, and from HEOG and VEOG channels were analyzed using EEGLAB (Delorme & Makeig, 2004) and Fieldtrip toolboxes (Oostenveld, Fries, Maris & Schoffelen, 2010) running on MATLAB, separately for middle-and long-latency ranges.

For the MLR analysis, data were re-referenced to the averaged mastoids, and bandpass filtered from 15 to 200 Hz (Kaiser windowed sinc FIR filter). For each participant epochs of 150 ms were extracted for analysis, including 50 ms of pre-stimulus baseline. Independent Component Analysis (ICA) with the Second Order Blind Identification (SOBI) method (Delorme & Makeig, 2004; Delorme, Sejnowski & Makeig, 2007) was applied to isolate and remove eye blinks, movement and myogenic artefacts. After ICA cleaning, epochs with amplitudes larger than 50 μV at any EEG channel, or larger than 100 μV at the EOG channels, were excluded from further analysis. One participant was excluded from further analysis because of contamination of the MLR with the post-auricular muscle artifact (Bell, Smith, Allen & Lutman, 2004). On average, 947 trials were retained for the reversed-standard stimulus, and 929, 926, and 931 for the deviant stimuli at 5%, 10%, and 20% probability, respectively.

For the LLR analysis, data were re-referenced to the averaged mastoids, and bandpass filtered from 3 to 30 Hz (Kaiser windowed sinc FIR filter). For each participant epochs of 500 ms were extracted for analysis, containing 100 ms of data before stimulus onset used as baseline. Epochs with amplitudes larger than 80 μV at any of the EEG channels, or larger than 100 μV at the EOG channels, were excluded from further analysis. The participant excluded for MLR analysis was also excluded from the LLR. On average, 888 trials were retained for the reversed-standard stimulus, and 870, 879, and 866 for the deviant stimuli at 5%, 10%, and 20% probability, respectively.

For each participant, epochs corresponding to deviant stimuli presented with probabilities of 5%, 10%, 20% and reversed-standards were averaged separately, resulting in four AEP averages for each latency range. Finally, grand-average with data of all participants was obtained for illustration purposes.

2.6. Statistical analysis

To analyze significant differences between AEPs elicited by different deviant probabilities, we applied a cluster-based nonparametric repeated measures ANOVA (Maris & Oostenveld, 2007), with one within-participant factor including the three deviant stimuli and the reversed-standard. Additionally, the same analysis was conducted over the difference waveforms computed by subtracting the AEP elicited in the reversed-standard condition to the one elicited by each of the deviants. The analyses were applied separately for MLR and LLR ranges, across all the channels. For MLR, analyses were run from 20 to 80 ms time-window, and for LLR from 80 to 400 ms, similar as done in a previous study from our laboratory (Aghamolaei et al., 2016).

For each time-point over these predefined time-windows, the procedure applied was as follows (Rivolta et al., 2014): First, electrodes adjacent to each other whose F-value was above that corresponding to a p-value < 0.05 were aggregated into clusters. At least two neighbouring electrodes were necessary to form a cluster. Second, the F-values of the electrodes forming a cluster were summed together, forming the cluster level statistics. And third, these cluster statistic-values were compared with the permutation distribution of the maximum cluster-level statistics under the null hypothesis obtained with the Monte Carlo randomization method (Manly, 1997), using 3000 permutations. Clusters were considered significant when having values higher than the 95th percentile of the statistic obtained by Monte Carlo randomization. In the time-window of the cluster with significant F-values, post-hoc t-tests were carried out to study the interactions between specific probabilities.

Furthermore, we compared the effects of different probability conditions on the voltage distribution over the scalp, by conducting a topographical analysis. A matrix of 25 electrodes was chosen (red square in Fig. 1C), where we defined five horizontal electrode lines distributed along the anterior-posterior axis of the scalp (e.g., the first horizontal electrode comprises electrodes F7, F3, Fz, F4 and F8), and five vertical electrode lines distributed along the left-right axis (e.g., the first vertical electrode comprises electrodes F7, FT7, T7, TP7 and P7). A three-way repeated measures ANOVA was then performed over the mean amplitudes of significant time-windows for MLR and MMN, with the three factors being Probability (four levels: 5%, 10%, 20% and 91.5%), Frontality (five levels: the five horizontal electrodes, inset in Fig. 1C) and Laterality (five levels: the five vertical electrodes, inset in Fig. 1C). With this analysis, we looked for significant interactions between Probability factor and Frontality/Laterality, which would indicate a different effect of probability on amplitude in different regions of the scalp, resulting in particular voltage distributions. To assess the effect of deviant probability manipulations on scalp topographies, the same analysis was applied including only the three deviant probabilities in the Probability factor. Twenty-five electrodes were used in these analyses (Fig. 1C). To exclude the effect of amplitude on differences in topographical distribution, for all topographical analyses data were normalized by dividing the amplitude at each electrode by the sum of squared voltages at all electrodes analyzed per participant and per condition (McCarthy & Wood, 1985). For each of the comparisons, whenever the assumption of sphericity was violated, degrees of freedom were corrected using Greenhouse-Geisser estimates. For all the statistical analyses, Bonferroni corrections for multiple comparisons were performed to adjust the p-values of the post-hoc tests.

3. Results

3.1. Middle-latency range

Stimuli presented in each condition and probability elicited sizable MLRs in all participants, with the following components and peak latencies: a brainstem waveform at 25 ms from stimulus onset, followed by the MLR components N0 (28,5 ms), P0 (35 ms), Na (35,5 ms), Pa (47 ms), Nb (55 ms) and Pb (68 ms). These peak latencies are delayed about 10 milliseconds from the typical MLR latencies (Picton et al., 1974) because of the use of up-chirp stimuli of 16,7 ms of duration, and resemble those found in previous studies eliciting MLR with the same stimuli (Aghamolaei et al., 2016; Leung et al., 2013). Up-chirp stimulus is known to yield this effect as a consequence of the simultaneous stimulation of different sections of the basilar membrane (Rupp et al., 2002). In the MLR grand-average waveform, the cluster-based-permutation ANOVA revealed a main effect of probability ($p = 0.037$) in the time-window from 50.5 to 59.5 ms, corresponding to the Nb component (Fig. 2A), thus indicating significant differences between amplitudes elicited by the different probabilities of the stimuli.

Post-hoc t-tests performed over the MLR significant cluster revealed significant amplitude differences between the 5% deviant and the reversed-standard ($p = 0.032$), as well as between the 20% deviant and the reversed-standard ($p = 0.008$) (Fig. 2B).

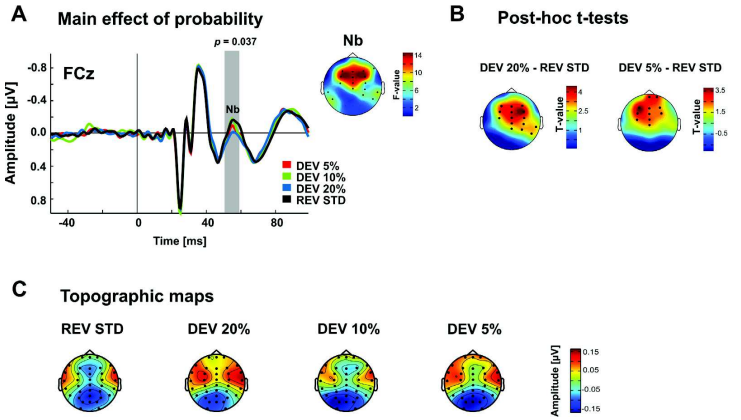

Fig. 2. A) Main effect of stimulus probability on MLR. Grand-average MLRs elicited by reversed-standard condition and deviant stimuli with 5%, 10% and 20% probabilities, recorded at FCz electrode. The gray bar shows the time window where a significant main effect of probability was found by non-parametric analysis (50.5–59.5 ms, roughly corresponding to Nb). The topographic map illustrates the F-values over the scalp in Nb time-window. Only electrodes for which the F-value was significant are depicted. B) Post-hoc *t*-tests over MLR significant time-window (50.5–59.5 ms). Deviance detection was observed for the 5% deviant ($p = 0.032$) and the 20% deviant ($p = 0.008$), but different deviant probabilities did not elicit significantly different responses. The topographic maps illustrate the t-values over the scalp for the two significant contrasts. Only electrodes for which the t-value was significant are depicted. C) Mean scalp topographies of amplitudes within the MLR significant cluster (50.5–59.5 ms).

Significant differences were also found between the 10% deviant and the reversed-standard, although these did not survive the Bonferroni correction ($p = 0.132$). Nb amplitudes elicited by the different deviant probabilities did not differ significantly among them, suggesting that the deviance effect was irrespective of deviant probability. Results from a subsequent analysis with the cluster-based-permutation ANOVA performed over the difference waveforms in the MLR went in the same direction, as no significant clusters were revealed, thus suggesting there are no significant differences between deviant conditions.

When assessing the effect of probability on the Nb cluster's scalp topographies (Fig. 2C), the 3-way repeated measures ANOVA reported no significant factor interactions, neither between Probability and Frontality ($F_{(4.277,94.094)} = 0.859$, $p = 0.590$) nor between Probability and Laterality ($F_{(5.445,119.787)} = 1.944$, $p = 0.086$). Thus, at the MLR level, deviance related effects were only reflected on the amplitude of Nb component, but not in the pattern of voltage distribution over the scalp. The same analysis including only the three deviant probabilities yielded the same lack of interaction between Probability and Frontality ($F_{(2.873,63.211)} = 0.847$, $p = 0.469$) and Probability and Laterality ($F_{(3.915,86.135)} = 0.463$, $p = 0.759$) indicating, in summary, that both the amplitude and the topographic features of the Nb component of the MLR remained unaffected by deviant probability manipulations.

3.2. Long-latency range

The cluster-based-permutation ANOVA returned three significant clusters in the LLR with a main effect of probability (Fig. 3A and B). The first of these clusters, within a time window from 80 to 202 ms ($p = 0.0003$) corresponded to a typical MMN, as described in the literature (Näätänen et al., 2007), with a maximum amplitude in the frontocentral scalp. Moreover, two additional clusters with significant differences between stimulus probabilities were found at latencies from 203.5 to 297 ms ($p = 0.0003$), and from 302 to 399.5 ms ($p = 0.0003$). These latency ranges roughly correspond, respectively, to the P3a (Escera, Alho, Schröger & Winkler, 2000) and a Late Negativity (LN), sometimes identified as the Reorienting Negativity (RON; Schröger & Wolff, 1996; Escera, Yago & Alho, 2001). In all the cases, the significant differences suggested that the components' amplitude increased as a function of the deviant stimulus probability.

Post-hoc *t*-tests were carried out within the first significant time-window of LLR grand-average, corresponding to the MMN (Fig. 3C). Here, reversed-standard amplitude significantly differed from that elicited by the 5% deviant ($p = 0.002$) and the 10% deviant ($p = 0.002$). Significant differences were also found between reversed-standard and the 20% deviant, although these did not survive the Bonferroni correction ($p = 0.232$). Moreover, responses elicited by distinct deviant probabilities significantly differed each from another. Particularly, amplitude elicited by the 20% deviant was smaller than that of the 10% deviant ($p = 0.002$), which in turn was smaller than that of the 5% deviant ($p = 0.014$). Also, significant differences occurred between deviant 20% and 5% ($p = 0.002$). This suggests that, in addition to a deviance-related response to each of the three deviant probabilities, at the MMN level the probability of the deviant stimulus was encoded too. Indeed, effects of deviant probability on MMN amplitude were also found when performing the cluster-based-permutation ANOVA over the difference waveforms in the LLR. Here three significant clusters were found, from 86 to 195 ms ($p = 0.0003$), from 203 to 273 ms ($p = 0.0003$) and from 300 to 362 ms ($p = 0.0016$), the first of them corresponding to MMN.

Comparisons between scalp topographies elicited by each deviant probability were carried out by means of a repeated-measures ANOVA within the first cluster time-window (Fig. 4A), corresponding to MMN. Here we found a significant combined effect of Probability and Frontality ($F_{(3.664,80.619)} = 6.524$, $p < 0.001$) and Probability and Laterality ($F_{(4.661,102.53)} = 8.558$, $p < 0.001$), indicating a deviance effect on the topographic distribution over the scalp, not observed in the MLR analyses. When performing the same analysis without the reversed-standard, significant interactions still were found between Probability and Frontality ($F_{(2.437,53.618)} = 3.502$, $p = 0.029$) and Probability and Laterality ($F_{(3.105,68.304)} = 3.872$, $p = 0.012$). Hence, in contrast with the MLR, at

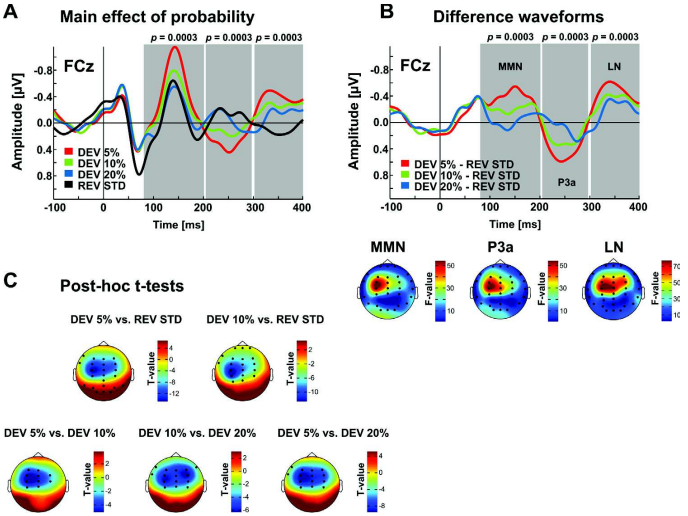

Fig. 3. A) Main effect of stimulus probability on LLR. Grand-average LLRs elicited by reversed-standard condition and deviant stimuli with 5%, 10% and 20% probability, recorded at FCz electrode. The shadowed areas show the three time windows where a significant main effect of probability was found (80–202 ms; 203.5–297 ms; 302–399.5 ms). The topographic maps illustrate the F-values over the scalp in each of the three clusters. Only electrodes for which the F-value was significant are depicted. B) Grand-average difference waveforms. LLR difference waveforms obtained by subtracting the standard response from each of the deviant's, evidences the correspondence of the three significant clusters with MMN, P3a and LN, respectively. C) Post-hoc *t*-tests over first LLR significant time-window (80–202 ms). Deviance detection was observed for the 5% deviant ($p = 0.002$) and the 10% deviant ($p = 0.002$), as well as significant amplitude differences were found among deviant probabilities 5% and 10% ($p = 0.014$), 10% and 20% ($p = 0.002$) and 5% and 20% ($p = 0.002$). The topographic maps illustrate the t-values over the scalp for the significant contrasts. Only electrodes for which the t-value was significant are depicted.

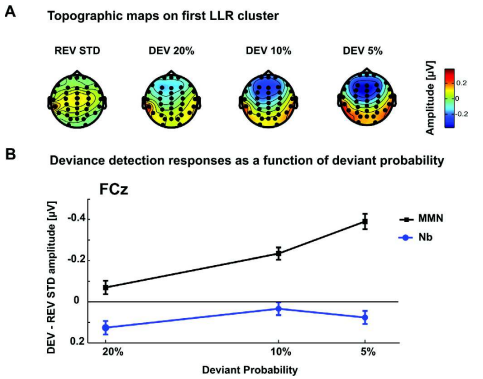

Fig. 4. A) Mean scalp topographies of amplitudes within the first LLR significant cluster (80–202 ms, corresponding to MMN). B) Deviance detection as a function of deviant probability. Mean amplitude of the difference waveforms for Nb (50.5–59.5 ms) and MMN (80–202 ms) components, at FCz electrode, were plotted as a function of deviant stimuli's probability. Probabilities are displayed on the x axis, whereas the y axis shows the mean amplitude of the difference waveforms between responses to deviant and reversed-standard stimuli, both for MMN (black) and Nb (blue) components. Vertical bars show the standard error of the mean (SEM) (for interpretation of the references to colour in this figure legend, the reader is referred to the web version of this article).

MMN latencies the voltage distribution over the scalp varied as a function of the deviant stimulus probability.

Finally, in the time-window of the only cluster with significant F-values in the MLR range (50.5–59.5 ms, roughly corresponding to Nb), and in the time-window of the first cluster with significant F-values in the LLR (80–202 ms, corresponding to MMN, see Fig. 3B), difference waveforms were retrieved at the FCz electrode. For illustration purposes, the mean amplitude of each of these waveforms was then obtained and plotted as a function of deviant stimulus probability (Fig. 4B).

4. Discussion

The present study was an attempt to further characterize the hierarchical organization of auditory novelty system, by testing the responsiveness of the MLR components to manipulations of the deviant stimulus probability, which are known to affect MMN amplitude. Specifically, our hypothesis was that MLR components would respond differently to progressively lower degrees of deviant probability, as it has been described for the MMN in humans and SSA in animals. Our results confirmed deviance detection at the MLR latency range for deviations in spatial location, in agreement with previous findings (Aghamolaei et al., 2016; Cornella et al., 2012; Grimm et al., 2012; Sonnadara et al., 2006b). Furthermore, in the LLR, our results replicated those of previous studies (Evstigneeva & Aleksandrov, 2009; Fisher et al., 2011; Haenschel et al., 2005; Sabri & Campbell, 2001; Sato et al., 2000; Sonnadara et al., 2006a) in finding a significant increase in the amplitude of MMN as a function of decreasing the deviant probability. However, contrary to our hypothesis, we did not observe MLR sensitivity to changes in the deviant stimulus probability, as no significant differences between responses elicited to deviant stimuli of different probabilities were found, neither in the amplitude of components

nor on the pattern of voltage distribution across the scalp. These findings suggest that, while regularity violations are encoded at stages of the auditory pathway eliciting the MLR, only at neural populations of higher stages, such as those generating the MMN, the probability contrast between the regular and the deviant sound is encoded.

4.1. Deviance detection in MLR

The results of the present study revealed an overall deviance-related reduction in the Nb component of MLR, whose neural generators have been found in the anterior rim of HG in a recent MEG study (Recasens, Grimm, Capilla, Nowak & Escera 2012). Such reduction replicates results from Shiga et al. (2015), who also found attenuation of Nb component, for frequency deviants. Additionally, deviance-related enhancement of Nb component has been shown when using deviant stimuli varying from the standard in other simple acoustic features than spatial location, such as frequency (Alho et al., 2012; Grimm et al., 2011; Leung et al., 2012; Recasens et al., 2014) intensity (Althen et al., 2011), or timing (Leung et al., 2013).

Regularity violations in location have been previously found in another MLR component, namely the Na (Cornella et al., 2012; Grimm et al., 2012; Sonnadara et al., 2006b). The apparent dissociation between the present results and those of previous studies could be explained, however, by the different experimental protocols used in all these studies. First, the type of stimuli used (Gaussian white noise bursts, pure tones and click sounds, respectively) were different than ours. Second, the way the location deviance was introduced in the first two studies, by manipulating interaural time difference (ITD) in the deviant tones delivered through headphones, also differed from the one used in the present study. Moreover, Aghamolaei et al. (2016), used a location deviant and the same type of stimulus as the one employed in the present study (chirps), but found MLR correlates of deviance detection in Pa and Pb components. These differences may be due to the different characteristics of our experimental designs: in their study, the deviant stimuli had equal probability in all conditions, but differed from each other in location from which they were presented; in our experiment, however, the deviant stimuli were always presented from the same location, but differed in the probability between conditions. Additionally, in their study multi-oddball paradigm was used, while in our study each deviant probability, for obvious reasons, was presented in a separate block. Furthermore, it has also been proposed that Nb and Pa components could in fact share neural generators (Yoshiura, Ueno, Iramina & Masuda, 1995).

As for the topographical distribution, our results yielded no differential effects of the probability factor among different scalp regions, neither between standard and deviants nor within deviants, thus suggesting that the pattern of voltage distribution across the scalp, as the amplitude of the components, was not affected differently by different deviant probabilities in MLR time-range. In any case, the results of the present study confirm that regularities in the acoustic environment are encoded in neural traces, and that stimuli that do not accommodate to these traces elicit deviant-related responses at early latency ranges in the auditory hierarchy.

4.2. Deviant probability effects on MMN

Significant differences were found between standard and deviant stimuli in the long-latency range (e.g., eliciting the MMN), thus showing deviance detection, as well as an effect of deviant probability manipulations on MMN amplitude. Different theories have been proposed for the sensitivity of MMN to deviant probability. As a deviance detection component, the MMN depends on the development an internal representation of the relationships between discrete sounds in the acoustic environment. Such representation patterns the repetitive attributes of auditory stimulation, which allows the auditory system to generate predictive models of the incoming acoustic information (Winkler, 2007). From that perspective, the decreased MMN amplitude may be interpreted as the consequence of the instability of this regularity template as the probability of the standard stimuli decreases, thus weakening the deviance detection signal (Sabri & Campbell, 2001). A recent study from Sculthorpe and Campbell (2011) supports this interpretation, as they found that increasing the deviant probability does not affect the MMN amplitude when obtained with a paradigm that allows the global rules of the standard sequence to be preserved. However, this phenomenon may also be caused by the ongoing formation of a separated representation of the regularities within deviant stimuli, as these deviant stimuli appear more frequently. Consequently, the two regularity representations could inhibit each other, resulting in the diminished MMN response (Fisher et al., 2011; Ritter et al., 1992; Rosburg, 2004). This last contribution appears to be more decisive, as increasing the number of deviants without altering the standards still affects MMN amplitude (Fisher et al., 2011).

Finally, results from scalp topography analyses indicate that the effect of probability manipulations in amplitude is significantly different over distinct frontal and lateral electrodes, which imply that differences in stimuli probabilities result also in different patterns of voltage distribution across the scalp in MMN, in contrast with MLR.

4.3. Deviant probability effects on MLR: hierarchical interpretation

Even though MLR has been consistently proven to encode for regularities in the acoustic environment, it appears that the MLR generating system is not sensitive to changes in deviant probability. In other words, the results suggest that the MLR generating system is sensitive to regularity violations, but not to the probability with which the encoded regularities are disrupted. Such sensitivity is however present at latter components in the LLR, such as the MMN. We interpret these results as another dissociation between MLR and LLR generating systems that goes in accordance with previous studies from our lab on deviance magnitude (Aghamolaei et al., 2016) or complex regularity violations (Cornella et al., 2012). These studies revealed that only at latter components of the human AEP specific characteristics of the regularity violations, such as the deviance magnitude, can be indexed. The rationale behind the differential sensitivity of MLR and MMN might rely on the fact that at higher levels of the auditory hierarchy the predictive models are complex enough as to encode the deviant stimulus statistics. However, we cannot fully disregard that the MLR deviance-detection system was sensitive to lower probabilities of the deviant (e.g., 3%, 1%) so that a gradual deviant-probability effect would have arisen on the MLR components at these probabilities.

Moreover, a functional dissociation between MLR and MMN would have its corresponding anatomical correlate, as the two neurophysiological responses are elicited by distinct regions in the auditory cortex, from primary to secondary areas (Recasens et al., 2012). From that perspective, our results would go in accordance with Schönwiesner et al. (2007), which revealed that the initial detection of deviance would take place in primary auditory cortex, whereas a more detailed analysis of the acoustic regularities, which, in our case, would correspond to deviance probability, would take place in the posterior superior temporal gyrus and the planum temporale. In summary, our results would reinforce the view that progressively more complex processes in the detection of regularity violations require higher-order regions in the auditory cortex that would elicit latter AEPs components, whereas hierarchically lower

areas, which include some of the known MLR generators, prioritize regularity encoding.

On the other hand, the observed insensitivity of MLR for the probability with which the acoustic regularities are altered is in apparent contradiction with animal studies recording SSA, that have found this effect in structures proposed as neural generators of earlier deviance-detection responses than MMN (Antunes et al., 2010; Malmierca et al., 2009; Patel et al., 2012; Ulanovsky et al., 2003). The differences in brain anatomy and physiology between humans and animals due to evolutionary aspects may account for these contradictory results, as it could be more advantageous for the animal species studied to encode deviant probability very early in the auditory hierarchy. Likewise, the gap between animal and human research, in their methodological approaches and the different characteristics of the phenomena studied (neurophysiological activity of single neurons and large mass potentials at the scalp). Further studies should aim at bridging these gaps in human and animal research towards completing a full picture of the hierarchy of deviance-related responses in the auditory system.

5. Conclusions

The results of the present study established yet another dissociation of middle-and long-latency response generators in their capacity to encode probability contingencies of the soundscape. From a physiological point of view, this suggests that processing deviant probabilities would require higher cerebral resources than the ones in charge of regularity encoding. Further research should address the question of the neurophysiological bases behind this dissociation, as well as the gap between animal and human findings on deviant probability manipulations in anatomically lower structures of the auditory pathway.

Conflict of interests

None.

Acknowledgments

This work was supported by the Spanish Ministry of Economy and Knowledge (PSI2012-37174), the Catalan Government (SGR2014-177), and the ICREA Academia Distinguished Professorship awarded to Carles Escera.

Special thanks to Johanna Frost Nylén, for her help in data collection.

References

Aghamolaei, M., Zarnowiec, K., Grimm, S., & Escera, C. (2016). Functional dissociation between regularity encoding and deviance detection along the auditory hierarchy. *European Journal of Neuroscience*, *43*, 529–535.

Alho, K., Grimm, S., Mateo-León, S., Costa-Faidella, J., & Escera, C. (2012). Early processing of pitch in the human auditory system. *European Journal of Neuroscience*, *36*(7), 2972–2978.

Althen, H., Grimm, S., & Escera, C. (2011). Fast detection of unexpected sound intensity decrements as revealed by human evoked potentials. *PLoS One*, *6*(12), e28522.

Althen, H., Grimm, S., & Escera, C. (2013). Simple and complex acoustic regularities are encoded at different levels of the auditory hierarchy. *European Journal of Neuroscience*, *38*(10), 3448–3455.

Anderson, L. A., Christianson, G. B., & Linden, J. F. (2009). Stimulus-specific adaptation occurs in the auditory thalamus. *Journal of Neuroscience*, *29*(22), 7359–7363.

Antunes, F. M., Nelken, I., Covey, E., & Malmierca, M. S. (2010). Stimulus-specific adaptation in the auditory thalamus of the anesthetized rat. *PLoS One*, *5*(11), e14071.

Bell, S. L., Smith, D. C., Allen, R., & Lutman, M. E. (2004). Recording the middle latency response of the auditory evoked potential as a measure of depth of anaesthesia. A technical note. *British Journal of Anaesthesia*, *92*(3), 442–445.

Brainard, D. H. (1997). The psychophysics toolbox. *Spatial Vision*, *10*, 433–436.

Cacciaglia, R., Escera, C., Slabu, L., Grimm, S., Sanjuán, A., Ventura-Campos, N., et al. (2015). Involvement of the human midbrain and thalamus in auditory deviance detection. *Neuropsychologia*, *68*, 51–58.

Cornella, M., Leung, S., Grimm, S., & Escera, C. (2012). Detection of simple and pattern regularity violations occurs at different levels of the auditory hierarchy. *PLoS One*, *7*(8), e43604.

Cornella, M., Leung, S., Grimm, S., & Escera, C. (2013). Regularity encoding and deviance detection of frequency modulated sweeps: Human middle-and long-latency auditory evoked potentials. *Psychophysiology*, *50*(12), 1275–1281.

Dau, T., Wegner, O., Mellert, V., & Kollmeier, B. (2000). Auditory brainstem responses with optimized chirp signals compensating basilar-membrane dispersion. *Journal of the Acoustical Society of America*, *107*(3), 1530–1540.

Delorme, A., & Makeig, S. (2004). EEGLAB: An open source toolbox for analysis of single-trial EEG dynamics including independent component analysis. *Journal of Neuroscience Methods*, *134*(1), 9–21.

Delorme, A., Sejnowski, T., & Makeig, S. (2007). Enhanced detection of artifacts in EEG data using higher-order statistics and independent component analysis. *Neuroimage*, *34*(4), 1443–1449.

Deouell, L. Y. (2007). The frontal generator of the mismatch negativity revisited. *Journal of Psychophysiology*, *21*(3–4), 188–203.

Elberling, C., Don, M., Cebulla, M., & Stürzebecher, E. (2007). Auditory steady-state responses to chirp stimuli based on cochlear traveling wave delay. *Journal of the Acoustical Society of America*, *122*(5), 2772–2785.

Escera, C., & Corral, M. J. (2007). Role of mismatch negativity and novelty-P3 in involuntary auditory attention. *Journal of Psychophysiology*, *21*(3-4), 251–264.

Escera, C., & Malmierca, M. S. (2014). The auditory novelty system: An attempt to integrate human and animal research. *Psychophysiology*, *51*, 111–123.

Escera, C., Alho, K., Winkler, I., & Näätänen, R. (1998). Neural mechanisms of involuntary attention to acoustic novelty and change. *Journal of Cognitive Neuroscience*, *10*(5), 590–604.

Escera, C., Alho, K., Schröger, E., & Winkler, I. (2000). Involuntary attention and distractibility as evaluated with event-related brain potentials. *Audiology and Neurotology*, *5*(3–4), 151–166.

Escera, C., Yago, E., & Alho, K. (2001). Electrical responses reveal the temporal dynamics of brain events during involuntary attention switching. *European Journal of Neuroscience*, *14*(5), 877–883.

Escera, C., Leung, S., & Grimm, S. (2014). Deviance detection based on regularity encoding along the auditory hierarchy: Electrophysiological evidence in humans. *Brain Topography*, *27*(4), 527–538.

Evstigneeva, M. D., & Aleksandrov, A. A. (2009). Mismatch negativity: The contribution of differences in the refractoriness of stimulus-specific neuron populations. *Neuroscience and Behavioral Physiology*, *39*(9), 833–840.

Farley, B. J., Quirk, M. C., Doherty, J. J., & Christian, E. P. (2010). Stimulus-specific adaptation in auditory cortex is an NMDA-independent process distinct from the sensory novelty encoded by the mismatch negativity. *Journal of Neuroscience*, *30*(49), 16475–16484.

Fisher, D. J., Grant, B., Smith, D. M., & Knott, V. J. (2011). Effects of deviant probability on the 'optimal'multi-feature mismatch negativity (MMN) paradigm. *International Journal of Psychophysiology*, *79*(2), 311–315.

Grimm, S., Escera, C., Slabu, L., & Costa-Faidella, J. (2011). Electrophysiological evidence for the hierarchical organization of auditory change detection in the human brain. *Psychophysiology*, *48*(3), 377–384.

Grimm, S., Recasens, M., Althen, H., & Escera, C. (2012). Ultrafast tracking of sound location changes as revealed by human auditory evoked potentials. *Biological Psychology*, *89*(1), 232–239.

Grimm, S., Escera, C., & Nelken, I. (2016). Early indices of deviance detection in humans and animal models. *Biological Psychology*, *116*, 23–27.

Haenschel, C., Vernon, D. J., Dwivedi, P., Gruzelier, J. H., & Baldeweg, T. (2005). Event-related brain potential correlates of human auditory sensory memory-trace formation. *Journal of Neuroscience*, *25*(45), 10494–10501.

Kleiner M., Brainard D. & Pelli D. (2007). "What's new in Psychtoolbox-3?" Perception 36 ECVP Abstract Supplement.

Leung, S., Cornella, M., Grimm, S., & Escera, C. (2012). Is fast auditory change detection feature specific? An electrophysiological study in humans. *Psychophysiology*, *49*(7), 933–942.

Leung, S., Recasens, M., Grimm, S., & Escera, C. (2013). Electrophysiological index of acoustic temporal regularity violation in the middle latency range. *Clinical Neurophysiology*, *124*(12), 2397–2405.

Malmierca, M. S., Cristaudo, S., Pérez-González, D., & Covey, E. (2009). Stimulus-specific adaptation in the inferior colliculus of the anesthetized rat. *Journal of Neuroscience*, *29*(17), 5483–5493.

Malmierca, M. S., Sanchez-Vives, M. V., Escera, C., & Bendixen, A. (2014). Neuronal adaptation, novelty detection and regularity encoding in audition. *Frontiers in Systems Neuroscience*, *8*, 111.

Manly, B. F. J. (1997). *Randomization, bootstrap and Monte Carlo methods in biology* (2nd ed.).

Maris, E., & Oostenveld, R. (2007). Nonparametric statistical testing of EEG-and MEG-data. *Journal of Neuroscience Methods*, *164*(1), 177–190.

McCarthy, G., & Wood, C. C. (1985). Scalp distributions of event-related potentials: An ambiguity associated with analysis of variance models. *Electroencephalography and Clinical Neurophysiology/Evoked Potentials Section*, *62*(3), 203–208.

Näätänen, R., & Picton, T. (1987). The N1 wave of the human electric and magnetic response to sound: A review and an analysis of the component structure. *Psychophysiology*, *24*(4), 375–425.

Näätänen, R., Gaillard, A. W., & Mäntysalo, S. (1978). Early selective-attention effect on evoked potential reinterpreted. *Acta Psychologica*, *42*(4), 313–329.
Näätänen, R., Sams, M., Järvilehto, T., & Soininen, K. (1980). Probability of deviant stimulus and event-related brain potentials. In R. Sinz, & M. R. Rosenzweig (Eds.), *Psychophysiology* (pp. 397–405). Amsterdam: Elsevier Biomedical Press.
Näätänen, R., Pakarinen, S., Rinne, T., & Takegata, R. (2004). The mismatch negativity (MMN): towards the optimal paradigm. *Clinical Neurophysiology*, *115*(1), 140–144.
Näätänen, R., Paavilainen, P., Rinne, T., & Alho, K. (2007). The mismatch negativity (MMN) in basic research of central auditory processing: A review. *Clinical Neurophysiology*, *118*(12), 2544–2590.
Nelken, I., & Ulanovsky, N. (2007). Mismatch negativity and stimulus-specific adaptation in animal models. *Journal of Psychophysiology*, *21*(3-4), 214–223.
Nordby, H., Roth, W. T., & Pfefferbaum, A. (1988). Event-related potentials to breaks in sequences of alternating pitches or interstimulus intervals. *Psychophysiology*, *25*(3), 262–268.
Oostenveld, R., Fries, P., Maris, E., & Schoffelen, J. M. (2010). FieldTrip: Open source software for advanced analysis of MEG, EEG, and invasive electrophysiological data. *Computational Intelligence and Neuroscience*, *2011*. Article ID 156869.
Opitz, B., Schröger, E., & Von Cramon, D. (2005). Sensory and cognitive mechanisms for preattentive change detection in auditory cortex. *European Journal of Neuroscience*, *21*(2), 531–535.
Pérez-González, D., Malmierca, M. S., & Covey, E. (2005). Novelty detector neurons in the mammalian auditory midbrain. *European Journal of Neuroscience*, *22*(11), 2879–2885.
Paavilainen, P. (2013). The mismatch-negativity (MMN) component of the auditory event-related potential to violations of abstract regularities: A review. *International Journal of Psychophysiology*, *88*(2), 109–123.
Patel, C. R., Redhead, C., Cervi, A. L., & Zhang, H. (2012). Neural sensitivity to novel sounds in the rat's dorsal cortex of the inferior colliculus as revealed by evoked local field potentials. *Hearing Research*, *286*(1), 41–54.
Pelli, D. G. (1997). The Video Toolbox software for visual psychophysics: Transforming numbers into movies. *Spatial Vision*, *10*(4), 437–442.
Picton, T. W., Hillyard, S. A., Krausz, H. I., & Galambos, R. (1974). Human auditory evoked potentials. I: Evaluation of components. *Electroencephalography and Clinical Neurophysiology*, *36*, 179–190.
Recasens, M., Grimm, S., Capilla, A., Nowak, R., & Escera, C. (2012). Two sequential processes of change detection in hierarchically ordered areas of the human auditory cortex. *Cerebral Cortex*, *24*(1), bhs295.
Recasens, M., Grimm, S., Wollbrink, A., Pantev, C., & Escera, C. (2014). Encoding of nested levels of acoustic regularity in hierarchically organized areas of the human auditory cortex. *Human Brain Mapping*, *35*(11), 5701–5716.
Richardson, B. D., Hancock, K. E., & Caspary, D. M. (2013). Stimulus-specific adaptation in auditory thalamus of young and aged awake rats. *Journal of Neurophysiology*, *110*(8), 1892–1902.
Ritter, W., Paavilainen, P., Lavikainen, J., Reinikainen, K., Alho, K., Sams, M., et al. (1992). Event-related potentials to repetition and change of auditory stimuli. *Electroencephalography and Clinical Neurophysiology*, *83*(5), 306–321.
Rivolta, D., Castellanos, N. P., Stawowsky, C., Helbling, S., Wibral, M., Grützner, C., et al. (2014). Source-reconstruction of event-related fields reveals hyperfunction and hypofunction of cortical circuits in antipsychotic-naive, first-episode schizophrenia patients during mooney face processing. *Journal of Neuroscience*, *34*(17), 5909–5917.
Rosburg, T. (2004). Effects of tone repetition on auditory evoked neuromagnetic fields. *Clinical Neurophysiology*, *115*(4), 898–905.
Rupp, A., Uppenkamp, S., Gutschalk, A., Beucker, R., Patterson, R. D., Dau, T., et al. (2002). The representation of peripheral neural activity in the middle-latency evoked field of primary auditory cortex in humans. *Hearing Research*, *174*(1), 19–31.
Saarinen, J., Paavilainen, P., Schöger, E., Tervaniemi, M., & Näätänen, R. (1992). Representation of abstract attributes of auditory stimuli in the human brain. *Neuroreport*, *3*(12), 1149–1151.
Sabri, M., & Campbell, K. B. (2001). Effects of sequential and temporal probability of deviant occurrence on mismatch negativity. *Cognitive Brain Research*, *12*(1), 171–180.
Sato, Y., Yabe, H., Hiruma, T., Sutoh, T., Shinozaki, N., Nashida, T., et al. (2000). The effect of deviant stimulus probability on the human mismatch process. *Neuroreport*, *11*(17), 3703–3708.
Schönwiesner, M., Novitski, N., Pakarinen, S., Carlson, S., Tervaniemi, M., & Näätänen, R. (2007). Heschl's gyrus, posterior superior temporal gyrus, and mid-ventrolateral prefrontal cortex have different roles in the detection of acoustic changes. *Journal of Neurophysiology*, *97*(3), 2075–2082.
Schröger, E., & Wolff, C. (1996). Mismatch response of the human brain to changes in sound location. *Neuroreport*, *7*(18), 3005–3008.
Sculthorpe, L. D., & Campbell, K. B. (2011). Evidence that the mismatch negativity to pattern violations does not vary with deviant probability. *Clinical Neurophysiology*, *122*(11), 2236–2245.
Shestakova, A., Brattico, E., Huotilainen, M., Galunov, V., Soloviev, A., Sams, M., et al. (2002). Abstract phoneme representations in the left temporal cortex: Magnetic mismatch negativity study. *Neuroreport*, *13*(14), 1813–1816.
Shiga, T., Althen, H., Cornella, M., Zarnowiec, K., Yabe, H., & Escera, C. (2015). Deviance-related responses along the auditory hierarchy: Combined FFR, MLR and MMN evidence. *PloS One*, *10*(9), e0136794.
Slabu, L., Escera, C., Grimm, S., & Costa-Faidella, J. (2010). Early change detection in humans as revealed by auditory brainstem and middle-latency evoked potentials. *European Journal of Neuroscience*, *32*(5), 859–865.
Slabu, L., Grimm, S., & Escera, C. (2012). Novelty detection in the human auditory brainstem. *Journal of Neuroscience*, *32*(4), 1447–1452.
Sonnadara, R. R., Alain, C., & Trainor, L. J. (2006a). Effects of spatial separation and stimulus probability on the event-related potentials elicited by occasional changes in sound location. *Brain Research*, *1071*(1), 175–185.
Sonnadara, R. R., Alain, C., & Trainor, L. J. (2006b). Occasional changes in sound location enhance middle latency evoked responses. *Brain Research*, *1076*(1), 187–192.
Ulanovsky, N., Las, L., & Nelken, I. (2003). Processing of low-probability sounds by cortical neurons. *Nature Neuroscience*, *6*(4), 391–398.
Ulanovsky, N., Las, L., Farkas, D., & Nelken, I. (2004). Multiple time scales of adaptation in auditory cortex neurons. *Journal of Neuroscience*, *24*(46), 10440–10453.
Von der Behrens, W., Bäuerle, P., Kössl, M., & Gaese, B. H. (2009). Correlating stimulus-specific adaptation of cortical neurons and local field potentials in the awake rat. *Journal of Neuroscience*, *29*(44), 13837–13849.
Winkler, I. (2007). Interpreting the mismatch negativity. *Journal of Psychophysiology*, *21*(3-4), 147–163.
Yoshiura, T., Ueno, S., Iramina, K., & Masuda, K. (1995). Source localization of middle latency auditory evoked magnetic fields. *Brain Research*, *703*(1), 139–144.
Yvert, B., Fischer, C., Bertrand, O., & Pernier, J. (2005). Localization of human supratemporal auditory areas from intracerebral auditory evoked potentials using distributed source models. *Neuroimage*, *28*(1), 140–153.

STUDY II:

The effects of cTBS on the Frequency-Following Response and other auditory evoked potentials

The effects of cTBS on the Frequency-Following Response and other auditory evoked potentials

Abbreviated title: cTBS and auditory evoked potentials

Author names and affiliations: Fran López-Caballero[a, b], Pablo Martin-Trias[c], Teresa Ribas-Prats[a, b, d], Natàlia Gorina-Careta[a, b, d], David Bartrés-Faz[a,c, e], Carles Escera[a, b, d]

[a] Institute of Neurosciences, University of Barcelona, Catalonia-Spain.

[b] Cognitive Neuroscience Research Group, Department of Clinical Psychology and Psychobiology, University of Barcelona, Catalonia-Spain.

[c] Medical Psychology Unit. Department of Medicine. Faculty of Medicine and Health Sciences. University of Barcelona, Spain.

[d] Institut de Recerca Sant Joan de Déu (IRSJD), Santa Rosa 39-57, 08950 Esplugues de Llobregat, Barcelona, Catalonia-Spain.

[e] Institut d'Investigacions Biomèdiques August Pi i Sunyer (IDIBAPS). Barcelona, Spain.

***Correspondence**: Carles Escera, PhD, Professor. Department of Clinical Psychology and Psychobiology, University of Barcelona. Passeig de la Vall d'Hebron 171, 08035 Barcelona, Catalonia-Spain. Tel: +34 933 125 048, Fax: +34 934 021 584, E-mail: cescera@ub.edu

Abstract

The Frequency-Following Response (FFR) is an auditory evoked potential that follows the periodic characteristics of a sound. FFR measures have proven to be sensitive to cognitive function, including language, learning and attention, as well as to several clinical conditions, such as autism or dyslexia. Despite being a widely studied biosignal in auditory cognitive neuroscience, the neural underpinnings of the FFR are still unclear. Traditionally, FFR has been associated with subcortical activity originating in the inferior colliculi, but recent evidence suggested cortical sources. Moreover, the cortical contribution to the FFR seems to be dependent on the stimulus frequency, being stronger with stimulus frequencies around 100 Hz. In the present study, we combined EEG with an inhibitory Transcranial Magnetic Stimulation (TMS) protocol, the continuous Theta Burst Stimulation (cTBS), to disentangle the cortical contribution to the FFR elicited to stimuli of high and low frequency. We recorded FFR to the syllable /ba/ at two fundamental frequencies (low: 113 Hz; high: 317 Hz) in healthy participants. FFR, Long Latency Response (LLR) and Auditory Brainstem Response (ABR) were recorded before and after real and sham cTBS administration in the right auditory cortex. Results showed that cTBS on the right auditory cortex did not produce a significant change in the FFR recorded, neither with low nor with high frequency stimulation. No effect was observed in the ABR and LLR components, despite LLR known contributions from auditory cortex. A follow up experiment confirmed that the lack of positive findings on LLR in the original study was not due to the reduction of the cTBS inhibitory effects with time. Possible reasons behind the negative results are discussed, including the inefficacy of cTBS when targeting the auditory cortex, compensatory mechanisms from the non-targeted areas and intraindividual variability of the cTBS effectiveness.

Keywords: Frequency-Following Response, Neural generators, Auditory Cortex, Transcranial Magnetic Stimulation, continuous Theta Burst Stimulation, Long-Latency Potentials

1. Introduction

The Frequency-Following Response (FFR) is a sustained evoked potential recorded with electroencephalography (EEG) that mimics the periodic features of the auditory stimulus waveform. It appears after the transient waves V and A of the phasic Auditory Brainstem Response (ABR), for which it is sometimes described as the sustained part of the ABR (Skoe and Kraus, 2010). FFR is thought to reflect phase-locked neural activity of the auditory system to the spectral and temporal components of the acoustic signal (Krishnan et al., 2004; Chandrasekaran and Kraus 2010; Skoe and Krauss, 2010), and can be elicited by different types of stimulus; such as pure tones, vowels or syllables. Moreover, it is sensitive to both the fine structure and the envelope of the signal. Given the properties of the FFR, it has been widely studied in the field of auditory neuroscience, and is considered a useful noninvasive tool to explore the neural mechanisms behind the representation of incoming sounds in the hearing brain.

FFR has been shown to be sensitive to different phenomena related with auditory perception and, in turn, to higher-level processing of language and music. This includes speech-in-noise perception (Chandrasekaran, Skoe and Kraus, 2014; Du et al., 2011), pitch discrimination training (Carcagno and Plack, 2011), rapid auditory

learning (Skoe, Krizman, Spitzer and Kraus, 2013), language experience and bilingualism (Kraus and Chandrasekaran, 2010; Krishnan et al., 2005; Krizman et al. 2012), musical training (Bidelman, 2013; Bidelman and Alain, 2015; Parbery-Clark et al. 2011; Skoe and Kraus, 2012), as well as age-related changes in auditory abilities (Anderson, White-Schwoch, Parbery-Clark and Kraus, 2013; Bidelman, Villafuerte, Moreno and Alain, 2014a). Moreover, FFR is sensitive to task-related attention (Hairston, Letowski and McDowell, 2013), stimulus probability (Skoe, Chandrasekaran, Spitzer, Wong and Kraus, 2014), and modulated by processes of regularity encoding, temporal predictability (Gorina-Careta, Zarnowiec, Costa-Faidella and Escera, 2016) and deviance detection (Slabu, Grimm and Escera, 2012; Escera, 2017). On the other hand, FFR has been shown to be affected in several clinical conditions, such as hearing impairment (Bellier, Veuillet, Vesson, Bouchet, Caclin and Thai-Van, 2015), language impairment (Rocha-Muniz, 2012), reading disorders (Billiet and Bellis, 2011; Chandrasekaran, Hornickel, Skoe, Nicol and Kraus, 2009) or Mild Cognitive Impairment (Bidelman et al., 2017). Furthermore, on the genetic aspects of the FFR, the involvement of the serotonin transporter expression has been revealed (Selinger, Zarnowiec, Via, Clemente and Escera, 2016).

To date, the neural generators of the FFR remain under debate. Yet, in order to properly interpret the results obtained by the studies mentioned above, it is critical to elucidate the contributions from different cerebral structures to the scalp-recorded signal. Traditionally, converging evidence from human and animal studies pointed to a subcortical origin of the FFR. Human EEG studies have shown that a high number of averages is needed to obtain a reliable response, suggesting a recording site far away from the generators, and human lesion studies revealed no FFR obtained from patients with upper brainstem lesions (Sohmer and Pratt, 1977). Additionally, evidence from source reconstruction techniques with EEG revealed major contributions to the FFR from the midbrain (Bidelman, 2015b). In line with the research conducted with humans, animal studies, using single-unit recordings, have shown that early auditory structures represent the incoming stimuli with high precision (Langner, 1992; Nelken, 2004), resembling FFR characteristics. Moreover, first spike latencies in the inferior colliculus (IC) of cat align with the onset latency of the FFR (Schreiner and Langner, 1988), with a phase correspondence between FFR and single unit activity in the cochlear nucleus and superior olivary complex (Marsh, Brown and Smith, 1974). Still in cats, cryogenic cooling of the IC was shown to reduce the FFR (Smith, Marsh and Brown, 1975). Gardi, Merzenich and McKean (1979) concluded that, in that species, ~95% of the scalp-recorded FFR can be attributed to activity from the cochlea, the cochlear nuclei and the superior olivary nuclei. Furthermore, in awake monkeys, the upper phase-locking limit in cortical neurons was shown to be of ~100 Hz (Steinschneider, Arezzo and Vaughan, 1980; Steinschneider, Fishman and Arezzo, 2008), way below the phase-locked activity recordable with FFR (e.g., Aiken and Picton, 2008), thus disregarding cortical contribution to the FFR.

Despite all of the evidence pointing to a subcortical origin of the FFR, in a recent human study using magnetoencephalography (MEG) a strong cortical contribution was found from FFRs recorded to speech syllables of 98 Hz fundamental frequency (F0), especially in the right hemisphere (Coffey, Chepesiuk, Herholz, Baillet and Zatorre,

2016). Such results would help re-interpreting the already mentioned findings of FFR modulation by factors theoretically associated with cortical plasticity, such as musical training or bilingualism. However, a crucial aspect arises when interpreting results in FFR studies, and that is the frequency of stimulation used, given the mentioned phase-locking limit of cortical neurons found in monkeys (~100 Hz). Notably, as discussed in Joris, Schreiner and Rees review (2004), phase-locking capacities of neurons along the auditory pathway are progressively reduced from brainstem to cortical levels, reaching the ~100 Hz limit at the cortex. Theoretically, this would imply that FFR sources vary depending on the frequency of the stimulus, and that FFR recorded to stimuli with frequencies above 100 Hz should be free of cortical contributions. To address these questions, a recent study by Bidelman (2018) applied source reconstruction techniques with EEG, using different stimulus frequencies, and found major contributions from the bilateral auditory nerve and the IC to all stimulus frequencies tested, as well as contributions from the primary auditory cortex (PAC) restricted to frequencies below 150 Hz.

Importantly, both EEG and MEG spatial resolution is low, since the signal recorded at the sensor level is the result of overlapping brain signals from different anatomical sites, and source reconstruction techniques have limitations, as they require to solve an inverse problem with infinite possible solutions (Mahjoory, Nikulin, Botrel, Linkenkaer-Hansen, Fato and Haufe, 2017). Given these limitations, in the present study we addressed the question of the anatomical sources of the FFR from a different perspective, trying to complement findings from inverse solution methods. Instead of reconstructing the sources from the scalp-recorded signal, we recorded FFR before and after a transient inactivation of the right auditory cortex, by means of the repetitive Transcranial Magnetic Stimulation (rTMS) patterned protocol known as continuous Theta Burst Stimulation (cTBS; Huang et al., 2005). The cTBS protocol can modulate cortical excitability producing long-term depression like phenomena, resulting in a downregulation of the cortical activation of the targeted region (e.g., Tupak et al., 2013). Using the measurable output of motor evoked potentials, a recent meta-analysis showed that the inhibitory post-effects of cTBS may remain significant after 60 minutes of stimulation, depending on the protocol employed (Chung, Hill, Rogasch, Hoy and Fitzgerald, 2016). In addition, neuronavigated rTMS has been successfully applied in a safe and precise manner to target primary (e.g., Schecklmann et al., 2016) and secondary (e.g., Slotema, Blom, van Lutterveld, Hoek and Sommer, 2014) auditory cortices.

The goal of the present study was hence to disentangle whether the right auditory cortex contributes to the scalp-recorded FFR, as well as to test whether this potential contribution is dependent on the frequency of the stimulus used to elicit the FFR (low, 113Hz; or High, 317 Hz). Our theoretical prediction was that FFR elicited to the low frequency would be modulated by the transient inactivation of the right auditory cortex with cTBS, whereas FFR to the high frequency would remain unaffected. As control conditions in our design, we also assessed whether the transient inactivation of the right auditory cortex would affect the Auditory Brainstem Response (ABR) and Long Latency Responses (LLR), to confirm whether cTBS in that area would induce changes in cortical evoked potentials, while not affecting subcortical ones (ABR).

2. Materials and Methods

2.1. Participants

Twenty participants (11 males), ranging in age from 18 to 34 years (mean = 24.3; standard deviation = 4.2), were included in the study, recruited among University of Barcelona students. All included participants, but one, were naïve to previous TMS administration and right handed (Edinburgh Handedness Inventory >40) to minimize variability in the localization of language areas (Knecht et al., 2000) and avoid a potential confound with our target area with cTBS. Exclusion criteria included history of neurologic or psychiatric condition, abnormal MRI structural measurements and abnormal hearing thresholds. A pure-tone audiometry (frequency range: 250-4000 Hz), using audiometric Beyerdynamic DT48-A headphones (Heilbronn, Germany), was performed for each participant at the screening session and before each experimental session, ensuring mean hearing thresholds below 20 dB NHL at each ear. In accordance with TMS safety guidelines (Rossi et al., 2009), pregnancy, previous history of losing consciousness, prior experience of a seizure or diagnosis of epilepsy were also among the exclusion criteria. In addition, participants with more than five years of musical training in the last five years before the study were also discarded, as musical training is known to modulate the FFR (e.g., Skoe and Kraus, 2012). Furthermore, in screening sessions, five participants were discarded due to hardly detectable FFRs, two due to the presence of post-auricular muscle response (PAM) artifact, and two decided not to participate in the study as they considered the cTBS pulse to be annoying. The experimental protocol was approved by the Bioethics Committee of the University of Barcelona and was in accordance with the WMA Declaration of Helsinki Ethical Principles for Medical Research Involving Human Subjects. At the beginning of the screening session, written informed consent was obtained from each participant after all the details of the research (except the hypotheses) were explained to them, including the characteristics of the EEG, MRI and TMS methods and the possibility to withdraw from the experiment at their wish. Upon completion of the four sessions of the study, they were compensated by monetary payment with 80€.

2.2. Procedure and experimental design

The study was conducted in four sessions for each participant, in separate days: screening session, MRI session and two experimental sessions (Sham and Active). The order of Sham and Active sessions was counterbalanced across participants, and they were separated by a minimum of 2 days and a maximum of 7 (study design represented in Figure 1A). During the screening session, after the audiometry, FFR and LLR recordings were obtained from each participant, ensuring FFR to both low and high frequency stimuli could be detected as well as the absence of PAM response. Because of our EEG acquisition montage, PAM response could not be cleaned in our data. Thus, it was crucial to identify participants displaying this kind of artifact beforehand. During the screening session also, we determined rMTH and aMTH for each participant, using a template MRI for neuronavigation, and applied a maximum of 4 seconds of the cTBS protocol placing the coil in the approximate position of the head where it would be placed in the experimental sessions (T4 electrode location according to the 10-20 EEG electrode system). With this, we aimed to allow participants to familiarize with the TMS before the real experiment and to let us know how much discomfort it produced due to the proximity of the coil to

the ear and ocular nerves. During the MRI session, the structural MRI from each participant were acquired. Participants who were already in possession of their structural MRI did not participate in this session. Sham and Active experimental sessions were identical except for the coil with which the cTBS pulse was applied, either the real one or the sham. In these sessions, after the audiometry, rMTH and aMTH were determined for each participant. Then, Baseline and Post EEG recordings were performed and, in between the two, the cTBS pulse was applied at the target coordinates of stimulation for each participant. Neuronavigation in experimental sessions was performed using participant's MRI. Both Baseline and Post EEG recordings consisted on two FFR blocks, one for each stimulation frequency, followed by the click ABR and the chirp LLR blocks. The FFR recordings of each stimulus frequency were divided in two separate blocks of 1000 sweeps each and interspersed between frequencies. Moreover, the starting frequency of the recordings (low or high) was counterbalanced across participants. With this, we avoided FFRs to a particular frequency to be more affected by the cTBS pulse, as inhibitory cTBS effects fade away with time (Chung, et al., 2016). During EEG recordings, participants were seated comfortably and instructed to perform a visual no go-go task while listening to the sounds, ensuring they were not paying attention to the auditory stimuli (minimum of 80% hit rate in the visual task). The task consisted on the random presentation of numbers from 2 to 9, with a SOA jittered between 850 and 1100 ms. During the visual task, participants had to press ENTER key as fast as possible when the same number appeared twice in succession (20% times). The visual task was concurrent with every EEG block, so the duration of the task was dependent on the duration of the EEG block. Participants were asked to refrain from alcohol intake and from taking any drugs during the 24 hours before any of the four sessions of the study. All sessions but the MRI one were held at the premises of the Medical Psychology Unit, located in the Faculty of Medicine and Health Sciences of the University of Barcelona.

2.3. Stimuli

For FFR recordings, the stimulus was the consonant-vowel (CV) syllable /ba/, created with the Klatt-based synthesizer (Klatt, 1976). The syllable duration was 170 ms, with 10 ms onset period, 45 ms consonant transition and 115 ms steady state part, corresponding to the vowel. The fundamental frequency (F0) was modified with Praat 6.0.10 software (Boersma, 2001; Boersma & Weenink, 2016) to create syllables with F0 of 113 Hz (low frequency) or 317 Hz (high frequency) (Figure 1B). The choice of these frequencies was performed on purpose to avoid contamination with harmonics of the 50 Hz electric line in Europe. During the consonant transition, first (F1) and second (F2) formants rise from 737 Hz to 842 Hz and from 1436 Hz to 1650 Hz, respectively. In the steady state part, both formants remain constant. Third formant (F3) stays at 3170 Hz along all syllable duration. Syllables were presented at 85 dB SPL with a Stimulus Onset Asynchrony (SOA) of 270 ms.

For ABR recordings, the stimulus was a 0.1 ms squarewave click, following recommended standards (American Neurophysiology Society, 2006). The stimulus was included in the default sound database of SmartEP platform (Intelligent Hearing Systems, Miami, Fl, EEUU). Clicks were presented at 85 dB SPL with a SOA of 52 ms.

For LLR recordings, the stimulus was an up-chirp (Dau, Wegner, Mellert & Kollmeier 2000; Figure 1C), with a length of 16.7 ms. It was created using MATLAB software (The Mathworks, Inc., Natick, MA) and the Psychophysics Toolbox extensions (Brainard, 1997; Kleiner, Brainard and Pelli, 2007) by summing rising harmonic series of cosine waveforms from 50 to 8000 Hz, in accordance with Elberling, Don, Cebulla and Stürzebecher study (2007). Chirps were presented at 70 dB SPL with a SOA of 500 ms.

All stimuli were presented to both ears, with alternating polarities and using Etymotic shielded insert earphones of 300 ohms (Etymotic Research, Inc., Elk Grove Village, IL, USA).

2.4. MRI acquisition

The anatomical Magnetic Resonance Imaging (MRI) session took place at the Department of Diagnostic Imaging of Sant Joan de Déu Hospital (Barcelona, Spain). 3D structural datasets were acquired (T1 sequences, 240 slices, slice thickness of 1 mm) using a 1.5T MRI scanner (Ingenia, Philips Medical Systems, Netherlands). Six participants of the sample were already in possession of their structural MRI from either a clinical examination or a previous study, and voluntarily provided it for the purposes of the study. Quality standards of all structural MRI were of sufficient quality for the purpose of TMS neuronavigation.

2.5. Neuronavigated TMS protocol

TMS was delivered with an eight-shaped coil using MagPro X100 magnetic stimulator (MagVenture A|S, Denmark). In all experimental sessions, stimulation was neuronavigated with a stereotactic system (eXimia Navigated Brain Stimulation, Nexstim, Finland) using individual MRI acquisition. Resting and active Motor Thresholds (rMTH and aMTH, respectively) were determined for each participant before cTBS was applied. To do this, single TMS pulses were applied in the area of the right M1 cortical region corresponding to the left first dorsal interosseous (FDI) muscle, while motor evoked potentials (MEPs) were monitored through a pair of Ag-AgCl surface electrodes in a belly-tendon montage, using AcqKnowledge 4.2 software and BIOPAC MP150 system (Biopac Systems Inc., Goleta, CA, USA). Single pulses were administered starting at intensities corresponding to 35% of stimulator output capacity and increased in steps of 5% until reaching rMTH and aMTH values (Rossini et al., 2015). rMTH was defined as the minimum stimulus intensity that elicited at least 5 out of 10 consecutive MEPs of at least 50 μv peak-to-peak amplitude, whereas aMTH was defined as the minimum stimulus intensity that elicited at least 5 out of 10 consecutive MEPs of at least 200 μv peak-to-peak amplitude during FDI soft contraction (approximately 20% of maximum muscle contraction).

cTBS protocol consisted in the repeated application of triplets of pulses (bursts) at 50 Hz, with an inter-train interval (ITI) of 200 ms (5 Hz; theta), during 40'' (200 triplets, 600 pulses in total, Figure 1D), and its administration intensity corresponds to 80% of aMTH (Huang et al., 2005) . This protocol has been described to produce a long-lasting (20-30 min) reduction in cortical excitability (Chung et al., 2016) and has been previously used to target primary auditory cortical areas (Schecklmann et al., 2016). The target location for the cTBS pulse was the right primary auditory cortex, Montreal Neurological Institute (MNI) coordinates (x, y, z) of 50, -21, 7. The coordinates of the stimulation target were defined individually

by transforming them into the participant's native MRI space, using MNI template-to-native transformation matrix with FSL software (Figure 1E). In two participant's MRIs the transformation matrix was not properly implemented, as checked by visual inspection, and thus the target location was defined manually conforming to MRI-determined landmarks for Heschl's gyri (Abdul-Kareem and Sluming, 2008). The coil was held tangentially to the skull, with the coil handle positioned upwards, as described in previous studies targeting auditory cortex with TMS (e.g., Schecklmann et al., 2016). For sham stimulation, a sham coil was used, mimicking the clicking sound of each TMS pulse. All TMS procedures were performed following international safety recommendations (Rossi et al., 2009), including cTBS only delivered in one single cerebral hemisphere, and the use of earplugs during cTBS.

Figure 1 (next page). (A) Experimental design. **(B)** Stimulus waveform for the syllable /ba/ of low frequency (F0: 113 Hz; top) and of high frequency (F0: 317 Hz; bottom), used to elicit the FFR **(C)** Stimulus waveform for the up-chirp (Dau et al., 2000), used to elicit the LLR. **(D)** Representation of the continuous Theta Burst Stimulation (cTBS) TMS protocol. Three pulses at 50 Hz (bursts) presented every 200 ms during 40'' (600 pulses in total). **(E)** example of target coordinates for the cTBS pulse in a participant's MRI. Right primary auditory cortex MNI coordinates (x, y, z) of 50, -21, 7, transformed into participant's native MRI space.

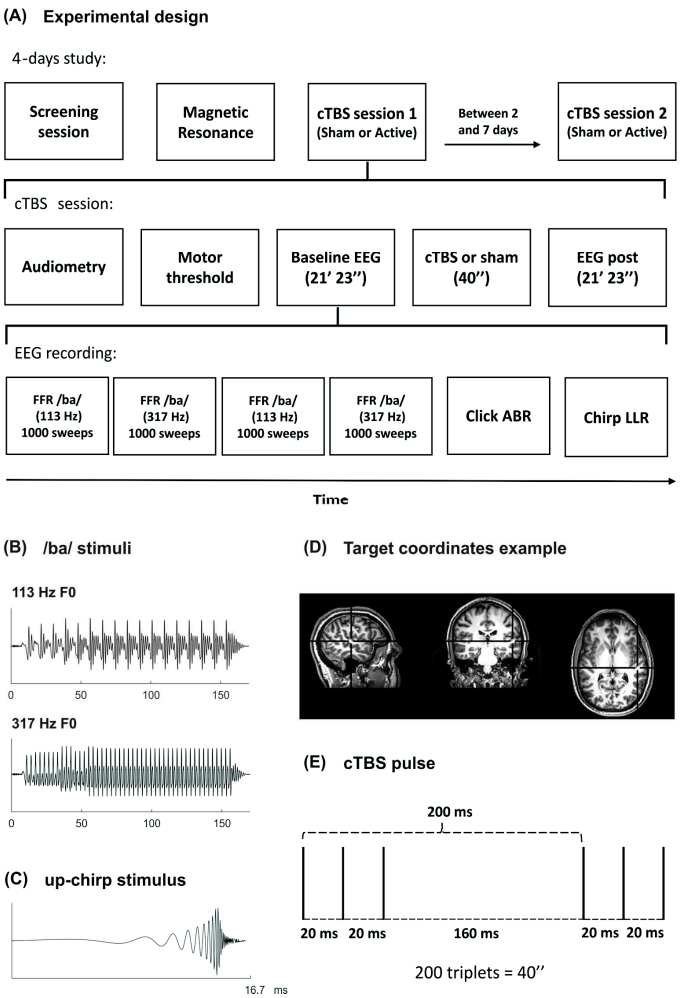

Image: Original figure created by the author

2.6. EEG acquisition

EEG recordings were performed using SmartEP platform with cABR and Advanced Hearing Research modules (Intelligent Hearing Systems, Miami, F1, EEUU). Disposable snap Ag/AgCl electrodes were used, with one active electrode located at Cz according to 10-20 EEG electrode system, a reference electrode placed at the left earlobe, and a ground electrode at the forehead. In four participants reference electrode was placed at left mastoid instead, but the protocol was later changed to use left earlobe due to the reduced probability of obtaining PAM artifact with this reference. Nevertheless, none of these four participants had PAM artifact and their EEG recordings were comparable to the rest of the sample. During the recordings, a tubular elastic net was placed on participant's head to help the fixation of the Cz electrode. All impedances were kept below 5kΩ.

The duration of the stimulation blocks was automatically adjusted until the total number of intended artifact-free sweeps were obtained per block and participant. Overall, the number of rejected-artifacts per block and participant was below 10%. In all EEG recordings, data was acquired with alternating polarities which were then averaged together (Aiken and Picton, 2008).

For FFR recordings, 2000 artifact-free sweeps (in two blocks of 1000 sweeps) were acquired for each stimulation frequency (Low and High), with a sampling rate of 13,333 Hz. Data was online band-pass filtered from 70 to 1500 Hz, and the amplitude rejection criteria was +/- 30 μV. Data was epoched in time windows from -40.88 to 229.35 ms (baseline corrected).

For ABR recordings, 2000 artifact-free sweeps were acquired, with a sampling rate of 40,000 Hz. Data was online band-pass filtered from 100 to 3000 Hz, and the amplitude rejection criteria was +/- 30 μV. Data was epoched in time windows from -10.9 to 40.9 (baseline corrected).

For LLR recordings, 200 artifact-free sweeps were acquired, with a sampling rate of 6,666 Hz. Data was online band-pass filtered from 1 to 30 Hz, and the amplitude rejection criteria was +/- 80 μV. Data was epoched in time windows from -100.88 to 399 ms (baseline corrected).

2.7. EEG analysis

Data from Cz electrode was analyzed using MATLAB software (The Mathworks, Inc., Natick, MA, USA). Average waveforms for FFR, ABR and LLR measures were obtained per participant, session (Sham or Active), measurement (Baseline or Post cTBS) and, in the case of FFR, frequency (low or high). FFRs from the two FFR blocks of 1000 sweeps each were averaged into a single FFR, separately for each frequency.

For the FFRs, different measures from both the time domain and the frequency domain were obtained, separately for each stimulus frequency, trying to portrait different aspects of this response as described in a recent study from our laboratory (Ribas-Prats et al., 2019). In that study, a detailed description on the aspects of the signal that each of these measures describe, as well as the way they were calculated, can be found. In the time domain, first, the stimulus-to-response cross-correlation (*Pearson's r*) was calculated (Russo et al., 2004), yielding the magnitude of the first maximum cross-correlation value and its associated stimulus-to-response delay (neural lag). Second, the signal-to-noise ratio (SNR; Liu et al., 2015) with root-mean-square amplitude (μV) was

calculated in three time-windows of the FFR corresponding to the consonant transition (10-55 ms) and vowel (55-170 ms) sections of the syllable /ba/, as well as to the whole stimulus (0-170 ms), considering a baseline from -40 to 0 ms. To calculate SNR, consonant transition, vowel and whole stimulus sections in the FFR were defined individually for every participant accounting for the neural lag obtained from the stimulus-to-response cross-correlation. Third, a sliding time-window autocorrelation was computed, from which pitch error (Hz) and pitch strength (*Pearson's r*) measures were extracted. To analyze FFRs in the frequency domain, a Fast-Fourier Transform (FFT), hanning windowed, was computed over the three time-windows previously defined (consonant transition, vowel and whole stimulus), again, adjusted accounting for the individual neural lag. From the resulting spectra, first, amplitude values (μV/Hz) within a window of 10 Hz surrounding the F0 of the stimulus were retrieved (e.g., 108-118 for Low frequency stimulus). Second, SNR were calculated by dividing the mean amplitude over the 10 Hz window at F0 peak by the noise on the peak flanks. This noise was calculated as the mean amplitude of two 10 Hz windows at each side of the peak, separated by 20 Hz from the peak frequency window. All FFR analyses were performed with scrips developed in our laboratory based on analysis routines provided by Intelligent Hearing Systems (Miami, Fl, EEUU).

For the ABRs, mean amplitude values (μV) of wave V were retrieved, defining a time window from 5 to 6.5 ms from sound onset. For the LLRs, amplitude analyses were performed over three different components, P50 (30 to 50 ms), N1 (70 to 110 ms) and P2 (120 to 160 ms). For both ABR and LLR analyses, time windows were defined based on peak values of the analyzed components on the grand-average waveforms.

2.8. Statistical analysis

Repeated measures ANOVA were performed separately for each of the FFR measures, the ABR wave 5 mean amplitudes, as well as P50, N1 and P2 mean amplitudes of LLR. For FFR measures, a three-way repeated measures ANOVA was performed, with the three levels being Session (Sham, Active), Measurement (Baseline, Post) and Frequency (Low, High). For ABR and LLR measures, a two-way repeated measures ANOVA was performed instead, with the two levels being Session and Measurement. For each of these comparisons, effect sizes were obtained using partial eta-squared and, whenever the assumption of sphericity was violated, degrees of freedom were corrected using *Greenhouse-Geisser* estimates.

Given our hypothesis, with these statistical comparisons, first, we expected a triple interaction between Session, Measurement and Frequency levels in the FFR, with statistically significant differences between Baseline and Post measurements only occurring in the Active session and for the Low frequency condition. Second, we did not expect interactions between Session and Measurement levels in the ABR, thus confirming no effect of cTBS at the brainstem level. Third, we expected an interaction between these two levels in the LLR components, with these cortical components only differing between Baseline and Post measurements in the Active session.

Additional statistical comparisons were computed in FFR, ABR and LLR measures. Specifically, we computed effect sizes between Baseline and Post measurements, separately for Active and Sham sessions

and, in the case of FFR, separately for each frequency of stimulation as well. We did so by using *Cohen's* d_{rm} as suggested by Lakens (2013). The formula used was as follows:

$$Cohen's\ d_{rm} = \frac{M_{diff}}{\sqrt{SD_1^2 + SD_2^2 - 2 \times r \times SD_1 \times SD_2}} \times \sqrt{2 \times (1-r)}$$

M_{diff} is the difference between the mean (M) of the difference scores and the comparison value m (e.g., 0) and r is the correlation between measures. Confidence intervals (CI) for each effect size are reported. The CI provides information about the precision of an estimate and its potential generalizability or replicability (Banjanovic and Osborne, 2016). We used the bias-corrected and accelerated bootstrap (BCa) method with the matlab function bootci (DiCicio and Efron, 1996; Efron and Tibshirani, 1993). First, the effect size is computed in each of the 10,000 replications of the original sample. Next, the resulting bootstrap distribution is corrected for bias (i.e., skew) and acceleration (i.e., nonconstant variance). Finally, the lower and upper bound of the CI is found at the 0.025 and 0.975 quantiles of the corrected distribution.

3. Results

3.1. FFR

Grand-average FFRs are shown in Figure 2A. FFRs to both low and high frequency stimuli were obtained, with a clear spectral peak at stimulus F0 (Figure 2B). For the low frequency stimulus, harmonics of the F0 can also be observed. For illustrative purposes, spectra shown were calculated over the FFR section corresponding to the vowel part of the stimuli (65 to 180 ms, assuming 10 ms of neural lag; shaded area in plots from Figure 2A).

Statistical comparisons of the time domain SNR revealed a main effect of Frequency factor in all three sections of the FFR (Transient, $F_{(1,19)} = 69.53$, $p < 0.001$, $n_p^2 = 0.785$; Constant, $F_{(1,19)} = 60.27$, $p < 0.001$, $n_p^2 = 0.760$; Total, $F_{(1,19)} = 72.23$, $p < 0.001$, $n_p^2 = 0.792$), indicating the magnitude of the neural activity relative to the baseline was larger for FFR elicited to low-frequency stimuli. Moreover, overall differences in time domain SNR were found also between Baseline and Post EEG measurements in the consonant transition section of the FFR (Table 1), indicating the magnitude of the neural activity relative to the baseline changed across measurements. However, such difference was independent of the Session and Frequency factors, and therefore it could not be attributed to the cTBS pulse. Such differences were also found for the total section of the FFR, but these did not survive for multiple comparison correction. For the mean spectral amplitude at the FFR F0, again, statistical comparisons revealed a main effect of Frequency in all three sections of the FFR (Transient, $F_{(1,19)} = 37.96$, $p < 0.001$, $n_p^2 = 0.666$; Constant, $F_{(1,19)} = 23.38$, $p < 0.001$, $n_p^2 = 0.552$; Total, $F_{(1,19)} = 35.45$, $p < 0.001$, $n_p^2 = 0.651$), with higher spectral amplitudes in FFR to the low frequency stimulus. Such effect was not found, as expected, when computing the spectral SNR (Transient, $F_{(1,19)} = 1.080$, $p = 0.312$, $n_p^2 = 0.054$; Constant, $F_{(1,19)} = 0.871$, $p = 0.363$, $n_p^2 = 0.044$; Total, $F_{(1,19)} = 0.669$, $p = 0.424$, $n_p^2 = 0.034$). No significant effects in Session or Measurement factors, or in their interaction, were found for F0 mean spectral amplitude values or spectral SNR, as shown in Table 1, thus suggesting no effect of the cTBS pulse in these FFR measures neither. To test more precisely whether the lack of effects in FFR measures would be expected in the population, comparisons between Baseline and Post values in these measures

were performed by computing *Cohen's d* and confidence intervals (CI) associated. Such analyses confirmed no effects in the main comparisons of interest given our hypothesis (i.e., Active sessions and FFR to low frequencies). Specifically, when comparing time domain SNR values from the total section of the FFR (Active Low Baseline vs Post: d = -0.054, CI [-0.050 0.366]), small size effects were obtained, as well as confidence intervals including 0, thus suggesting the lack of effect at the population level. Same results were obtained for mean spectral amplitude at F0 (Active Low Baseline vs Post: d = 0.033, CI [-0.53 0.44]) as well as in spectral SNR (Active Low Baseline vs Post: d = -0.155, CI [-0.61 0.25]).

Figure 2. Time domain FFRs (μV) **(A)** and FFR spectra (μV/Hz) **(B)** elicited to syllable /ba/ with Low (113 Hz, top) and High (317 Hz, bottom) F0, in Sham (left side) and Active (right side) sessions. In blue, baseline FFR recordings before the cTBS pulse. In orange, Post cTBS FFR recordings. Shaded areas (65-180 ms) in time-domain FFRs represent time-windows of the response corresponding to the vowel section of the stimulus, assuming 10 ms of neural lag, from where spectra were calculated for illustrative purposes. All recordings were obtained at Cz electrode.

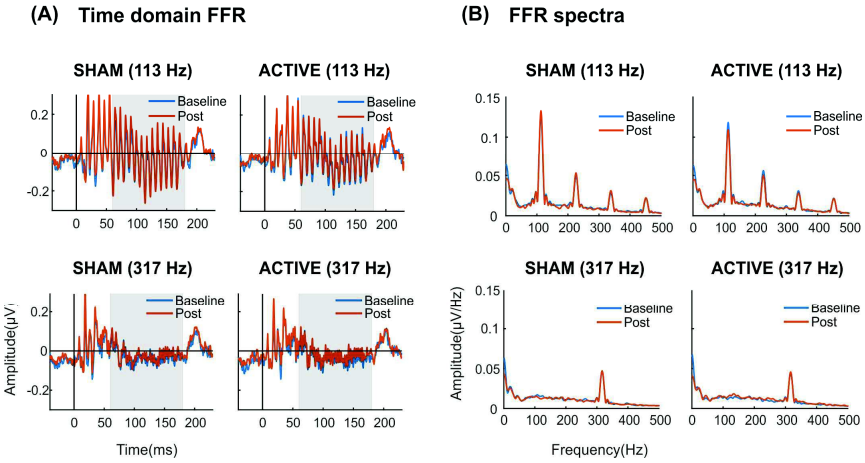

Image: Original figure created by the author

Table 1. Results of repeated measures ANOVA on FFR measures: time domain SNR with root-mean-square amplitudes (SNR time domain; TD), mean spectral amplitude of peak at F0 (F0 amplitude; μV/Hz) and SNR comparing spectral peak at F0 with its flanks (SNR spectral). Each measure was calculated at three time-windows of the FFR corresponding to different sections of the stimulus: consonant transition (10-55 ms), vowel (55-170 ms) and whole stimulus (0-170-ms), adjusted for each participant accounting for the individual neural lag. Session factor includes Sham and Active levels, Measurement factor includes Baseline and Post levels, and Frequency factor includes Low and High frequency levels. Session and Measurement factors, the interaction between them (Ses*Meas) and a thriple interaction between Session, Measurement and Frequency (Ses*Meas*Freq) are reported. For each factor and their interaction, F and p values are presented (degrees of freedom: 1,19) along with effect sizes (n_p^2). p values below 0.05 are highlighted.

FFR statistics	**Transient**			**Constant**			**Total**		
	F	p	n_p^2	F	p	n_p^2	F	p	n_p^2
SNR TD									
Session	1.649	0.215	0.080	0.341	0.566	0.018	0.000	0.988	0.000
Measurement	19.16	**< 0.001**	0.502	0.881	0.360	0.044	4.688	**0.043**	0.198
Ses*Meas	3.636	0.072	0.161	0.127	0.725	0.007	0.989	0.332	0.049
Ses*Meas*Freq	0.234	0.634	0.012	0.610	0.444	0.031	0.394	0.538	0.020
F0 amplitude									
Session	0.400	0.535	0.021	0.464	0.504	0.024	0.155	0.698	0.008
Measurement	0.659	0.427	0.034	0.007	0.936	0.000	0.020	0.889	0.001
Ses*Meas	0.566	0.461	0.029	0.219	0.645	0.011	0.538	0.472	0.028
Ses*Meas*Freq	2.005	0.173	0.095	0.185	0.672	0.010	0.496	0.490	0.025
SNR spectral									
Session	0.020	0.890	0.001	0.008	0.929	0.001	0.032	0.860	0.002
Measurement	1.194	0.288	0.059	0.343	0.565	0.018	0.180	0.676	0.009
Ses*Meas	0.286	0.599	0.015	1.727	0.204	0.083	0.459	0.506	0.024
Ses*Meas*Freq	2.149	0.159	0.102	1.985	0.175	0.095	2.392	0.138	0.112

*p values in the table are non-corrected for multiple comparisons

Grand-average spectrograms were also computed for illustrative purposes (Figure 3A and 3B), where maximum amplitudes can be observed at frequencies corresponding to syllables F0 along the duration of the stimuli. Observable harmonics are also present in the FFR to low frequencies. Moreover, autocorrelogram plots (Figure 4A and 4B), for both low and high frequency stimuli, show the FFR phase-locking to the stimulus F0. Statistical comparisons for pitch strength measures revealed a main effect of Frequency ($F_{(1,19)} = 57.411$, $p < 0.001$, $n_p^2 = 0.751$), thus showing the robustness of the response's phase-locking to the syllable F0 contour (Jeng et al., 2013) was higher for FFR to low frequency stimuli. Same effect on Frequency factor was found for pitch error, reflecting higher pitch encoding accuracy for low frequency FFR ($F_{(1,19)} = 76.600$, $p < 0.001$, $n_p^2 = 0.801$), and for maximum stimulus-to-response cross-correlation ($F_{(1,19)} = 36.006$, $p < 0.001$, $n_p^2 = 0.655$).

However, none of these measures yielded significant effects among Session or Measurement factors, or their interaction (Table 2), with no effects attributable to cTBS. Again, statistical comparisons with *Cohen's d* for the main comparison of interest confirmed the lack of significant differences between Baseline and Post measurements in any of these FFR measures (Active Low Baseline vs Post: pitch strength, d = -0.044, CI [-0.56 0.40]; pitch error, d = 0.119, CI [-0.10 0.36], max stimulus-to-response cross correlation, d = 0.056, CI [-0.20 0.26]).

Figure 3. Spectrograms of the grand-averaged FFRs elicited to syllable /ba/ with **(A)** Low (113 Hz) and **(B)** High (317 Hz) F0. Top panels for Sham sessions and bottom ones for Active sessions. Baseline measurements to the left, Post cTBS measurements to the right. Darkest to lighter colors indicate spectral amplitude (μV) from lower to higher values, as a function of time and frequency. The black line shows time points with maximum amplitudes.

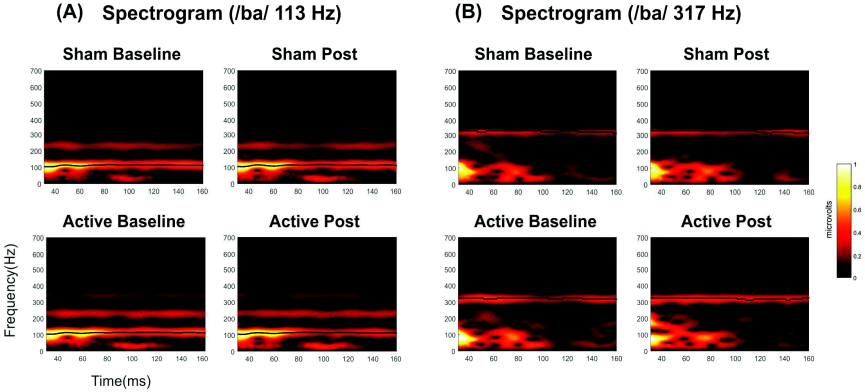

Image: Original figure created by the author

Figure 4. Autocorrelogram of the gran-averaged FFRs elicited to syllable /ba/ with **(A)** Low (113 Hz) and **(B)** High (317 Hz) F0. Top panels for Sham sessions and bottom ones for Active sessions. Baseline measurements to the left, Post cTBS measurements to the right. Darker to lighter colors indicate autocorrelation values from -1 to 1 (*Pearson's r*), as a function of time and lag. The black line shows time points with maximum autocorrelation values.

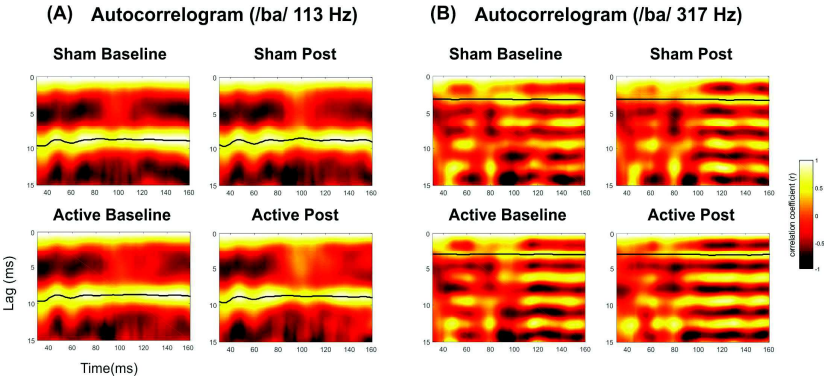

Image: Original figure created by the author

Table 2. Results of repeated measures ANOVA on FFR measures: first maximum stimulus-to-response cross-correlation (Maxcorr; *Pearson's r*), Pitch strength (*Pearson's r*) and Pitch error (Hz). Session factor includes Sham and Active levels, Measurement factor includes Baseline and Post levels, and Frequency factor includes Low and High frequency levels. Session and Measurement factors, the interaction between them (Ses*Meas) and a thriple interaction between Session, Measurement and Frequency (Ses*Meas*Freq) are reported. For each factor and their interaction, *F* and *p* values are presented (degrees of freedom: 1,19) along with effect sizes (n_p^2).

FFR statistics	***F***	***p***	$\boldsymbol{n_p^2}$
Maxcorr			
Session	0.008	0.928	0.000
Measurement	2.173	0.157	0.103
Ses*Meas	0.370	0.550	0.019
Ses*Meas*Freq	0.701	0.413	0.036
Pitch strength			
Session	1.964	0.177	0.094
Measurement	0.042	0.839	0.002
Ses*Meas	1.763	0.200	0.085
Ses*Meas*Freq	0.060	0.809	0.003
Pitch error			
Session	0.842	0.370	0.042
Measurement	0.379	0.545	0.020
Ses*Meas	0.004	0.951	0.000
Ses*Meas*Freq	0.000	0.998	0.000

**p* values in the table are non-corrected for multiple comparisons

Overall, from all these different approaches to the FFR data we obtained no differences between Baseline and Post recordings in neither the Sham nor the Active sessions, regardless of the stimulus fundamental frequency. Despite not being reported in the tables, interactions between Frequency and Measurement or Frequency and Session factors were not significant neither for any of the FFR measures. Furthermore, the hypothesized triple interaction between Session, Measurement and Frequency was not found (see Tables 1 and 2), in any of the FFR measures studied.

3.2. ABR and LLR

Amplitude of ABR wave V (Figure 5A) was overall larger ($F_{(1,19)} = 4.539$, $p = 0.046$, $n_p^2 = 0.193$) in the Post measurements (Table 3), although no interaction with Session factor was found, thus suggesting no effect of cTBS applied to the right auditory cortex in subcortical auditory evoked potentials. *Cohen's d* analyses confirmed such negative results (Active Baseline vs Post, $d = -0.133$, CI [-0.30 0.008]; Sham Baseline vs Post, $d = -0.235$, CI [-0.43 0.016]), with small size effects and confidence intervals including 0 value.

LLR components (Figure 5B) were not affected by the cTBS pulse neither. Specifically, mean amplitudes of LLR components analyzed, P50, N1 and P2, were not significantly different across measurements or sessions, and no significant interaction between these two factors was found in ANOVA (Table 3). LLR was a crucial indicator in our study to prove the effect of cTBS on the auditory cortex, yet we found no significant results. Results from *Cohen's d* and confidence intervals also pointed towards the lack of significant differences between Baseline and Post mean amplitude values in either Active (P50, d = -0.134, CI [-0.59 0.49]; N1, d = -0.317, CI [-0.04 0.80]; P2, d = -0.160, CI [-0.74 0.34]) or Sham (P50, d = -0.184, CI [-0.55 0.15]; N1, d = -0.144, CI [-0.37 0.51]; P2, d = -0.151, CI [-0.45 0.18]) sessions.

Figure 5. (A) Grand-averaged ABR waveforms elicited by auditory click stimulus in Sham (left) and Active (right) sessions. Shaded areas (5 to 6.5 ms) represent time-windows of wave V, for where mean amplitude values (μV) were taken for statistical comparisons. **(B)** Grand-averaged LLR waveforms elicited by up-chirp stimulus in Sham (top) and Active (bottom) sessions. Shaded areas represent time-windows of P50 (30 to 50 ms), N1 (70 to 110 ms) and P2 (120 to 160 ms) components, for where mean amplitude values (μV) were taken for statistical comparisons. For all figures, in blue, baseline recordings before cTBS pulse; in orange, Post cTBS recordings.

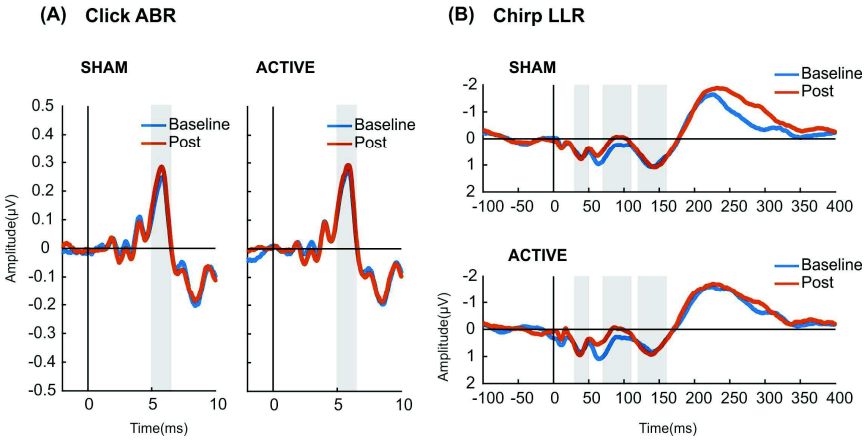

Image: Original figure created by the author

Table 3. Results of repeated measures ANOVA on ABR wave V (5 to 6.5 ms) and LLR components P50 (30 to 50 ms), N1 (70 to 110 ms) and P2 (120 to 160 ms) amplitude values (μV). Session factor includes Sham and Active levels and Measurement factor includes Baseline and Post levels. Session and Measurement factors, as well as the interaction between them (Ses*Meas) are reported. For each factor and their interaction, *F* and *p* values are presented (degrees of freedom: 1,19), along with effect sizes (n_p^2). *p* values below 0.05 are highlighted.

ABR/LLR stats	*F*	*p*	n_p^2
Wave V ABR			
Session	2.162	0.158	0.102
Measurement	4.539	**0.046**	0.193
Ses*Meas	0.685	0.418	0.035
P50 LLR			
Session	0.433	0.519	0.022
Measurement	1.009	0.328	0.050
Ses*Meas	0.045	0.834	0.002
N1 LLR			
Session	0.093	0.764	0.005
Measurement	1.878	0.187	0.090
Ses*Meas	0.463	0.505	0.024
P2 LLR			
Session	4.074	0.058	0.177
Measurement	1.172	0.292	0.058
Ses*Meas	0.000	0.955	0.000

**p* values in the table are non-corrected for multiple comparisons

3.3. Additional control: LLR experiment

Since we did not observe any effect of the cTBS on cortical evoked potentials, we argued that one possibility was that the LLR blocks were acquired way after the cTBS administration (e.g., 21 min) and therefore the potential inhibitory effects may have vanished away at the time of our recordings. To control for such possibility, an additional experiment a few months after the completion of the original one was conducted in a sub-sample of 11 participants from the original study, who voluntarily took part in it. In this control experiment, we used the exact same parameters as described in the methods section, with the exception that only an LLR block before and after the cTBS pulse (Baseline and Post) was recorded. In such block, four LLR recordings of 200 artifact-free sweeps each were acquired, both in Sham and Active Sessions. Among these four recordings, two were using the same up-chirp stimuli from the original study, and the other two, interspersed between those, were using a pure tone of 880 Hz and 100 ms duration. Therefore, the LLR blocks followed the sequence: Chirp – Pure Tone – Chirp – Pure Tone, with the starting type of stimuli counterbalanced across subjects. The rationale behind the use of additional LLR recordings in this new experiment was to assess whether the hypothetical cTBS effects would be present at LLR recordings

immediately after the cTBS pulse but fade away in the successive recording, although such effect was not observed. Moreover, this time, we aimed to test cTBS effects both with the stimuli used in the original study and with a pure tone, since this second stimulus elicited a larger N1 response.

Results from the additional experiment are shown in Figure 6. LLR waveforms from the two recordings of the same Session (Active, Sham), Measurement (Baseline, Post) and stimulus type (Pure Tone and Chirp stimulus), were averaged together, and mean amplitudes at the N1 peak (75 to 115 ms for LLR to chirp, 75 to 125 ms for LLR to pure tone; defined based on the grand-average waveforms) were retrieved for statistical analyses. Two-way repeated measures ANOVA revealed no significant effects of Session factor ($F_{(1,10)} = 0.403$, $p = 0.540$), Measurement factor ($F_{(1,10)} = 0.210$, $p = 0.657$) and the interaction between them ($F_{(1,10)} = 4.005$, $p = 0.073$) for N1 elicited by chirp stimulus. For N1 elicited by pure tone stimulus, a main effect of Measurement ($F_{(1,10)} = 12.329$, $p = 0.006$) was found, thus revealing that, overall, N1 amplitude changed between Baseline and Post measurements, but regardless of the session. Alternatively, no effects were found for Session factor ($F_{(1,10)} = 0.653$, $p = 0.438$) and Session*Measurement interaction ($F_{(1,10)} = 1.330$, $p = 0.276$). Further statistical testing with *Cohens's d* and confidence intervals revealed moderate to strong size effects when comparing Baseline to Post mean N1 amplitudes elicited by chirp stimulus, but such effects were found both in Active and Sham sessions (Active: $d = -1.0658$, CI [-1.84 -0.02]; Sham: $d = 0.533$, CI[0.09 0.96]). With pure tone stimulus, a moderate size effect was found for Baseline vs Post comparison in Active session ($d = 0.481$, CI[0.0261.10]), with confidence intervals excluding the 0 value, in contrast with results in Sham session ($d = 0.246$, CI[-0.03 0.66]). However, no differences were found between N1 amplitudes of the two Post measurements (Sham vs Active: $d = -0.07$, CI[-0.54 0.25]).

Figure 6. Results of additional control experiment **(A)** Grand-averaged LLR waveforms elicited by up-chirp stimulus in Sham (cool colors) and Active (warm colors) sessions. The shaded area (75 to 115 ms) represent the time-window of N1 component, for where mean amplitude values (μV) were taken for statistical comparisons. **(B)** Grand-averaged LLR waveforms elicited by pure tone stimulus in Sham (cool colors) and Active (warm colors) sessions. The shaded area (75 to 125 ms) represent the time-window of N1 component, for where mean amplitude values (μV) were taken for statistical comparisons. For all figures, lighter colors refer to baseline recordings before cTBS pulse; darker ones correspond to Post cTBS recordings.

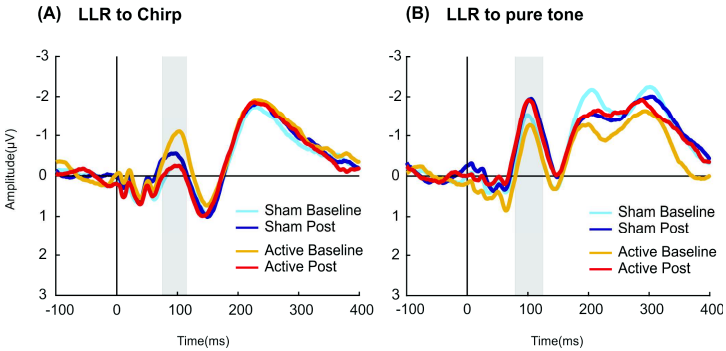

Image: Original figure created by the author

In summary, the results of the additional control experiment ruled out the attribution of the lack of effects in cortical potentials to the time delay between the administration of the cTBS pulse and the LLR recordings, as well as further confirmed the lack of effects of cTBS over the right auditory cortex on cortical potentials (LLR). Indeed, the fact alone that FFR measures were not affected in any of the stimulation frequencies could have driven the conclusion that the scalp-recorded FFR had no cortical contribution, as the transient inactivation of the right auditory cortex did not affect FFR measurements to any of the stimulation frequencies. However, given the results in LLR, the lack of effects on the FFR measures cannot be attributed to the lack of cortical contribution to this evoked potential.

4. Discussion

In the present study, we applied cTBS, an inhibitory rTMS pulse, in the right primary auditory cortex aiming to produce a transient inactivation in this region that would last for approximately 20-30 minutes (Chung et al., 2016). Within this time window, we recorded FFR, ABR and LLR evoked potentials and tested whether these would be affected by the hypothesized transient inactivation. Specifically, our hypothesis was that FFR recorded to low (113 Hz) stimulus fundamental frequency, as compared to high (317 Hz), would be modulated by that inactivation, provided auditory cortex contributes to FFR signal at low but not high stimulus frequencies. Moreover, LLR but no ABR potentials would be modulated as well, as the former have proven cortical contributions. However, our results suggest no effect of cTBS on the auditory cortex, as

LLR potentials were not affected, therefore leaving results on the FFR uninterpretable. Several reasons behind this lack of effects are discussed, which yield interesting highlights regarding the use of cTBS protocols in the auditory cortex.

The first possible cause of our negative findings is that the cTBS pulse was largely ineffective in our target area of stimulation, the primary auditory cortex. Reviewing the efficacy of rTMS protocols in producing transient inhibitory effects at the neuronal level, on the one hand, we find studies on neuron-enriched primary cortical cultures (Grehl et al., 2015) revealing that TBS protocols increase intracellular calcium, which can modulate synaptic plasticity (Hulme, Jones, Ireland and Abraham, 2012) leading to long-term depression mechanisms. Moreover, TBS regulates the expression of genes related with dendritic growth, which is associated with morphological changes in neuronal projections (Grehl et al., 2015). On the other hand, in humans, cTBS has been shown effective to produce long-term depression-like effects in a targeted neural population (Huang et al., 2005; for a review, see Chung et al., 2016). However, in these last studies evidence comes from the measurement of activity from motor cortex.

Importantly, few studies have addressed the question on whether cTBS produces measurable changes in auditory cortical areas, and these have always been related with clinical populations, specially, tinnitus. For instance, Schecklmann et al. (2014), using functional near-infrared spectroscopy in tinnitus patients, found that cTBS produced changes in sound-evoked brain oxygenation in primary auditory cortex, with reversed patterns for active and placebo conditions, as well as different results for block and event-related designs. Moreover, clinical effects of repetitive TMS protocols, including cTBS, over the primary auditory cortex have been measured on tinnitus, aiming to reduce the symptomatology (Barwood et al., 2013; Schecklmann et al., 2016; Sahlsten et al., 2017). From these studies, only one (Barwood et al., 2013), with four patients, found significant improvement in tinnitus when comparing active and placebo TMS conditions. In the other two studies, improvement of tinnitus scores was not superior in active than in placebo condition, thus suggesting no clinically relevant effects. Still within auditory cortex, evidence on the inhibitory effects of rTMS comes also from studies on schizophrenia patients, in which the transient inactivation of areas within this region (e.g. heschl's gyrus, temporoparietal cortex, language areas determined with fMRI) is intended to ameliorate auditory hallucinations. To this regard, some studies show benefits from rTMS in reducing auditory hallucinations (Hoffman, Hawkings, Gueorgieva et al., 2003), whereas others find no differences between active and placebo groups (McIntosh, et al., 2004; Blumberger et al., 2012; Paillère-Martinot et al., 2017), as well as several meta-analyses show an overall small but present effects of rTMS on auditory hallucinations (Aleman, Sommer and Kahn, 2007; Freitas, Fregni and Pasual-Leone, 2009). In summary, despite clear and long-lasting inhibitory effects described for cTBS (Huang et al., 2005; Chung et al., 2016), which prompted its use in the present study, no clear conclusions on the effectiveness of cTBS or rTMS over auditory cortex can be drawn from the literature.

In comparison to effects on auditory cortical areas, repeated TMS protocols applied to other sensory areas of the cortex, including primary ones, have been proven to produce robust effects. For instance, rTMS impaired motion discrimination and accuracy when

applied in primary visual cortex and secondary areas (Thompson, Deblieck, Wu, Iacoboni and Liu, 2016). In the somatosensory cortex, cTBS over primary somatosensory areas (S1) impaired tactile acuity (Rai, Premji, Tommerdahl and Nelson, 2012), rTMS over S1 impaired the processing of contralateral visual stimuli of human bodyparts being touched only by an human agents (Rossetti, Miniussi, Maravita and Bolognini, 2012), and rTMS over S2 produced changes in BOLD response in the area, as well as decreased participant's ratings of touch intensity (using a H8 deep TMS coil; Case, Richards, Spagnolo, Olausson and Bushnell, 2017). Notably, a crucial element when considering the effectiveness of any TMS protocol in cortical areas is how deep within the brain the stimulation target is. In addition to fMRI-measured and sensory processing effects observed in the studies described, several studies measuring rTMS effects on event-related potentials, as we do, have targeted areas of superficial cortex (e.g., prefrontal areas: Sokhadze, et al., 2018; Lowe, Staines, Manocchio and Hall, 2018; or somatosensory areas: Poreisz, Antal, Boros, Brepohl, Csifcsák and Paulus, 2008). However, our target area of stimulation, the primary auditory cortex, includes a part of cortex buried within the temporal lobe, at the supratemporal plane (i.e., Heschl's gyri; Abdul-Kareem and Sluming, 2008). According to TMS physics described in Rossi et al. (2009), the Figure 8 coil that we used produces a more focal but shallower stimulation and, with pulse intensities below 120% of MTH, the stimulation cannot induce direct activation at depth of more than 2 cm beneath the scalp (Roth et al., 2002, 2007; Zangen et al., 2005). Considering our pulse intensities were determined as 80% of aMTH, following safety guidelines, the possibility exists that our TMS pulses were not reaching the target area. In fact, this may help explain the overall more consistent findings in the literature on rTMS inhibitory effects on visual or somatosensory primary areas of the cortex, in comparison with auditory ones. Moreover, determining the intensity of the TMS pulse using motor cortex (superficial cortex) as a reference, again following standard procedures, may undermine our success when trying to target an area of cortex with a greater separation from the coil than the motor cortex.

A different but related interpretation on the lack of effects observed in the present study would be that, despite cTBS producing a transient inactivation of the auditory cortex, the effects were not reflected in the auditory evoked potentials (AEP) recorded. To this regard, to the best of our knowledge, no previous study has addressed whether cTBS over the auditory cortex affects AEPs. There are, however, studies combining EEG and TMS over auditory cortex using paired associative stimulation (PAS), that is, pairing external acoustic stimuli with TMS pulses applied to the corresponding cortical region where stimuli would be processed (Stefan, Kunesch, Cohen, Benecke and Classen, 2000). When performing PAS so that the TMS pulse occurs right before the incoming acoustic stimulus, for instance, long term depression-like mechanisms can be generated, reducing synaptic connectivity. In these studies, several auditory evoked potentials were modulated when performing PAS protocols over auditory cortex, including N1-P2 complex (Schecklmann, et al., 2011), Auditory Steady-State Responses (Engel, Markewitz, Langguth and Schecklmann, 2017), or late auditory evoked potentials (Markewitz, Engel, Langguth and Schecklmann, 2019). These studies demonstrate that, indeed, TMS over auditory cortical areas can modulate AEPs. Despite their findings, the kind of TMS protocols used in these designs, with almost simultaneous

EEG recordings and TMS pulses, differs considerably from our protocol with cTBS, in which EEG recordings were separated in time from TMS administration.

Compensatory mechanisms from the non-targeted areas contributing to the signal recorded could also potentially explain our negative results. Following international standards for the use of rTMS (Rossi et al., 2009), the administration of cTBS was restricted to only one hemisphere. In our case, we chose the right one as our primary goal was to assess FFR, as contribution from the right hemisphere to this evoked potential was found to be more prominent (Coffey et al., 2016). However, the possibility remains that left auditory cortex compensates for the transient inactivation of the right one. Indeed, contralateral activation of temporoparietal areas compensating right sided inactivation with rTMS has been described in healthy individuals (Tracy et al., 2010). This possibility applies as well to our LLR recordings, the control condition to demonstrate the effect of cTBS in the present study, as long latency potentials such as N1 are known to have contributions from both auditory cortices (Näätänen and Picton, 1987; Recasens, Grimm, Capilla, Nowak and Escera, 2012), as well as from frontal areas, such as premotor cortices, supplementary motor area or anterior cingulate (Alcaini et al., 1994; Giard et al., 1994; Näätänen and Picton, 1987; Picton et al., 1995; see Bender, Oelkers-Ax, Resch and Weisbrod, 2006). These areas could in fact partially contribute to the amplitude of components. Therefore, a transient inactivation of a small area of the right auditory cortex may have been insufficient to affect amplitude of the signal to a significant degree.

A further important element to consider when performing cTBS protocols is the effectiveness inter and intraindividual variability described for the pulse in motor areas (Vallence et al., 2015; Jannati, Block, Oberman, Rotenberg and Pascual-Leone, 2017). Importantly, some studies performing rTMS protocols (Martin-Trias et al., 2018) and intermittent theta burst stimulation (López-Alonso, Cheeran, Río-Rodríguez and Fernández-Del-Olmo, 2014) in dorsolateral prefrontal cortex and motor cortex, respectively, report responsiveness values in approximately 40% of participants. Several factors have been described as influencing this variability in motor areas (see Martin-Trias et al., 2018), including coil orientation discrepancies among studies (Talelli, Cheeran, Teo and Rothwell, 2007) and subject factors such as age (Todd, Kimber, Ridding and Semmler, 2010), gender (Chaieb, Antal and Paulus, 2008), genetics (Cheeran et al., 2008; Jannati et al., 2017) or relative levels of excitability in neuronal populations, affected by participant's individual state (levels of fatigue, sleep or wakefulness, etc: Silvanato, Muggleton and Walsh, 2008; Hordacre et al., 2017). Considering this variability has been described in areas of motor cortex, we don't know to what extent it could be influencing results in a much less studied area such as the auditory cortex, and therefore it constitutes a relevant factor to understand the lack of confirmation of our hypothesis.

5. Conclusions

The present study addresses an important question in the field of auditory neuroscience, such as the neural origins of the FFR, and uses a novel and methodologically rigorous approach to answer it, alternative to EEG source reconstruction techniques, by combining EEG and cTBS. No effects of cTBS were observed in FFR or cortical potentials, suggesting that the inactivation of an auditory sensory area with this protocol

is ineffective. Nevertheless, this absence of effects is of particular relevance (The importance of no evidence, March 2019), as this is, to the best of our knowledge, the first attempt to record auditory evoked potentials after a cTBS pulse in a primary auditory area. Moreover, possible reasons behind this lack of effects are discussed, which may be relevant to other studies using cTBS protocol in auditory cortical areas.

Author Contributions

FLC, DB and CE designed the study; FLC, PM and NGC performed data acquisition, FLC and TR carried out data analysis; FLC, DB and CE wrote the manuscript; all coauthors revised and approved the final version of the manuscript.

Conflict of Interest Statement

The authors declare that the research was conducted in the absence of any commercial or financial relationships that could be construed as a potential conflict of interest.

Acknowledgments

This work was supported by the Spanish Ministry of Economy and Knowledge (PSI2015-63664-P), the Catalan Government (SGR2014-177), and the ICREA Academia Distinguished Professorship awarded to Carles Escera. David Bartrés-Faz was partially supported by a Spanish Ministry of Economy and Competitiveness (MINECO) 35 grant to D-BF [grant number PSI2015-64227-R].

Special thanks to Jordi Tobajas Arbós for his help in data collection, and to Mercedes Atienza Ruiz for her help in statistical analysis.

References

Abdul□Kareem, I. A., & Sluming, V. (2008). Heschl gyrus and its included primary auditory cortex: structural MRI studies in healthy and diseased subjects. *Journal of Magnetic Resonance Imaging: An Official Journal of the International Society for Magnetic Resonance in Medicine*, *28*(2), 287-299.

Aiken, S. J., & Picton, T. W. (2008). Envelope and spectral frequency-following responses to vowel sounds. *Hearing research*, *245*(1-2), 35-47.

Alcaini, M., Giard, M. H., Thevenet, M., & Pernier, J. (1994). Two separate frontal components in the N1 wave of the human auditory evoked response. *Psychophysiology*, *31*(6), 611-615.

Aleman, A., Sommer, I. E., & Kahn, R. S. (2007). Efficacy of slow repetitive transcranial magnetic stimulation in the treatment of resistant auditory hallucinations in schizophrenia: a meta-analysis. *Journal of Clinical Psychiatry*, *68*(3), 416-421.

Anderson, S., White-Schwoch, T., Parbery-Clark, A., & Kraus, N. (2013). Reversal of age-related neural timing delays with training. *Proceedings of the National Academy of Sciences*, *110*(11), 4357-4362.

Banjanovic, E. S., & Osborne, J. W. (2016). Confidence Intervals for Effect Sizes: Applying Bootstrap Resampling. *Practical Assessment, Research & Evaluation*, *21*.

Barwood, C. H., Wilson, W. J., Malicka, A. N., McPherson, B., Lloyd, D., Munt, K., & Murdoch, B. E. (2013). The effect of rTMS on auditory processing in adults with chronic, bilateral tinnitus: a placebo-controlled pilot study. *Brain stimulation*, *6*(5), 752-759.

Bellier, L., Veuillet, E., Vesson, J. F., Bouchet, P., Caclin, A., & Thai-Van, H. (2015). Speech auditory brainstem response through hearing aid stimulation. *Hearing research*, *325*, 49-54.

Bender, S., Oelkers-Ax, R., Resch, F., & Weisbrod, M. (2006). Frontal lobe involvement in the processing of meaningful auditory stimuli develops during childhood and adolescence. *Neuroimage*, *33*(2), 759-773.

Bidelman, G. M. (2013). The role of the auditory brainstem in processing musically relevant pitch. *Frontiers in psychology*, *4*, 264.

Bidelman, G. M. (2015). Multichannel recordings of the human brainstem frequency-following response: scalp topography, source generators, and distinctions from the transient ABR. *Hearing research*, *323*, 68-80.

Bidelman, G. M. (2018). Subcortical sources dominate the neuroelectric auditory frequency-following response to speech. *Neuroimage*, *175*, 56-69.

Bidelman, G. M., & Alain, C. (2015). Musical training orchestrates coordinated neuroplasticity in auditory brainstem and cortex to counteract age-related declines in categorical vowel perception. *Journal of Neuroscience*, *35*(3), 1240-1249.

Bidelman, G. M., Lowther, J. E., Tak, S. H., & Alain, C. (2017). Mild cognitive impairment is characterized by deficient brainstem and cortical representations of speech. *Journal of Neuroscience*, *37*(13), 3610-3620.

Bidelman, G. M., Villafuerte, J. W., Moreno, S., & Alain, C. (2014). Age-related changes in the subcortical–cortical encoding and categorical perception of speech. *Neurobiology of aging*, *35*(11), 2526-2540.

Billiet, C. R., & Bellis, T. J. (2011). The relationship between brainstem temporal processing and performance on tests of central auditory function in children with

reading disorders. *Journal of Speech, Language, and Hearing Research*.

Blumberger, D. M., Christensen, B. K., Zipursky, R. B., Moller, B., Chen, R., Fitzgerald, P. B., & Daskalakis, Z. J. (2012). MRI-targeted repetitive transcranial magnetic stimulation of Heschl's gyrus for refractory auditory hallucinations. *Brain stimulation*, *5*(4), 577-585.

Boersma, Paul & Weenink, David (2016). Praat: doing phonetics by computer [Computer program]. Version 6.0.10, retrieved from http://www.praat.org/

Boersma, Paul (2001). Praat, a system for doing phonetics by computer. *Glot International* **5:9/10**, 341-345

Brainard, D. H., & Vision, S. (1997). The psychophysics toolbox. *Spatial vision*, *10*, 433-436.

Carcagno, S., & Plack, C. J. (2011). Subcortical plasticity following perceptual learning in a pitch discrimination task. *Journal of the Association for Research in Otolaryngology*, *12*(1), 89-100.

Case, L. K., Laubacher, C. M., Richards, E. A., Spagnolo, P. A., Olausson, H., & Bushnell, M. C. (2017). Inhibitory rTMS of secondary somatosensory cortex reduces intensity but not pleasantness of gentle touch. *Neuroscience letters*, *653*, 84-91.

Chaieb, L., Antal, A., & Paulus, W. (2008). Gender-specific modulation of short-term neuroplasticity in the visual cortex induced by transcranial direct current stimulation. *Visual neuroscience*, *25*(1), 77-81.

Chandrasekaran, B., & Kraus, N. (2010). The scalp□recorded brainstem response to speech: Neural origins and plasticity. *Psychophysiology*, *47*(2), 236-246.

Chandrasekaran, B., Hornickel, J., Skoe, E., Nicol, T., & Kraus, N. (2009). Context-dependent encoding in the human auditory brainstem relates to hearing speech in noise: implications for developmental dyslexia. *Neuron*, *64*(3), 311-319.

Chandrasekaran, B., Skoe, E., & Kraus, N. (2014). An integrative model of subcortical auditory plasticity. *Brain topography*, *27*(4), 539-552.

Cheeran, B., Talelli, P., Mori, F., Koch, G., Suppa, A., Edwards, M., ... & Rothwell, J. C. (2008). A common polymorphism in the brain□derived neurotrophic factor gene (BDNF) modulates human cortical plasticity and the response to rTMS. *The Journal of physiology*, *586*(23), 5717-5725.

Chung, S. W., Hill, A. T., Rogasch, N. C., Hoy, K. E., & Fitzgerald, P. B. (2016). Use of theta-burst stimulation in changing excitability of motor cortex: a systematic review and meta-analysis. *Neuroscience & Biobehavioral Reviews*, *63*, 43-64.

Coffey, E. B., Herholz, S. C., Chepesiuk, A. M., Baillet, S., & Zatorre, R. J. (2016). Cortical contributions to the auditory frequency-following response revealed by MEG. *Nature communications*, *7*, 11070.

DiCiccio, T. J., & Efron, B. (1996). Bootstrap confidence intervals. *Statistical science*, 189-212.

Du, Y., Kong, L., Wang, Q., Wu, X., & Li, L. (2011). Auditory frequency-following response: a neurophysiological measure for studying the "cocktail-party problem". *Neuroscience & Biobehavioral Reviews, 35*(10), 2046-2057.

Efron, B., & Tibshirani, R. J. (1993). An Introduction to the Bootstrap, volume 57 of. *Monographs on Statistics and applied probability*, 17.

Elberling, C., Don, M., Cebulla, M., & Stürzebecher, E. (2007). Auditory steady-state responses to chirp stimuli based on cochlear traveling wave delay. *The Journal of the Acoustical Society of America*, *122*(5), 2772-2785.

Engel, S., Markewitz, R. D. H., Langguth, B., & Schecklmann, M. (2017). Paired associative stimulation of the Temporal cortex: effects on the auditory steady-state response. *Frontiers in psychiatry*, *8*, 227.

Escera., C. (2017) The Role of the Auditory Brainstem in Regularity Encoding and Deviance Detection. In Kraus, N., Anderson, S., White-Schwoch., T., Fay, R. & Popper, A. (Eds.), *The Frequency Following Response. A Window into Human Communication* (pp 101-120). Springer.

Freitas, C., Fregni, F., & Pascual-Leone, A. (2009). Meta-analysis of the effects of repetitive transcranial magnetic stimulation (rTMS) on negative and positive symptoms in schizophrenia. *Schizophrenia research*, *108*(1-3), 11-24.

Gardi, J., Merzenich, M., & McKean, C. (1979). Origins of the scalp-recorded frequency-following response in the cat. *Audiology*, *18*(5), 353-380.

Giard, M. H., Perrin, F., Echallier, J. F., Thevenet, M., Froment, J. C., & Pernier, J. (1994). Dissociation of temporal and frontal components in the human auditory N1 wave: a scalp current density and dipole model analysis. *Electroencephalography and Clinical Neurophysiology/Evoked Potentials Section*, *92*(3), 238-252.

Gorina-Careta, N., Zarnowiec, K., Costa-Faidella, J., & Escera, C. (2016). Timing predictability enhances regularity encoding in the human subcortical auditory pathway. *Scientific reports*, *6*, 37405.

Grehl, S., Viola, H. M., Fuller-Carter, P. I., Carter, K. W., Dunlop, S. A., Hool, L. C., ... & Rodger, J. (2015). Cellular and molecular changes to cortical neurons following low intensity repetitive magnetic stimulation at different frequencies. *Brain stimulation*, *8*(1), 114-123.

Hairston, W. D., Letowski, T. R., & McDowell, K. (2013). Task-related suppression of the brainstem frequency following response. *PLoS One*, *8*(2), e55215.

Herbsman, T., Avery, D., Ramsey, D., Holtzheimer, P., Wadjik, C., Hardaway, F., ... & Nahas, Z. (2009). More lateral and anterior prefrontal coil location is associated with better repetitive transcranial magnetic stimulation antidepressant response. *Biological psychiatry*, *66*(5), 509-515.

Hoffman, R. E., Hawkins, K. A., Gueorguieva, R., Boutros, N. N., Rachid, F., Carroll, K., & Krystal, J. H. (2003). Transcranial magnetic stimulation of left temporoparietal cortex and medication-resistant auditory hallucinations. *Archives of general psychiatry*, *60*(1), 49-56.

Hordacre, B., Goldsworthy, M. R., Vallence, A. M., Darvishi, S., Moezzi, B., Hamada, M., ... & Ridding, M. C. (2017). Variability in neural excitability and plasticity induction in the human cortex: a brain stimulation study. *Brain stimulation*, *10*(3), 588-595.

Huang, Y. Z., Edwards, M. J., Rounis, E., Bhatia, K. P., & Rothwell, J. C. (2005). Theta burst stimulation of the human motor cortex. *Neuron*, *45*(2), 201-206.

Hulme, S. R., Jones, O. D., Ireland, D. R., & Abraham, W. C. (2012). Calcium-dependent but action potential-independent BCM-like metaplasticity in the hippocampus. *Journal of Neuroscience*, *32*(20), 6785-6794.

Jannati, A., Block, G., Oberman, L. M., Rotenberg, A., & Pascual-Leone, A. (2017). Interindividual variability in response to continuous theta-burst stimulation in healthy adults. *Clinical Neurophysiology*, *128*(11), 2268-2278.

Jannati, A., Block, G., Oberman, L. M., Rotenberg, A., & Pascual-Leone, A. (2017). Interindividual variability in response to

continuous theta-burst stimulation in healthy adults. *Clinical Neurophysiology*, *128*(11), 2268-2278.

Jeng, F. C., Peris, K. S., Hu, J., & Lin, C. D. (2013). Evaluation of an automated procedure for detecting frequency-following responses in American and Chinese neonates. *Perceptual and motor skills*, *116*(2), 456-465.

Joris, P. X., Schreiner, C. E., & Rees, A. (2004). Neural processing of amplitude-modulated sounds. *Physiological reviews*, *84*(2), 541-577.

Klatt, D. (1976, April). A digital filter bank for spectral matching. In *ICASSP'76. IEEE International Conference on Acoustics, Speech, and Signal Processing* (Vol. 1, pp. 573-576). IEEE.

Kleiner, M., Brainard, D., Pelli, D., Ingling, A., Murray, R., & Broussard, C. (2007). What's new in Psychtoolbox-3. *Perception*, *36*(14), 1.

Knecht, S., Dräger, B., Deppe, M., Bobe, L., Lohmann, H., Flöel, A., ... & Henningsen, H. (2000). Handedness and hemispheric language dominance in healthy humans. *Brain*, *123*(12), 2512-2518.

Kozel, F. A., Nahas, Z., Debrux, C., Molloy, M., Lorberbaum, J. P., Bohning, D., ... & George, M. S. (2000). How coil–cortex distance relates to age, motor threshold, and antidepressant response to repetitive transcranial magnetic stimulation. *The Journal of neuropsychiatry and clinical neurosciences*, *12*(3), 376-384.

Kraus, N., & Chandrasekaran, B. (2010). Music training for the development of auditory skills. *Nature reviews neuroscience*, *11*(8), 599.

Krishnan, A., Xu, Y., Gandour, J. T., & Cariani, P. A. (2004). Human frequency-following response: representation of pitch contours in Chinese tones. *Hearing research*, *189*(1-2), 1-12.

Krishnan, A., Xu, Y., Gandour, J., & Cariani, P. (2005). Encoding of pitch in the human brainstem is sensitive to language experience. *Cognitive Brain Research*, *25*(1), 161-168.

Krizman, J., Marian, V., Shook, A., Skoe, E., & Kraus, N. (2012). Subcortical encoding of sound is enhanced in bilinguals and relates to executive function advantages. *Proceedings of the National Academy of Sciences*, *109*(20), 7877-7881.

Lakens, D. (2013). Calculating and reporting effect sizes to facilitate cumulative science: a practical primer for t-tests and ANOVAs. *Frontiers in psychology*, *4*, 863.

Langner, G. (1992). Periodicity coding in the auditory system. *Hearing research*, *60*(2), 115-142.

Liu, F., Maggu, A. R., Lau, J. C., & Wong, P. (2015). Brainstem encoding of speech and musical stimuli in congenital amusia: evidence from Cantonese speakers. *Frontiers in human neuroscience*, *8*, 1029.

López-Alonso, V., Cheeran, B., Río-Rodríguez, D., & Fernández-del-Olmo, M. (2014). Inter-individual variability in response to non-invasive brain stimulation paradigms. *Brain stimulation*, *7*(3), 372-380.

Lowe, C. J., Staines, W. R., Manocchio, F., & Hall, P. A. (2018). The neurocognitive mechanisms underlying food cravings and snack food consumption. A combined continuous theta burst stimulation (cTBS) and EEG study. *Neuroimage*, *177*, 45-58.

Mahjoory, K., Nikulin, V. V., Botrel, L., Linkenkaer-Hansen, K., Fato, M. M., & Haufe, S. (2017). Consistency of EEG source localization and connectivity estimates. *Neuroimage*, *152*, 590-601.

Markewitz, R., Engel, S., Langguth, B., & Schecklmann, M. (2019). Effects of

Acoustic Paired Associative Stimulation on Late Auditory Evoked Potentials. *Brain topography*, *32*(3), 343-353.

Marsh, J. T., Brown, W. S., & Smith, J. C. (1974). Differential brainstem pathways for the conduction of auditory frequency-following responses. *Electroencephalography and clinical neurophysiology*, *36*, 415-424.

Martin-Trias, P., Lanteaume, L., Solana, E., Cassé-Perrot, C., Fernández-Cabello, S., Babiloni, C., ... & Truillet, R. (2018). Adaptability and reproducibility of a memory disruption rTMS protocol in the PharmaCog IMI European project. *Scientific reports*, *8*(1), 9371.

McIntosh, A. M., Semple, D., Tasker, K., Harrison, L. K., Owens, D. G., Johnstone, E. C., & Ebmeier, K. P. (2004). Transcranial magnetic stimulation for auditory hallucinations in schizophrenia. *Psychiatry Research*, *127*(1-2), 9-17.

Näätänen, R., & Picton, T. (1987). The N1 wave of the human electric and magnetic response to sound: a review and an analysis of the component structure. *Psychophysiology*, *24*(4), 375-425.

Nelken, I. (2004). Processing of complex stimuli and natural scenes in the auditory cortex. *Current opinion in neurobiology*, *14*(4), 474-480.

Paillère□Martinot, M. L., Galinowski, A., Plaze, M., Andoh, J., Bartrés□Faz, D., Bellivier, F., ... & Artiges, E. (2017). Active and placebo transcranial magnetic stimulation effects on external and internal auditory hallucinations of schizophrenia. *Acta Psychiatrica Scandinavica*, *135*(3), 228-238.

Parbery-Clark, A., Strait, D. L., Anderson, S., Hittner, E., & Kraus, N. (2011). Musical experience and the aging auditory system: implications for cognitive abilities and hearing speech in noise. *PloS one*, *6*(5), e18082.

Picton, T. W., Lins, O. G., & Scherg, M. (1995). The recording and analysis of event-related potentials. *Handbook of neuropsychology*, *10*, 3-3.

Poreisz, C., Antal, A., Boros, K., Brepohl, N., Csifcsák, G., & Paulus, W. (2008). Attenuation of N2 amplitude of laser-evoked potentials by theta burst stimulation of primary somatosensory cortex. *Experimental brain research*, *185*(4), 611-621.

Rai, N., Premji, A., Tommerdahl, M., & Nelson, A. J. (2012). Continuous theta-burst rTMS over primary somatosensory cortex modulates tactile perception on the hand. *Clinical Neurophysiology*, *123*(6), 1226-1233.

Recasens, M., Grimm, S., Capilla, A., Nowak, R., & Escera, C. (2012). Two sequential processes of change detection in hierarchically ordered areas of the human auditory cortex. *Cerebral Cortex*, *24*(1), 143-153.

Ribas-Prats, T., Almeida, L., Costa-Faidella, J., Plana, M., Corral, M. J., Gómez-Roig, M. D., & Escera, C. (2019). The frequency-following response (FFR) to speech stimuli: A normative dataset in healthy newborns. *Hearing research*, *371*, 28-39.

Rocha-Muniz, C. N., Befi-Lopes, D. M., & Schochat, E. (2012). Investigation of auditory processing disorder and language impairment using the speech-evoked auditory brainstem response. *Hearing research*, *294*(1-2), 143-152.

Rossetti, A., Miniussi, C., Maravita, A., & Bolognini, N. (2012). Visual perception of bodily interactions in the primary somatosensory cortex. *European Journal of Neuroscience*, *36*(3), 2317-2323.

Rossi, S., Hallett, M., Rossini, P. M., Pascual-Leone, A., & Safety of TMS Consensus Group. (2009). Safety, ethical considerations, and application guidelines for the use of transcranial magnetic

stimulation in clinical practice and research. *Clinical neurophysiology*, *120*(12), 2008-2039.

Rossini, P. M., Burke, D., Chen, R., Cohen, L. G., Daskalakis, Z., Di Iorio, R., ... & Hallett, M. (2015). Non-invasive electrical and magnetic stimulation of the brain, spinal cord, roots and peripheral nerves: basic principles and procedures for routine clinical and research application. An updated report from an IFCN Committee. *Clinical Neurophysiology*, *126*(6), 1071-1107.

Roth, Y., Amir, A., Levkovitz, Y., & Zangen, A. (2007). Three-dimensional distribution of the electric field induced in the brain by transcranial magnetic stimulation using figure-8 and deep H-coils. *Journal of Clinical Neurophysiology*, *24*(1), 31-38.

Roth, Y., Zangen, A., & Hallett, M. (2002). A coil design for transcranial magnetic stimulation of deep brain regions. *Journal of Clinical Neurophysiology*, *19*(4), 361-370.

Russo, N., Nicol, T., Musacchia, G., & Kraus, N. (2004). Brainstem responses to speech syllables. *Clinical Neurophysiology*, *115*(9), 2021-2030.

Sahlsten, H., Virtanen, J., Joutsa, J., Niinivirta-Joutsa, K., Löyttyniemi, E., Johansson, R., ... & Holm, A. (2017). Electric field-navigated transcranial magnetic stimulation for chronic tinnitus: a randomized, placebo-controlled study. *International journal of audiology*, *56*(9), 692-700.

Schecklmann, M., Giani, A., Tupak, S., Langguth, B., Raab, V., Polak, T., ... & Fallgatter, A. J. (2016). Neuronavigated left temporal continuous theta burst stimulation in chronic tinnitus. *Restorative neurology and neuroscience*, *34*(2), 165-175.

Schecklmann, M., Giani, A., Tupak, S., Langguth, B., Raab, V., Polak, T., ... & Fallgatter, A. J. (2014). Functional near-infrared spectroscopy to probe state-and trait-like conditions in chronic tinnitus: a proof-of-principle study. *Neural plasticity*, *2014*.

Schecklmann, M., Volberg, G., Frank, G., Hadersdorfer, J., Steffens, T., Weisz, N., ... & Langguth, B. (2011). Paired associative stimulation of the auditory system: a proof-of-principle study. *PloS one*, *6*(11), e27088.

Schreiner, C. E., & Langner, G. E. R. A. L. D. (1988). Periodicity coding in the inferior colliculus of the cat. II. Topographical organization. *Journal of neurophysiology*, *60*(6), 1823-1840.

Selinger, L., Zarnowiec, K., Via, M., Clemente, I. C., & Escera, C. (2016). Involvement of the serotonin transporter gene in accurate subcortical speech encoding. *Journal of Neuroscience*, *36*(42), 10782-10790.

Silvanto, J., Muggleton, N., & Walsh, V. (2008). State-dependency in brain stimulation studies of perception and cognition. *Trends in cognitive sciences*, *12*(12), 447-454.

Skoe, E., & Kraus, N. (2010). Auditory brainstem response to complex sounds: a tutorial. *Ear and hearing*, *31*(3), 302.

Skoe, E., & Kraus, N. (2012). A little goes a long way: how the adult brain is shaped by musical training in childhood. *Journal of Neuroscience*, *32*(34), 11507-11510.

Skoe, E., Chandrasekaran, B., Spitzer, E. R., Wong, P. C., & Kraus, N. (2014). Human brainstem plasticity: the interaction of stimulus probability and auditory learning. *Neurobiology of learning and memory*, *109*, 82-93.

Skoe, E., Krizman, J., Spitzer, E., & Kraus, N. (2013). The auditory brainstem is a barometer of rapid auditory learning. *Neuroscience*, *243*, 104-114.

Slabu, L., Grimm, S., & Escera, C. (2012). Novelty detection in the human auditory brainstem. *Journal of Neuroscience*, *32*(4), 1447-1452.

Slotema, C. W., Blom, J. D., van Lutterveld, R., Hoek, H. W., & Sommer, I. E. (2014). Review of the efficacy of transcranial magnetic stimulation for auditory verbal hallucinations. *Biological psychiatry*, *76*(2), 101-110.

Smith, J. C., Marsh, J. T., & Brown, W. S. (1975). Far-field recorded frequency-following responses: evidence for the locus of brainstem sources. *Electroencephalography and clinical neurophysiology*, *39*(5), 465-472.

Sohmer, H., Pratt, H., & Kinarti, R. (1977). Sources of frequency following responses (FFR) in man. *Electroencephalography and clinical neurophysiology*, *42*(5), 656-664.

Sokhadze, E. M., Lamina, E. V., Casanova, E. L., Kelly, D. P., Opris, I., Tasman, A., & Casanova, M. F. (2018). Exploratory study of rTMS neuromodulation effects on electrocortical functional measures of performance in an oddball test and behavioral symptoms in autism. *Frontiers in systems neuroscience*, *12*, 20.

Stefan, K., Kunesch, E., Cohen, L. G., Benecke, R., & Classen, J. (2000). Induction of plasticity in the human motor cortex by paired associative stimulation. *Brain*, *123*(3), 572-584.

Steinschneider, M., Arezzo, J., & Vaughan Jr, H. G. (1980). Phase-locked cortical responses to a human speech sound and low-frequency tones in the monkey. *Brain research*, *198*(1), 75-84.

Steinschneider, M., Fishman, Y. I., & Arezzo, J. C. (2007). Spectrotemporal analysis of evoked and induced electroencephalographic responses in primary auditory cortex (A1) of the awake monkey. *Cerebral Cortex*, *18*(3), 610-625.

Talelli, P., Cheeran, B. J., Teo, J. T. H., & Rothwell, J. C. (2007). Pattern-specific role of the current orientation used to deliver Theta Burst Stimulation. *Clinical Neurophysiology*, *118*(8), 1815-1823.

The importance of no evidence [Editorial]. *Nature human behaviour, 3*. Published 12 March 2019. Retrieved from https://doi.org/10.1038/s41562-019-0569-7

Thompson, B., Deblieck, C., Wu, A., Iacoboni, M., & Liu, Z. (2016). Psychophysical and rTMS evidence for the presence of motion opponency in human V5. *Brain stimulation*, *9*(6), 876-881.

Todd, G., Kimber, T. E., Ridding, M. C., & Semmler, J. G. (2010). Reduced motor cortex plasticity following inhibitory rTMS in older adults. *Clinical Neurophysiology*, *121*(3), 441-447.

Tracy, D. K., O'daly, O., Joyce, D. W., Michalopoulou, P. G., Basit, B. B., Dhillon, G., ... & Shergill, S. S. (2010). An evoked auditory response fMRI study of the effects of rTMS on putative AVH pathways in healthy volunteers. *Neuropsychologia*, *48*(1), 270-277.

Tupak, S. V., Dresler, T., Badewien, M., Hahn, T., Ernst, L. H., Herrmann, M. J., ... & Fallgatter, A. J. (2013). Inhibitory transcranial magnetic theta burst stimulation attenuates prefrontal cortex oxygenation. *Human brain mapping*, *34*(1), 150-157.

Vallence, A. M., Goldsworthy, M. R., Hodyl, N. A., Semmler, J. G., Pitcher, J. B., & Ridding, M. C. (2015). Inter-and intra-subject variability of motor cortex plasticity following continuous theta-burst stimulation. *Neuroscience*, *304*, 266-278.

Zangen, A., Roth, Y., Voller, B., & Hallett, M. (2005). Transcranial magnetic stimulation of deep brain regions: evidence for efficacy of the H-coil. *Clinical neurophysiology*, *116*(4), 775-779.

STUDY III:

Binaural beat: A failure to enhance EEG power and emotional arousal

frontiers in Human Neuroscience

ORIGINAL RESEARCH
published: 15 November 2017
doi: 10.3389/fnhum.2017.00557

Binaural Beat: A Failure to Enhance EEG Power and Emotional Arousal

Fran López-Caballero[1,2] *and Carles Escera*[1,2,3]*

[1]*Brainlab-Cognitive Neuroscience Research Group, Department of Clinical Psychology and Psychobiology, University of Barcelona, Barcelona, Spain,* [2]*Institute of Neurosciences, University of Barcelona, Barcelona, Spain,* [3]*Institut de Recerca Sant Joan de Déu (IRSJD), Barcelona, Spain*

When two pure tones of slightly different frequencies are delivered simultaneously to the two ears, is generated a beat whose frequency corresponds to the frequency difference between them. That beat is known as acoustic beat. If these two tones are presented one to each ear, they still produce the sensation of the same beat, although no physical combination of the tones occurs outside the auditory system. This phenomenon is called binaural beat. In the present study, we explored the potential contribution of binaural beats to the enhancement of specific electroencephalographic (EEG) bands, as previous studies suggest the potential usefulness of binaural beats as a brainwave entrainment tool. Additionally, we analyzed the effects of binaural-beat stimulation on two psychophysiological measures related to emotional arousal: heart rate and skin conductance. Beats of five different frequencies (4.53 Hz -theta-, 8.97 Hz -alpha-, 17.93 Hz -beta-, 34.49 Hz -gamma- or 57.3 Hz -upper-gamma) were presented binaurally and acoustically for epochs of 3 min (Beat epochs), preceded and followed by pink noise epochs of 90 s (Baseline and Post epochs, respectively). In each of these epochs, we analyzed the EEG spectral power, as well as calculated the heart rate and skin conductance response (SCR). For all the beat frequencies used for stimulation, no significant changes between Baseline and Beat epochs were observed within the corresponding EEG bands, neither with binaural or with acoustic beats. Additional analysis of spectral EEG topographies yielded negative results for the effect of binaural beats in the scalp distribution of EEG spectral power. In the psychophysiological measures, no changes in heart rate and skin conductance were observed for any of the beat frequencies presented. Our results do not support binaural-beat stimulation as a potential tool for the enhancement of EEG oscillatory activity, nor to induce changes in emotional arousal.

Keywords: binaural beats, acoustic beats, EEG bands, heart rate, skin conductance

OPEN ACCESS

Edited by:
Vladimir Litvak,
UCL Institute of Neurology, United Kingdom

Reviewed by:
William Sedley,
Newcastle University, United Kingdom
Adam Tierney,
Birkbeck University of London, United Kingdom

***Correspondence:**
Carles Escera
cescera@ub.edu

Received: *27 July 2017*
Accepted: *02 November 2017*
Published: *15 November 2017*

Citation:
López-Caballero F and Escera C (2017) Binaural Beat: A Failure to Enhance EEG Power and Emotional Arousal. Front. Hum. Neurosci. 11:557. doi: 10.3389/fnhum.2017.00557

INTRODUCTION

When two pure-tone sinewaves with slightly different frequencies (e.g., 300 and 305 Hz) are presented simultaneously to the same ear, a periodic two-tone complex with a frequency corresponding to the frequency difference between the two tones (e.g., 5 Hz) can be perceived as a "beat". In such a phenomenon, known as "acoustic beat", the two input frequencies are physically mixed in the signal before they reach the auditory system. In contrast, when the same two tones with slightly different frequencies are played binaurally, one to each ear, the same beat is perceived,

although no physical combination of these tones occurs outside the auditory system, hence pointing to a central nervous origin. This latter effect is known as the "binaural beat", and can be perceived if the carrier frequency is lower than 1000 Hz, and the two frequencies differ from each other by approximately less than 35 Hz (Licklider et al., 1950).

First described by Dove (1841) and further characterized by Thompson (1877), binaural-beat phenomena reflect the convergence of neural activity from the auditory nerves in binaurally sensitive networks (Moore, 1997). There is agreement on the involvement of the auditory cortex and the brainstem in the neural mechanisms behind binaural beats perception. In animal studies, single-unit recordings have disclosed the earliest responses evoked by binaural-beat stimulation in neurons of the superior olivary complex of the brainstem (Wernick and Starr, 1968; Spitzer and Semple, 1998), the first nucleus in the ascending auditory pathway receiving bilateral input. Moreover, these studies have disclosed responses in the inferior colliculus of the midbrain that are phase-locked to the binaural-beat frequency (Kuwada et al., 1979; McAlpine et al., 1996).

In humans, magnetoencephalographic (MEG) studies have recorded auditory steady-state responses to binaural beats from various sources in the parietal, frontal and temporal areas of the cerebral cortex, including the auditory cortices (Karino et al., 2006). Moreover, similar studies have suggested the involvement of the medial superior olive and the inferior colliculus in their generation mechanism (Draganova et al., 2008). In contrast with binaural beats, neuronal correlates of acoustic beats, physically present in the acoustic signal, have been found in the cochlear nuclei, the earliest relay of the auditory pathway (Draganova et al., 2008). Interestingly, at cortical level, results from electroencephalographic (EEG) studies with event-related potentials have suggested a similar involvement of the cortex in the processing of both acoustic and binaural beats (Pratt et al., 2010). Altogether, these studies suggest that binaural beat perception is the result of the integration of auditory signals from each ear in the superior olivary complex and the inferior colliculus, with a resulting neuroelectrical discharge that travels along the brainstem up to the auditory cortex.

A controversial aspect of binaural-beat research is their claimed benefit for the enhancement of specific brain wave oscillatory activity. Such research field acquires particular relevance as the traditional EEG frequency bands, such as theta (4–7 Hz), alpha (8–12 Hz), beta (13–30 Hz) and gamma (30–100 + Hz) have been associated with specific cognitive functions, such as selective attention and memory (for a review, see Herrmann et al., 2016), and the modulation or entrainment of neural oscillatory activity may constitute an effective approach for their enhancement (Huang and Charyton, 2008). As the human hearing range excludes frequencies below 20 Hz, which fall within the range of some of the relevant EEG bands for cognitive enhancement, stimulation with binaural beats has been suggested as a potential beneficial tool to alter brainwave rhythmicity in a non-invasive manner (for a review, see Vernon, 2009).

Some empirical studies have addressed the intriguing question whether binaural beats could indeed modulate specific brain rhythms leading to enhanced cognitive functions, yet with contradictory results. From studies examining the effects of binaural beats in cognitive functions, binaural-beat stimulation with frequencies within EEG theta band has resulted in no effects on vigilance task performance (Goodin et al., 2012), whereas binaural-beat stimulation with "beta" frequencies has been shown to increase performance in tasks related to verbal span, working memory, executive functions (Kennerly, 1996) and vigilance (Lane et al., 1998). Moreover, stimulation with binaural beats with frequencies in the range of the EEG gamma band affects divergent thinking (Reedijk et al., 2013) and attentional control (Reedijk et al., 2015).

Studies addressing the effects of binaural-beat stimulation on neuroelectric brain activity have reported induced oscillatory activity in the EEG theta band after binaural-beat stimulation within this very same range (Brady and Stevens, 2000), although subsequent experiments failed to replicate these effects (Stevens et al., 2003; Wahbeh et al., 2007; Gao et al., 2014). Also, other studies failed to elicit entrainment of EEG oscillatory activity to binaural alpha-beats (Gao et al., 2014; Vernon et al., 2014), as well as to binaural beta-beats (Goodin et al., 2012; Gao et al., 2014; Vernon et al., 2014). Furthermore, when using beats with frequencies within EEG gamma band, some studies revealed induced EEG gamma-band oscillatory activity with both binaural (Lavallee et al., 2011; Ross et al., 2014) and acoustic (Ross et al., 2014) beat stimulation. Entrainment effects were also reported in EEG gamma band with acoustic beats within gamma frequencies in intracranial recordings (Becher et al., 2015). In addition to induced activity at EEG bands, several studies have addressed binaural-beat effects on EEG evoked activity. Ioannou et al. (2015) recorded auditory steady-state responses to binaural alpha-beats but not to binaural gamma-beats, whereas the already cited MEG study by Draganova et al. (2008) reported auditory steady-state responses to binaural gamma-beats.

Beyond EEG entrainment and cognitive enhancement, binaural-beat stimulation has also been related with other clinically relevant dimensions, such as parasympathetic activation and self-reported relaxation (McConnell et al., 2014), heart rate variability (Palaniappan et al., 2015) and acute pre-operative anxiety (Padmanabhan et al., 2005), for theta-, alpha- and delta-beat stimulation, respectively. On the other hand, a recent comprehensive review concludes a diminishing impact of binaural-beat stimulation on anxiety levels (Chaieb et al., 2015). Overall, stimulation with binaural beats could be a tool not only to entrain brain rhythms, but also to induce changes in autonomic functions, which may be helpful in clinical populations such as those suffering from hypertension, sleep or anxiety disorders, among others.

From the studies reviewed above, regarding the effects of binaural beats on electrophysiological, cognitive and affective measures, no conclusions can be drawn. The different experimental protocols in these studies, including stimulus duration, the specific beat frequencies used within the same range, the participant's attention to the stimuli (Schwarz and Taylor, 2005), as well as individual differences (Reedijk et al., 2015) may account for the observed contradictory results. In addition, in several of the studies, the lack of proper control

conditions, the lack of details about the experimental protocols, as well as the fact that binaural-beat effects on cognitive processes were assessed without monitoring brain oscillatory activity, result in methodological limitations that leave the issue controversial. In fact, electrophysiological research comparing the effects of beat stimulation under different conditions is still rare (Chaieb et al., 2015). On the other hand, from the reviewed literature it is also under debate the role of binaural beat stimulation in modulating autonomic functions. Disentangling such role may help to prove the potential clinical effectiveness of binaural beats.

The goal of the present study was therefore to elucidate whether binaural-beat stimulation at different beat frequencies would affect EEG oscillatory activity at the particular frequency of the beat stimulation, to test the potential usefulness of binaural beats as a brainwave entrainment tool. Particularly, we addressed this question by using a paradigm that allowed us to disentangle the specific and differential contribution of binaural beats over that of acoustic beats. Despite the exploratory nature of the present study and the inconclusive evidence on the topic, our theoretical prediction was that binaural beat stimulation would induce an enhancement of EEG power at the specific frequency of the beat. A secondary goal was to explore the effects of binaural-beat at different frequencies on psychophysiological measurements traditionally related to emotional arousal, such as heart rate and skin conductance, to test their suggested potential effect on autonomic function (McConnell et al., 2014) and thus further understand their potential clinical usefulness.

MATERIALS AND METHODS

Participants

Fourteen participants (five males), ranging in age from 20 to 31 years (mean = 23.3; standard deviation = 3.3) were recruited among University of Barcelona students, and compensated by monetary payment (8 €/h). Exclusion criteria for the selection of participants were history of neurologic or psychiatric condition, as well as abnormal hearing. A pure-tone audiometry (frequency range: 250–4000 Hz), using audiometric Beyerdynamic DT48-A headphones (Heilbronn, Germany), was performed for each participant before the experiment started, ensuring mean hearing thresholds below 20 dB NHL at each ear. The experimental protocol was approved by the Bioethics Committee of the University of Barcelona, and was in accordance with the WMA Declaration of Helsinki Ethical Principles for Medical Research Involving Human Subjects. Before the experimental sessions, written informed consent was obtained from each participant after all the details of the research (except the hypotheses) were explained to them, including the characteristics of the EEG method and the possibility to withdraw from the experiment at their wish.

Stimuli

Stimuli were pure tones delivered at 75 dB SPL. Acoustic and binaural beats were generated by presenting two pure tones with slightly different frequencies, either simultaneously to both ears (acoustic beat) or separately with one tone to each ear (binaural beat; **Figures 1A,B**). The frequency of one of the pure tones in all conditions was set to 373 Hz, and the beats were created by adding a second sinewave differing from the first in 4.53 Hz (theta-beat), 8.97 Hz (alpha-beat), 17.93 Hz (beta-beat), 34.49 Hz (gamma-beat) or 57.3 Hz (upper gamma-beat; exceeding the frequency limit above which the perception of binaural beats was suggested to be not possible; Licklider et al., 1950). We selected these frequency values as an intermediate point within the typical EEG frequency bands. Particularly, we set for the gamma-beat to be below 35 Hz because of the already mentioned limitation to the perception of binaural beats (Licklider et al., 1950). Besides, we included an "upper gamma"-beat to surpass this limit, in order to test the effects on the EEG of a beat that cannot be perceived. All stimuli were created and presented using MATLAB software (The Mathworks, Inc., Natick, MA, USA) and the Psychophysics Toolbox extensions (Brainard, 1997; Pelli, 1997; Kleiner et al., 2007).

Procedure and Experimental Design

The EEG experiments were conducted on a single 3-h session, including subject preparation and recording. During the experimental sessions, participants were seated comfortably in an electrically shielded and sound-attenuated chamber, while passively listening to the auditory stimuli presented through ER-3A ABR insert earphones (Etymotic Research, Inc., Elk Grove Village, IL, USA). Participants were instructed to watch a silent movie with subtitles.

There were two conditions: *binaural-beat*, in which binaural beats in one of the five frequencies were presented, and *acoustic-beat*, in which acoustic beats of the same five frequencies were presented instead. Stimuli were presented in 10 blocks lasting 6 min each (**Figure 1C**): one acoustic and one binaural block for each of the five beat frequencies of the study. Each block started with 90 s of a constant background pink noise (65 dB SPL), followed by 180 s of acoustic- or binaural-beat stimulation delivered +10 dB over the pink noise (i.e., 75 dB SPL), and subsequently followed by 90 additional seconds of pink noise (65 dB SPL). Binaural or acoustic beats were presented in a continuous fashion. Between blocks, there were from 45 s to 75 s of silence. The order of the blocks was randomized across participants, with the only restriction that two blocks with the same frequency could not be presented in a row (e.g., binaural theta-beat preceded by acoustic theta-beat).

Data Acquisition

Continuous EEG recordings were carried out from 36 scalp electrodes (Fp1, Fpz, Fp2, F7, F3, Fz, F4, F8, FT7, FC3, FCz, FC4, FT8, T7, C3, Cz, C4, T8, TP7, CP3, CPz, CP4, TP8, P7, P3, Pz, P4, P8, PO5, POz, PO6, O1, Oz, O2, CB1 and CB2; **Figure 1D**) and two additional electrodes placed on the left and right mastoids (M1 and M2). An electrode on the tip of the nose served as online reference. To control for eye movements, the electrooculogram (EOG) was also monitored with two bipolar electrodes placed above and below the left eye (VEOG), and two bipolar electrodes placed on the outer canthi of the eyes (HEOG). The scalp electrodes were mounted on an elastic

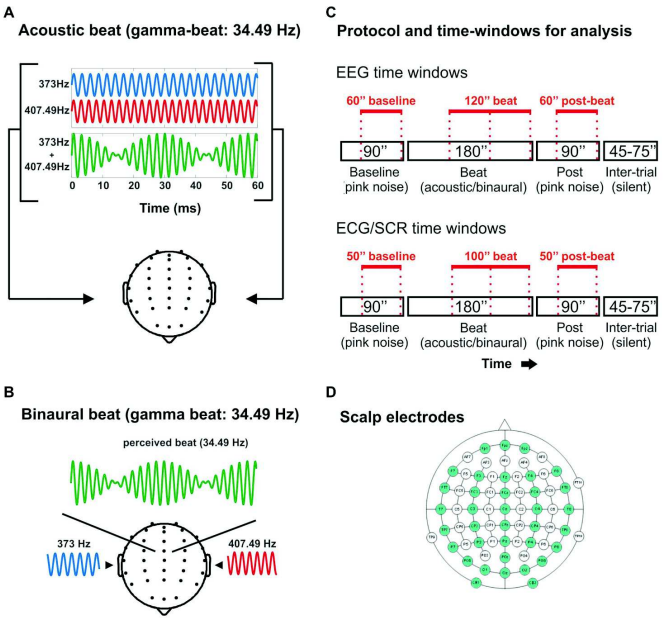

FIGURE 1 | (A) Illustration of the acoustic-beat condition with a beat frequency within the electroencephalographic (EEG) gamma range. Two pure tones of slightly different frequencies (373 Hz and 407.49 Hz) were presented simultaneously to the two ears. Consequently, a beat is generated whose frequency corresponds to the frequency difference between them (34.49 Hz). **(B)** Illustration of the binaural-beat condition with a beat frequency within the EEG gamma range. One pure tone (373 Hz) is presented to one ear while another (407.49 Hz) is presented to the other ear. Thus, a beat whose frequency corresponds to the frequency difference between them (34.49 Hz) is generated within the auditory pathway. **(C)** Experimental protocol and time-windows for analysis. Experimental blocks consisted on 90 s of pink noise, followed by 180 s of acoustic or binaural beat at the corresponding frequency, followed in turn by 90 s of pink noise. In red, the time windows used for the analyses of the EEG band power (EEG: above) and psychophysiological measures (electrocardiogram, ECG and skin conductance response, SCR: below). **(D)** Scalp electrodes used in the EEG recording (in green).

nylon cap (Quickcap, Neuroscan, Compumedics, Charlotte, NC, USA), in accordance with the extended 10–20 system. EEG signals were amplified using SynAmps RT amplifier (NeuroScan, Compumedics, Charlotte, NC, USA), digitized with a sampling rate of 1000 Hz, and online-low-pass filtered to 200 Hz using Neuroscan 4.4 software (NeuroScan, Compumedics, Charlotte, NC, USA). During the acquisition, all electrode impedances were kept below 10 kΩ.

The electrocardiogram and the skin conductance response (SCR) data were acquired using AcqKnowledge 4.2 software and Biopac MP150 acquisition system (Biopac Systems Inc., Goleta, CA, USA), with a sampling rate of 1000 Hz. Electrocardiogram data were collected using the Biopac ECG100C-MRI amplifier (Biopac Systems Inc., Goleta, CA, USA), with disposable Ag–AgCl electrodes aligned in a standard configuration (Right and Left sides of the body, under the rib and right sternum, just below the clavicle). SCR was obtained using the Biopac EDA100C-MRI amplifier (Biopac Systems Inc., Goleta, CA, USA) with the electrodes placed on the upper phalange of the middle and index fingers of the left hand.

Data Analysis

Data from 25 scalp electrodes (F7, F3, Fz, F4, F8, FT7, FC3, FCz, FC4, FT8, T7, C3, Cz, C4, T8, TP7, CP3, CPz, CP4, TP8, P7, P3, Pz, P4, P8), and from HEOG and VEOG channels were analyzed using EEGLAB (Delorme and Makeig, 2004) and Fieldtrip toolboxes (Oostenveld et al., 2011) running on MATLAB. EEG responses were re-referenced to the average of all scalp electrodes, and filtered from 0.1 Hz to 200 Hz. Eye blinks, large saccades and other muscular artifacts were removed from the data by means of Independent Component Analysis (ICA), with the Second Order Blind Identification (SOBI) method (Delorme and Makeig, 2004; Delorme et al., 2007). Since we were interested in induced activity within the EEG gamma band, among others, we followed recommendations from Keren et al. (2010) when performing ICA artifact rejection, to avoid

the contribution of micro-saccade muscular activity to gamma activity at the scalp level (Yuval-Greenberg and Deouell, 2011).

Four epochs of 60 s were defined for analysis of EEG data after disregarding the initial 30 and 60 s of the noise and the beat parts, respectively (**Figure 1C**), to allow the signal to stabilize. The resulting first epoch of each block was considered as "Baseline", the two subsequent epochs, with binaural or acoustic beat stimulation, were called "Beat1" and "Beat2", and the last epoch in the run was considered as post-treatment, and hence called "Post". For the electrocardiogram and SCR data, epochs lasted 50 s, with the noise epochs (Baseline and Post) starting 5 s after and ending 5 s before the pink noise stimulation, and with the two beat epochs arranged as Beat1, which started 10 s after the onset of the beat, and Beat2 ending 10 s before the beat offset (**Figure 1C**).

For each of the EEG epochs, Baseline, Beat1, Beat2 and Post, data were analyzed in the spectral domain, separately for each block and electrode by means of the Fast-Fourier Transform (FFT; Slepian windowed). Separated EEG spectra were calculated for the two epochs of the beat, Beat1 and Beat2, ensuring the frequency resolution in the FFT was identical for the noise and beat epochs. Yet, results from these two beat epochs were averaged together into a single epoch (Beat). In each of the three resulting EEG spectra, Baseline, Beat and Post, for each block, power values were obtained from a window of 3.5 Hz centered at the frequencies of interest, corresponding to the frequencies of the beat stimulation in each block: 4.53 Hz (theta-beat), 8.97 Hz (alpha-beat), 17.93 Hz (beta-beat), 34.49 Hz (gamma-beat) or 57.3 Hz (upper gamma-beat). Power values within these frequency ranges were normalized by means of the following formula:

$$Freq_{dB} = 10 * \log\left(\frac{Pi}{Pa}\right)$$

where Pi is the power value of the frequency of interest in the corresponding block, and Pa is the average power of the frequency of interest in the remaining blocks, for the same epoch (Baseline, Beat or Post) and condition (binaural-beat or acoustic-beat). For example, EEG power in the defined alpha window during the first noise epoch (Baseline) of the binaural alpha-beat block was divided by the average of power in alpha window in the first noise epoch of binaural theta-, beta-, gamma- and upper-gamma-beat blocks. Then, the resulting value was transformed into dB. By means of this transformation, we obtained a normalized power value for each epoch (Baseline, Beat, Post) and for each condition (binaural, acoustic) in each frequency of interest.

Scalp distribution of spectral power within each EEG frequency-window studied (theta, alpha, beta, gamma and upper-gamma) were obtained for illustrative purposes, and analyzed by taking averaged power values within two anterior (one left one right) and two posterior clusters of three electrodes each (F3, FC3, C3; F4, FC4, C4; CP3, P3, O1; CP4, P4, O2). Data from spectral EEG topographies were normalized by dividing the amplitude at each electrode by the sum of squared voltages at all electrodes analyzed per participant and per condition (McCarthy and Wood, 1985). With these analyses, we aimed to disentangle whether binaural beats at each frequency could induce changes in the scalp distribution within EEG bands.

As for the psychophysiological measures, heart rate was calculated from electrocardiogram data as the mean instantaneous heart rate averaged in 50-s time windows with no overlap, resulting in two values during noise epochs (Baseline and Post), and two values, during beat epochs (Beat1 and Beat2), averaged together (Beat). Similarly, we calculated the mean amplitude of the SCR, measured in microSiemens, in 50-s time windows with no overlap, resulting in two values during noise epochs (Baseline and Post), and two values, during beat epochs (Beat1 and Beat2), averaged together (Beat).

Statistical Analysis

Statistical comparisons of normalized EEG spectral power were performed, separately for each of the frequency ranges studied, by means of a three-way repeated measures analysis of variance (ANOVA), with the three factors being Session (three levels: Baseline, Beat, Post), Treatment (two levels: binaural, acoustic) and Electrode (15 levels: 15 electrodes). Similarly, statistical comparisons of heart rate and SCR averages were performed by means of a two-way repeated measures ANOVA, with the two factors being Session (three levels: Baseline, Beat, Post) and Treatment (two levels: binaural, acoustic). We examined Session effects, with significant interactions between Session and Treatment factors.

Analyses of scalp distribution of EEG spectral power were performed, separately for each of the frequency ranges studied, by means of a repeated measures ANOVA with four factors: Session (three levels: Baseline, Beat, Post), Treatment (two levels: binaural, acoustic), Frontality (two levels: anterior or posterior clusters) and Laterality (two factors: left and right clusters).

For EEG spectral power, we aimed to compare the power within the frequency range of interest in the noise epochs with that in the epochs of beat stimulation, separately for acoustic- and binaural-beat conditions. For each frequency of interest, and for each type of beat (binaural or acoustic), increased EEG power in the defined frequency range during epochs of beat stimulation, in comparison of epochs of noise, would indicate an enhancement effect of the stimulation. An interaction with the Treatment factor would indicate if that effect is attributable to the binaural beat. The same rationale applied for changes in heart rate and the SCR.

For each of the comparisons, whenever the assumption of sphericity was violated, degrees of freedom were corrected using Greenhouse-Geisser estimates. The alpha level was set to 0.05. Effect size and observed power values were calculated for each statistical test. For all the statistical analyses, Bonferroni corrections for multiple comparisons were performed to adjust the p-values.

RESULTS

EEG Frequency Analysis

If brainwave entrainment at the specific frequency of the binaural beat had occurred, we would observe a power enhancement at

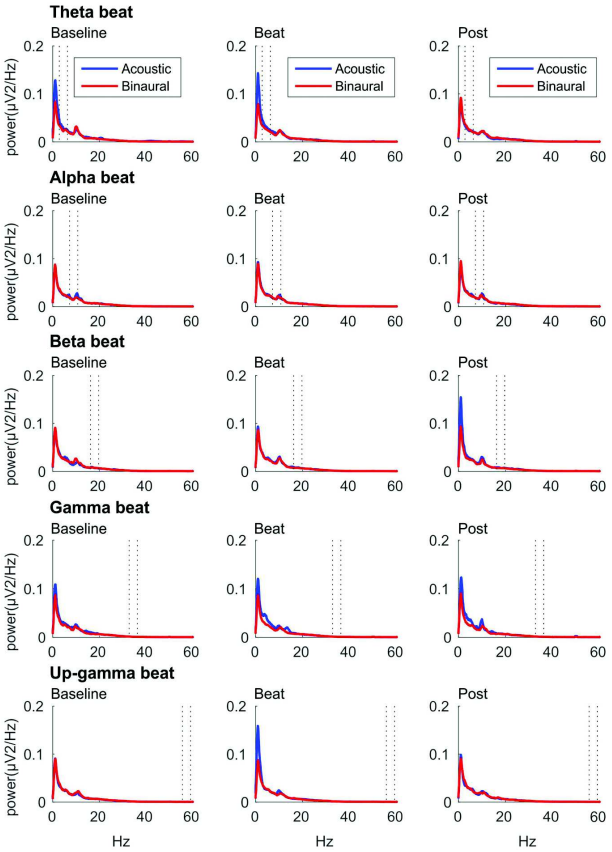

FIGURE 2 | EEG spectra for each epoch of the block (three columns, from left to right: Baseline, Beat, Post) and each of the five beat frequencies of stimulation (five rows, from top to bottom: theta, alpha, beta, gamma and upper gamma), before normalization. Red lines correspond to EEG spectra obtained in binaural-beat blocks, and blue lines in acoustic-beat blocks. Dotted lines in each spectrum show the frequency window from which power values were obtained and normalized for statistical analyses.

that specific frequency in the EEG spectrum when binaural beats were presented. However, such power enhancement was not observed for any of the tested beat frequencies, as well as no differences were observed between the EEG spectra obtained for binaural and acoustic beat conditions in the epochs of auditory stimulation. For illustrative purposes, in **Figure 2** we include the EEG spectrum obtained for each epoch of the block (Baseline, Beat, Post) and each of the five beat frequencies used (theta, alpha, beta, gamma and upper gamma).

After normalization, as summarized in **Table 1**, no significant effects whatsoever were found in the EEG spectral power within the theta, alpha, beta or gamma frequency ranges analyzed. Specifically, ANOVA analyses yielded no effect for the Session factor, indicating no differences in the normalized spectral power values, within the EEG bands analyzed, between the noise and beat epochs of the block. No significant effects were found for the Treatment factor neither, indicating no overall differences between binaural-beat and acoustic-beat stimulation. Furthermore, no interaction between Session and Treatment factors were found. According to these results, no enhancement of EEG spectral power would be induced neither with

TABLE 1 | Results of analysis of variance (ANOVA) on normalized values of electroencephalographic (EEG) power within theta (2.78–6.28 Hz), alpha (7.22–10.72 Hz), beta (16.18–19.68 Hz), gamma (32.74–36.24 Hz) and upper-gamma (55.55–59.05 Hz) bands.

Beat frequency	*df*	*F*	*p*	η_p^2	Observed power[a]
Theta					
Session	2, 22	0.641	0.536	0.055	0.144
Treatment	1, 11	0.662	0.433	0.057	0.116
Session*Treatment	2, 22	1.195	0.180	0.017	0.076
Electrode	24, 264	0.641	0.903	0.055	0.544
Alpha					
Session	2, 22	2.358	0.115	0.154	0.434
Treatment	1, 13	1.010	0.333	0.072	0.154
Session*Treatment	2, 26	0.611	0.551	0.045	0.141
Electrode	24, 264	3.253	**>0.001**	0.200	1
Beta					
Session	2, 26	0.594	0.559	0.044	0.138
Treatment	1, 13	0.026	0.874	0.002	0.053
Session*Treatment	1.22, 15.96	0.554	0.582	0.041	0.132
Electrode	24, 264	0.641	0.904	0.047	0.550
Gamma					
Session	1.43, 18.6	0.019	0.981	0.001	0.053
Treatment	1, 13	0.081	0.781	0.006	0.058
Session*Treatment	2, 26	1.273	0.297	0.089	0.251
Electrode	3.08, 40.05	1.401	0.254	0.097	0.364
Upper-gamma					
Session	1.43, 18.6	1.185	0.312	0.084	0.236
Treatment	1, 13	0.811	0.384	0.059	0.133
Session*Treatment	2, 26	0.089	0.915	0.007	0.062
Electrode	24, 264	2.743	0.054	0.174	0.628

*Session factor includes three levels refering to the different epochs of the block (Baseline, Beat and Post), whereas Treatment factor refers to binaural or acoustic beat condition. Session*Treatment refers to the interaction between them. Electrode factor includes 25 levels for the 25 electrodes analyzed. For each factor and their interaction, degrees of freedom (df), F and p values, size effects (η_p^2) and observed power are presented. P values below 0.05 are highlighted in bold. P values in the table are non-corrected for multiple comparisons. [a]calculated for alpha = 0.05.*

binaural or with acoustic beats of the reported frequencies. With binaural beats in the upper gamma frequency, which cannot be perceived (Licklider et al., 1950), EEG spectral power in the upper gamma frequency range analyzed showed no significant increase in relation to acoustic beats.

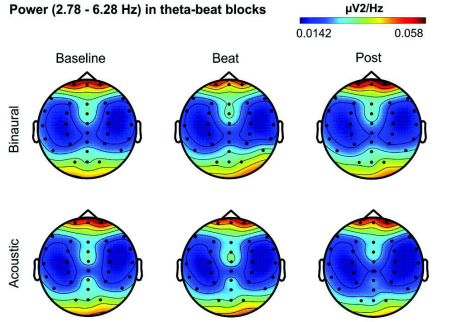

FIGURE 3 | Scalp distribution of EEG spectral power during blocks with theta-beat stimulation. From left to right, scalp maps correspond to Baseline, Beat, Post epochs of the blocks, respectively. On top, scalp maps in blocks with binaural-beat stimulation. At the bottom, scalp maps in blocks with acoustic-beat stimulation. EEG spectral power corresponds to a frequency window of 3.5 Hz around the frequency of stimulation (4.53 Hz). Black dots correspond to electrode positions.

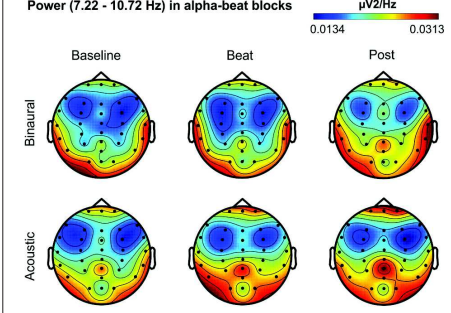

FIGURE 4 | Scalp distribution of EEG spectral power during blocks with alpha-beat stimulation. From left to right, scalp maps correspond to Baseline, Beat, Post epochs of the blocks, respectively. On top, scalp maps in blocks with binaural-beat stimulation. At the bottom, scalp maps in blocks with acoustic-beat stimulation. EEG spectral power corresponds to a frequency window of 3.5 Hz around the frequency of stimulation (8.97 Hz). Black dots correspond to electrode positions.

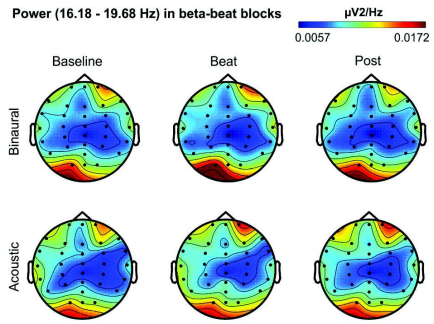

FIGURE 5 | Scalp distribution of EEG spectral power during blocks with beta-beat stimulation. From left to right, scalp maps correspond to Baseline, Beat, Post epochs of the blocks, respectively. On top, scalp maps in blocks with binaural-beat stimulation. At the bottom, scalp maps in blocks with acoustic-beat stimulation. EEG spectral power corresponds to a frequency window of 3.5 Hz around the frequency of stimulation (17.93 Hz). Black dots correspond to electrode positions.

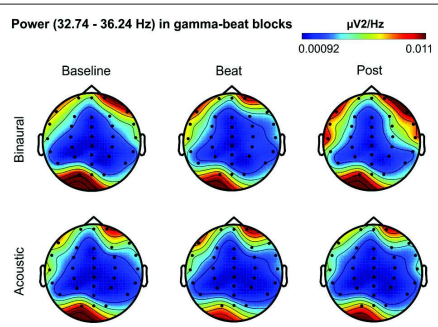

FIGURE 6 | Scalp distribution of EEG spectral power during blocks with gamma-beat stimulation. From left to right, scalp maps correspond to Baseline, Beat, Post epochs of the blocks, respectively. On top, scalp maps in blocks with binaural-beat stimulation. At the bottom, scalp maps in blocks with acoustic-beat stimulation. EEG spectral power corresponds to a frequency window of 3.5 Hz around the frequency of stimulation (34.49 Hz). Black dots correspond to electrode positions.

Besides changes in EEG spectra, we also examined differences in the spectral EEG topographies among conditions. In **Figures 3**–**7**, we show the scalp distribution of EEG spectral power within the theta, alpha, beta, gamma and upper gamma bands studied, respectively, for the Baseline, Beat and Post epochs of the blocks. For this analysis, we used two anterior and two posterior clusters of electrodes, aiming to explore interactions between Session or Treatment

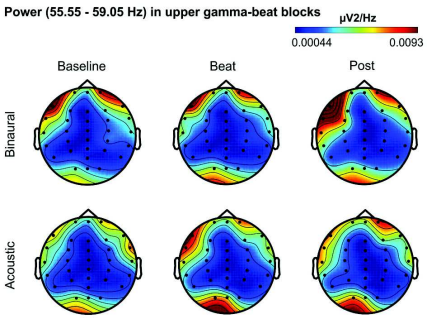

FIGURE 7 | Scalp distribution of EEG spectral power during blocks with upper-gamma-beat stimulation. From left to right, scalp maps correspond to Baseline, Beat, Post epochs of the blocks, respectively. On top, scalp maps in blocks with binaural-beat stimulation. At the bottom, scalp maps in blocks with acoustic-beat stimulation. EEG spectral power corresponds to a frequency window of 3.5 Hz around the frequency of stimulation (57.3 Hz). Black dots correspond to electrode positions.

factors with different regions of the scalp (studied through Frontality and Laterality factors). If binaural beats would affect the distribution of EEG spectral power across the scalp, we would observe an interaction between Session and Treatment factors, and Frontality and/or Laterality factors. That is, changes in spectral power would be different across different Frontality or Laterality levels, thus revealing different topographical distributions of EEG spectral power. However, no significant interactions between Session or Treatment, and Frontality or Laterality factors, were found within any of the EEG bands tested. In topographies within alpha band, only two triple interactions between Session, Treatment and Frontality ($F_{(2,24)}$ = 3.829, p = 0.036), and between Session, Frontality and Laterality ($F_{(2,24)}$ = 4.055, p = 0.030) yielded p values below 0.05 which, however, did not survive the Bonferroni correction for the multiple comparisons. The same occurred for topographies within upper gamma band, where an interaction between Session and Laterality ($F_{(2,24)}$ = 4.891, p = 0.017) vanished out after the Bonferroni correction.

Psychophysiological Measures

As summarized in **Table 2**, analyses on the two psychophysiological measures studied yielded negative results for beta- and gamma-beat stimulation, as well as for the upper gamma condition. ANOVA showed no effects of Session or Treatment factors, as well as no interaction between them, neither for heart rate or for skin conductance measures. With regard to the SCR for theta- and alpha-beats, the ANOVA yielded p values below 0.05 for the Session factor (**Table 2**) which, nevertheless, vanished out after the Bonferroni correction for the multiple comparisons.

TABLE 2 | Results of ANOVA on heart rate and skin conductance response (SCR; microSiemens) values in blocks of theta (4.53 Hz), alpha (8.97 Hz), beta (17.93 Hz), gamma (34.49 Hz) and upper-gamma (57.3 Hz) stimulation.

Heart rate	*df*	*F*	*p*	η_p^2	Observed power[a]
Theta-beat					
Session	2, 26	2.560	0.097	0.165	0.466
Treatment	1, 13	0.314	0.585	0.024	0.082
Session*Treatment	2, 26	0.883	0.425	0.064	0.185
Alpha-beat					
Session	2, 26	0.950	0.400	0.068	0.197
Treatment	1, 13	1.586	0.230	0.109	0.215
Session*Treatment	2, 26	0.049	0.952	0.004	0.057
Beta-beat					
Session	2, 26	0.640	0.535	0.047	0.145
Treatment	1, 13	0.993	0.337	0.071	0.152
Session*Treatment	2, 26	0.314	0.733	0.024	0.095
Gamma-beat					
Session	2, 26	0.156	0.854	0.012	0.072
Treatment	1, 13	0.603	0.451	0.044	0.111
Session*Treatment	2, 26	0.370	0.694	0.028	0.103
Upper-gamma-beat					
Session	2, 26	2.901	0.073	0.182	0.518
Treatment	1, 13	0.030	0.865	0.002	0.053
Session*Treatment	2, 26	1.514	0.239	0.104	0.293
Skin conductance					
Theta-beat					
Session	2, 26	3.934	**0.032**	0.232	0.655
Treatment	1, 13	2.164	0.165	0.143	0.276
Session*Treatment	2, 26	1.109	0.345	0.079	0.223
Alpha-beat					
Session	2, 26	4.845	**0.016**	0.271	0.751
Treatment	1, 13	0.001	0.980	0.000	0.050
Session*Treatment	1.39, 18.05	0.999	0.359	0.071	0.174
Beta-beat					
Session	2, 26	0.102	0.903	0.008	0.064
Treatment	1, 13	0.444	0.517	0.033	0.095
Session*Treatment	2, 26	0.294	0.748	0.022	0.092
Gamma-beat					
Session	2, 26	0.021	0.980	0.002	0.053
Treatment	1, 13	0.067	0.800	0.005	0.057
Session*Treatment	2, 26	1.411	0.262	0.098	0.275
Upper-gamma-beat					
Session	2, 26	1.225	0.310	0.086	0.243
Treatment	1, 13	0.655	0.433	0.048	0.117
Session*Treatment	2, 26	0.963	0.395	0.069	0.199

*Session factor includes three levels refering to different epochs of the block (Baseline, Beat and Post), whereas Treatment factor refers to binaural or acoustic beat condition. Session*Treatment refers to the interaction between them. For each factor and their interaction, degrees of freedom (df), F and p values, size effects (η_p^2) and observed power are presented. P values below 0.05 are highlighted in bold. P values in the table are non-corrected for multiple comparisons. [a]calculated for alpha = 0.05.*

These results indicate that no changes occurred in these psychophysiological parameters between the noise and beat epochs the block, neither with binaural or with acoustic theta-, alpha-, beta-, gamma- or upper gamma-beats, as well as there were no overall differences between the effects of the two types of beats.

Despite being not statistically significant, it is interesting to notice that, in the case of alpha-beat stimulation, skin conductance increased along the block, contrary to what would be expected if we consider increased SCR as associated to stress (see **Figure 8A**). In contrast, there was a decrease in skin conductance along the block with theta-beat stimulation, suggesting a relaxation effect with beats in this range, independently of the type of beat (see **Figure 8B**). Such trends along the session occur only with the two slowest beat frequencies studied here, theta and alpha, the typical beat frequencies reported in previous studies as related to clinically relevant psychophysiological dimensions (Padmanabhan et al., 2005; McConnell et al., 2014; Palaniappan et al., 2015).

DISCUSSION

Summary of Results

The main goal of the present study was to disentangle the specific contribution of binaural-beat stimulation at different beat frequencies on specific EEG frequency bands. Particularly, we aimed to explore binaural beat effects on EEG power. Results yielded no effects of binaural beats in the theta, alpha, beta, gamma and upper gamma beat frequencies in the enhancement

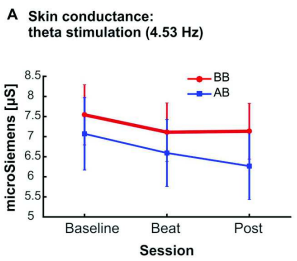

FIGURE 8 | (A) SCR (microSiemens) during blocks with binaural beats (BB; red) or acoustic beats (AB; blue) of theta frequency (4.53 Hz). **(B)** SCR (microSiemens) during blocks with BB (red) or AB (blue) of alpha frequency (8.97 Hz). Error bars show the standard error of the mean.

of EEG spectral power in their corresponding frequencies; similar negative results were also obtained with acoustic beats. Additionally, no effects from binaural or acoustic beats in the spectral EEG topographies were found either. As a secondary objective, we aimed to study whether binaural-beat stimulation would induce changes in two psychophysiological parameters, heart rate and skin conductance. Both binaural and acoustic beats produced no effect on these measures, although theta and alpha beats, independently on whether they were acoustic or binaural, yielded changes in skin conductance, yet vanishing out after multiple-comparison correction.

Effects of Binaural Beats on Brain Rhythms

Previous attempts to study binaural beats have hypothesized that oscillatory brain activity recorded through EEG could be modulated by binaural beats of specific frequencies. Particularly, we focused on studies where binaural beats would induce changes in EEG power. The modulation of EEG rhythms would be genuinely generated by the binaural beat and would be distinct from the one produced with an acoustic beat, as binaural beats are generated within the central auditory system. Our results for all the beat frequencies tested do not support this hypothesis, and suggest no enhancement of EEG spectral power within classical EEG bands is induced with binaural beats. Using beats in the theta frequency range, with frequencies from 5 Hz to 8.5 Hz, similar negative results were found by Stevens et al. (2003), Wahbeh et al. (2007) and, more recently, Gao et al. (2014), who failed to elicit an increase in theta EEG band. In all these studies, binaural beat stimulation had longer duration than in the present study, up to 4 h, yet they yielded similar negative results on EEG theta band. For beats with frequencies within the EEG alpha band, our results go in accordance with those of Gao et al. (2014) and Vernon et al. (2014) in finding no increase in EEG alpha band with binaural-beat stimulation. Similarly, for binaural beta-beats, although findings of increased performance in cognitive-demanding tasks suggested promising results, we failed to observe a power enhancement on the EEG beta band analyzed, in accordance with findings from previous studies (Goodin et al., 2012; Gao et al., 2014; Vernon et al., 2014).

Regarding binaural gamma-beats, our results within gamma band contrast with findings from Lavallee et al. (2011), which suggested enhancement of EEG gamma band relative to baseline using binaural beats. However, binaural beat frequencies used to achieve such results were in the beta range (15 Hz). Furthermore, Becher et al. (2015) reported an EEG spectral power increase with acoustic beats of 40 Hz, contrasting with our negative results with gamma-beats, with similar frequencies. Our results also contrast with others assessing binaural beats effects on cognitive functions associated with gamma band, such as selective attention (Gruber et al., 1999; Sokolov et al., 2004). In this regard, Reedijk et al. (2015) reported improvements in selective attention with binaural-beat stimulation at gamma frequency, but the present findings suggest the mechanism by which such improvements were obtained do not involve EEG gamma band enhancement. Finally, binaural beats in the upper gamma range (e.g., 57.3 Hz), exceeding the frequency limit for the perception of binaural beats (Licklider et al., 1950), seem unable to induce changes in the corresponding EEG spectral power.

One limitation to take into consideration for the lack of positive findings in the present study is the sample size (14 participants), which may be too small to yield a statistically significant result in the event that a real effect of binaural beats may exist. As reported in the results' tables, the observed power of our ANOVA tests is overall small. Therefore, caution should be taken when interpreting the present negative results, as the sample size may account for the null effects reported.

Previous studies on event-related potential modulation and auditory steady-state responses suggest that entrainment effects occur within seconds of the binaural beat stimulation (Karino et al., 2006; Kasprzak, 2011). Additionally, as mentioned, in previous studies testing the same hypothesis binaural beats were presented for a longer duration obtaining similar negative results (Wahbeh et al., 2007; Goodin et al., 2012; Gao et al., 2014). Therefore, we consider unlikely that the lack of increased EEG spectral power within specific bands in the present study is related with the short duration of 3 min used here for beat stimulation. In this regard, as suggested by some authors (Becher et al., 2015), another important factor to consider when trying to induce changes in EEG oscillatory activity at a particular frequency is the use of continuous tones or short repetitive bursts of stimulation. Studies recording evoked responses to binaural beats typically used short bursts of binaural beat stimulation. For example, Schwarz and Taylor (2005) elicited

a 40 Hz binaural beat auditory steady-state response with binaural beats presented in short bursts of 1200 ms, with intervals of 1200 ms; Draganova et al. (2008), similarly, found a 40 Hz auditory steady-state response using pure tones of 1000 ms duration and 2000 ms stimulus onset asynchrony, and Pratt et al. (2010) elicited event-related potential components followed by oscillations corresponding to 3 and 6 Hz binaural beats, using bursts of 2000 ms, with inter-stimulus intervals between 950 ms and 1050 ms. On the other hand, some other studies investigating induced EEG oscillatory activity with binaural beats (Wahbeh et al., 2007; Goodin et al., 2012; Gao et al., 2014; Vernon et al., 2014) used, like we did, continuous stimulation, and expected enhancement of power along the whole session. Thus, in the context of previous studies, the use of continuous presentation instead of short burst for stimulation seems appropriate, and is probably not related with the lack of effects observed here for the EEG bands studied.

Apart from results in the EEG spectra, spectral EEG topographies within theta, alpha, beta, gamma and upper gamma frequencies did not seem to be affected by binaural beats in their corresponding frequencies. This suggests that binaural beats do not have any impact in scalp distribution of EEG spectral power neither.

Psychophysiological Measures

Our results on heart rate and skin conductance do no support the proposal suggesting an effect of binaural beats on measures related with emotional arousal. In contrast with previous findings on heart rate variability (Palaniappan et al., 2015), parasympathetic activation (McConnell et al., 2014) or anxiety (Padmanabhan et al., 2005), we did not find a specific effect of binaural beat on heart rate and skin conductance for any of the beat frequencies tested here. On the other hand, our results go in accordance with the findings of Chaieb et al. (2015) regarding diminishing effects of binaural-beat stimulation on anxiety levels. Thus, our results suggest no effects of binaural or acoustic beats on autonomic responses. A limitation to consider when interpreting such lack of effects, as in the case of EEG analyses, is the small observed power of our statistical tests, given our small sample size. Another possible limitation is the short duration of stimulation used in the present study (3 min), which highly contrasts with the length of the stimulation used in previous studies (e.g., 20 and 30 min in Padmanabhan et al., 2005; McConnell et al., 2014 respectively). Whereas the stimulation length used in the present study may be appropriate to investigate effects on the EEG, it could be insufficient to induce changes in psychophysiological parameters, such as heart rate and skin conductance.

CONCLUSION

This study has provided a thorough research on the potential effects of binaural-beat stimulation on enhancing EEG activity on specific frequency bands. Our aim was to verify the theoretical assumption on the effects of binaural beats in both EEG rhythms and psychophysiological responses. The literature on the field was inconclusive: we reviewed studies on the effects of binaural beats in EEG oscillatory activity, as well as on the effects of binaural beats in measures related with autonomic responses. We performed an experimental design using rigorous methodological controls, with baseline-treatment-washout sessions and treatment vs. "placebo" condition (a beat with the same frequency, but generated acoustically).

No effects of binaural-beat stimulation on EEG spectral power occurred with beat frequencies belonging to theta, alpha, beta, or gamma EEG ranges, as well as with those belonging to upper gamma band. On the other hand, our measures of heart rate and skin conductance did not support the effect of binaural beats on emotional arousal. Thus, our results altogether do not support binaural beats as a potential brainwave entrainment tool, nor they suggest any beneficial effect on clinically relevant dimensions.

AUTHOR CONTRIBUTIONS

FL-C and CE designed the study, designed and carried out data analysis and wrote the manuscript. FL-C supervised data acquisition.

ACKNOWLEDGMENTS

This work was supported by the Spanish Ministry of Economy and Knowledge (PSI2015-63664-P), the Catalan Government (SGR2017-974) and the ICREA Academia Distinguished Professorship awarded to CE. Special thanks to Andrea Canturri, Koldo González and Pablo Reguilon, for their help in data collection and analysis.

REFERENCES

Becher, A. K., Höhne, M., Axmacher, N., Chaieb, L., Elger, C. E., and Fell, J. (2015). Intracranial electroencephalography power and phase synchronization changes during monaural and binaural beat stimulation. *Eur. J. Neurosci.* 41, 254–263. doi: 10.1111/ejn.12760

Brady, B., and Stevens, L. (2000). Binaural-beat induced theta EEG activity and hypnotic susceptibility. *Am. J. Clin. Hypn.* 43, 53–69. doi: 10.1080/00029157.2000.10404255

Brainard, D. H. (1997). The psychophysics toolbox. *Spat. Vis.* 10, 433–436. doi: 10.1163/156856897x00357

Chaieb, L., Wilpert, E. C., Reber, T. P., and Fell, J. (2015). Auditory beat stimulation and its effects on cognition and mood states. *Front. Psychiatry* 6:70. doi: 10.3389/fpsyt.2015.00070

Delorme, A., and Makeig, S. (2004). EEGLAB: an open source toolbox for analysis of single-trial EEG dynamics including independent component analysis. *J. Neurosci. Methods* 134, 9–21. doi: 10.1016/j.jneumeth.2003.10.009

Delorme, A., Sejnowski, T., and Makeig, S. (2007). Enhanced detection of artifacts in EEG data using higher-order statistics and independent component analysis. *Neuroimage* 34, 1443–1449. doi: 10.1016/j.neuroimage.2006.11.004

Dove, H. W. (1841). über die combination der eindrücke beider ohren und beider augen zu einem eindruck. *Monat. Ber. Akad.* 41, 251–252.

Draganova, R., Ross, B., Wollbrink, A., and Pantev, C. (2008). Cortical steady-state responses to central and peripheral auditory beats. *Cereb. Cortex* 18, 1193–1200. doi: 10.1093/cercor/bhm153

Gao, X., Cao, H., Ming, D., Qi, H., Wang, X., Wang, X., et al. (2014). Analysis of EEG activity in response to binaural beats with different frequencies. *Int. J. Psychophysiol.* 94, 399–406. doi: 10.1016/j.ijpsycho.2014.10.010

Goodin, P., Ciorciari, J., Baker, K., Carrey, A. M., Harper, M., and Kaufman, J. (2012). A high-density EEG investigation into steady state binaural beat stimulation. *PLoS One* 7:e34789. doi: 10.1371/journal.pone.0034789

Gruber, T., Müller, M. M., Keil, A., and Elbert, T. (1999). Selective visual-spatial attention alters induced gamma band responses in the human EEG. *Clin. Neurophysiol.* 110, 2074–2085. doi: 10.1016/s1388-2457(99)00176-5

Herrmann, C. S., Strüber, D., Helfrich, R. F., and Engel, A. K. (2016). EEG oscillations: from correlation to causality. *Int. J. Psychophysiol.* 103, 12–21. doi: 10.1016/j.ijpsycho.2015.02.003

Huang, T. L., and Charyton, C. (2008). A comprehensive review of the psychological effects of brainwave entrainment. *Altern. Ther. Health Med.* 14, 38–50.

Ioannou, C. I., Pereda, E., Lindsen, J. P., and Bhattacharya, J. (2015). Electrical brain responses to an auditory illusion and the impact of musical expertise. *PLoS One* 10:e0129486. doi: 10.1371/journal.pone.0129486

Karino, S., Yumoto, M., Itoh, K., Uno, A., Yamakawa, K., Sekimoto, S., et al. (2006). Neuromagnetic responses to binaural beat in human cerebral cortex. *J. Neurophysiol.* 96, 1927–1938. doi: 10.1152/jn.00859.2005

Kasprzak, C. (2011). Influence of binaural beats on EEG signal. *Acta Phys. Pol. A* 119, 986–990. doi: 10.12693/aphyspola.119.986

Kennerly, R. (1996). An empirical investigation into the effect of beta frequency binaural beat audio signals on four measures of human memory. *Hemi-Synch J.* 14, 1–4.

Keren, A. S., Yuval-Greenberg, S., and Deouell, L. Y. (2010). Saccadic spike potentials in gamma-band EEG: characterization, detection and suppression. *Neuroimage* 49, 2248–2263. doi: 10.1016/j.neuroimage.2009.10.057

Kleiner, M., Brainard, D. H., Pelli, D., and Broussard, C. (2007). What's new in psychtoolbox-3? *Perception* 36, 1–16. doi: 10.1068/v070821

Kuwada, S., Yin, T. C., and Wickesberg, R. E. (1979). Response of cat inferior colliculus neurons to binaural beat stimuli: possible mechanisms for sound localization. *Science* 206, 586–588. doi: 10.1126/science.493964

Lane, J. D., Kasian, S. J., Owens, J. E., and Marsh, G. R. (1998). Binaural auditory beats affect vigilance performance and mood. *Physiol. Behav.* 63, 249–252. doi: 10.1016/s0031-9384(97)00436-8

Lavallee, C. F., Koren, S. A., and Persinger, M. A. (2011). A quantitative electroencephalographic study of meditation and binaural beat entrainment. *J. Altern. Complement. Med.* 17, 351–355. doi: 10.1089/acm.2009.0691

Licklider, J. C. R., Webster, J. C., and Hedlun, J. M. (1950). On the frequency limits of binaural beats. *J. Acoust. Soc. Am.* 22, 468–473. doi: 10.1121/1.1906629

McAlpine, D., Jiang, D., and Palmer, A. R. (1996). Interaural delay sensitivity and the classification of low best-frequency binaural responses in the inferior colliculus of the guinea pig. *Hear. Res.* 97, 136–152. doi: 10.1016/0378-5955(96)00068-8

McCarthy, G., and Wood, C. C. (1985). Scalp distributions of event-related potentials: an ambiguity associated with analysis of variance models. *Electroencephalogr. Clin. Neurophysiol.* 62, 203–208. doi: 10.1016/0168-5597(85)90015-2

McConnell, P. A., Froeliger, B., Garland, E. L., Ives, J. C., and Sforzo, G. A. (2014). Auditory driving of the autonomic nervous system: listening to theta-frequency binaural beats post-exercise increases parasympathetic activation and sympathetic withdrawal. *Front. Psychol.* 5:1248. doi: 10.3389/fpsyg.2014.01248

Moore, B. C. J. (1997). *An Introduction to the Psychology of Hearing.* San Diego, CA: Academic Press.

Oostenveld, R., Fries, P., Maris, E., and Schoffelen, J. M. (2011). FieldTrip: open source software for advanced analysis of MEG, EEG, and invasive electrophysiological data. *Comput. Intell. Neurosci.* 2011:156869. doi: 10.1155/2011/156869

Padmanabhan, R., Hildreth, A. J., and Laws, D. (2005). A prospective, randomised, controlled study examining binaural beat audio and pre-operative anxiety in patients undergoing general anaesthesia for day case surgery. *Anaesthesia* 60, 874–877. doi: 10.1111/j.1365-2044.2005.04287.x

Palaniappan, R., Phon-Amnuaisuk, S., and Eswaran, C. (2015). On the binaural brain entrainment indicating lower heart rate variability. *Int. J. Cardiol.* 190, 262–263. doi: 10.1016/j.ijcard.2015.04.175

Pelli, D. G. (1997). The video toolbox software for visual psychophysics: transforming numbers into movies. *Spat. Vis.* 10, 437–442. doi: 10.1163/156856897x00366

Pratt, H., Starr, A., Michalewski, H. J., Dimitrijevic, A., Bleich, N., and Mittelman, N. (2010). A comparison of auditory evoked potentials to acoustic beats and to binaural beats. *Hear. Res.* 262, 34–44. doi: 10.1016/j.heares.2010.01.013

Reedijk, S. A., Bolders, A., Colzato, L. S., and Hommel, B. (2015). Eliminating the attentional blink through binaural beats: a case for tailored cognitive enhancement. *Front. Psychiatry* 6:82. doi: 10.3389/fpsyt.2015.00082

Reedijk, S. A., Bolders, A., and Hommel, B. (2013). The impact of binaural beats on creativity. *Front. Hum. Neurosci.* 7:786. doi: 10.3389/fnhum.2013.00786

Ross, B., Miyazaki, T., Thompson, J., Jamali, S., and Fujioka, T. (2014). Human cortical responses to slow and fast binaural beats reveal multiple mechanisms of binaural hearing. *J. Neurophysiol.* 112, 1871–1884. doi: 10.1152/jn.00224.2014

Schwarz, D. W., and Taylor, P. (2005). Human auditory steady state responses to binaural and monaural beats. *Clin. Neurophysiol.* 116, 658–668. doi: 10.1016/j.clinph.2004.09.014

Sokolov, A., Pavlova, M., Lutzenberger, W., and Birbaumer, N. (2004). Reciprocal modulation of neuromagnetic induced gamma activity by attention in the human visual and auditory cortex. *Neuroimage* 22, 521–529. doi: 10.1016/j.neuroimage.2004.01.045

Spitzer, M. W., and Semple, M. N. (1998). Transformation of binaural response properties in the ascending auditory pathway: influence of time-varying interaural phase disparity. *J. Neurophysiol.* 80, 3062–3076.

Stevens, L., Haga, Z., Queen, B., Brady, B., Adams, D., Gilbert, J., et al. (2003). Binaural beat induced theta EEG activity and hypnotic susceptibility: contradictory results and technical considerations. *Am. J. Clin. Hypn.* 45, 295–309. doi: 10.1080/00029157.2003.10403543

Thompson, S. P. (1877). XXXVI. On binaural audition. *Lond. Edinb. Dubl. Philos. Mag. J. Sci.* 4, 274–276. doi: 10.1080/14786447708639338

Vernon, D. (2009). *Human Potential: Exploring Techniques Used to Enhance Human Performance.* London: Routledge.

Vernon, D., Peryer, G., Louch, J., and Shaw, M. (2014). Tracking EEG changes in response to alpha and beta binaural beats. *Int. J. Psychophysiol.* 93, 134–139. doi: 10.1016/j.ijpsycho.2012.10.008

Wahbeh, H., Calabrese, C., and Zwickey, H. (2007). Binaural beat technology in humans: a pilot study to assess psychologic and physiologic effects. *J. Altern. Complement. Med.* 13, 25–32. doi: 10.1089/acm.2006.6196

Wernick, J. S., and Starr, A. (1968). Binaural interaction in the superior olivary complex of the cat: an analysis of field potentials evoked by binaural-beat stimuli. *J. Neurophysiol.* 31, 428–441.

Yuval-Greenberg, S., and Deouell, L. Y. (2011). Scalp-recorded induced γ-band responses to auditory stimulation and its correlations with saccadic muscle-activity. *Brain Topogr.* 24, 30–39. doi: 10.1007/s10548-010-0157-7

Conflict of Interest Statement: The authors declare that the research was conducted in the absence of any commercial or financial relationships that could be construed as a potential conflict of interest.

Summary of results

In the first study, as shown in Figures 2 and 3 of the corresponding publication, effects of deviant probability were found for LLR but not for MLR. Even though MLR has been consistently proven to encode for regularities in the acoustic environment, it appears that the MLR generating system is not sensitive to changes in deviant probability. In other words, the MLR generating system is sensitive to regularity violations, but not to the probability with which the encoded regularities are disrupted. Such sensitivity is however present at latter components in the LLR, such as the MMN. Thus, we show yet another dissociation between MLR and LLR generating systems that goes in accordance with previous studies on deviance magnitude (Aghamolaei et al., 2015) or complex regularity violations (Cornella et al., 2012). These studies revealed that only at latter components of the human AEP specific characteristics of the regularity violations, such as the deviance magnitude, can be indexed. Therefore, our findings suggest a functional dissociation between two different elements of the auditory hierarchy, as reflected in MLR and LLR.

In the second study, we aimed to assess the cortical contribution to the scalp-recorded FFR with different stimulus frequencies. Results showed that the continuous Theta Burst Stimulation (cTBS) technique used for the transient inactivation of the right auditory cortex did not produce a significant modulation in the FFRs recorded (Figures 2, 3 and 4 of corresponding manuscript), neither with low nor with high frequency stimulation. No effect was observed in the ABR and LLR components neither (Figures 5 and 6), despite LLR known contributions from auditory cortex. Such results did not allow us to conclude or discard a cortical contribution to the FFR, since no effects were found on LLR, that is, no effect on cortical potentials was observed with cTBS. Reasons behind the lack of effects discussed include compensatory effects from the left hemisphere, variability in the effectiveness of this pulse among individuals, and the stimulation target being too deep for the TMS to reach (Heschl's gyrus).

In the third study, we studied induced brain oscillations with binaural beats, and no effects of binaural-beat stimulation on EEG spectral power occurred with beat frequencies belonging to theta, alpha, beta, or gamma EEG ranges, as well as with those belonging to upper gamma band (see Figure 2 of corresponding publication). Thus, our results altogether did not support binaural beats as a potential tool to induce ongoing oscillatory activity in the brain. As a secondary finding, we also provide evidence towards binaural beats lack of effects to

modulate autonomic responses, such as heart rate and skin conductance, in a significant manner. Given the controversy on the literature on induced brain oscillatory activity with binaural beats, results from this study, using strict controls, with treatment versus placebo, and baseline-treatment-washout sessions, provide a valuable piece of evidence towards the understanding of these auditory illusions and its effects on the EEG signal.

General discussion

With the three studies of the present thesis, we hope to have contributed to the knowledge of two different mechanisms of the auditory brain function as reflected in two main domains of EEG activity, evoked and induced. Specifically, the questions addressed concerned, first, different brain auditory evoked responses (MLR: Picton et al., 1974; and MMN component of the LLR: Näätanen, Gaillard and Mäntysalo, 1978) to acoustic stimuli breaking a previous stablished regularity, allowing for the better understanding on the hierarchical organization of deviance detection along different stages of the auditory pathway. Second, a traditionally brainstem-associated auditory evoked potential whose neural generators are currently under discussion, the FFR (see Skoe and Kraus, 2010; Bidelman, 2018), aiming to better characterize the neural generators of this response and, thus, the mechanisms of neural phase-locking to external stimuli that it reflects. The third question addressed on the present thesis concerned the analysis of brain rhythms, or ongoing brain oscillations, a different phenomenon than evoked activity that reflects higher order processes of information transfer (Singer and Gray, 1995) and is associated with several cognitive functions (e.g., Mathewson et al., 2009; Kamiński, et al., 2012), with the objective to disentangle whether different brain rhythms could be induced by means of binaural beat stimuli. Across all three studies, we aimed to contribute to the better understanding of the neurophysiological basis of auditory perception and, for all these questions, EEG, given its temporal resolution, served as the main tool for the study of the auditory system, matching its characteristic temporal precision (Kraus et al, 2017; Long, et al., 2018).

Hierarchical organization of deviance detection under predictive coding theory

Going further in the interpretation of our results, beyond the individual discussion on each article, new insights on the hierarchical organization of deviance detection phenomena along the auditory pathway are provided by predictive coding theory (see Heilbron and Chait, 2017), which may help explain the findings from the first study. Within this comprehensive theoretical framework, as mentioned in the introduction, deviance detection signals are partially the result of a mismatch between the representation of an incoming

stimulus and the predictive model generated internally, rather than the result of a comparison with a memory-trace (Näätänen et al., 1978) or solely neuronal refractoriness (adaptation hypothesis; May et al., 1999). Interestingly, according to predictive coding theory, predictions on the incoming stimulus are generated hierarchically so that specific inferences of progressively greater complexity are built from lower to higher stages of the auditory processing (see Carbajal and Malmierca, 2018 for a review). For instance, in a local/global paradigm (e.g., AAAB AAAB AAAB; Chennu et al., 2016), predictions on the local rule would be performed at lower stages of the hierarchy (e.g., the stimulus A is going to be next), whereas prediction on the global rule (e.g., stimulus B is coming after the third stimulus A) would only occur at higher levels. Consequently, in the context of a highly interconnected network, the same stimulus may generate prediction error signals in one stage of the hierarchy while being redundant (predicted) in another, and therefore suppressed by repetition suppression mechanisms (Barlow 1961; Friston 2005). Moreover, given that at lower stages predictions are based on very basic interstimulus relationships, these can be explained by simple synaptic depression. However, moving forward in the hierarchy, from lemniscal to non-lemniscal regions and from brainstem nuclei to cortical regions, recent evidence from animal studies suggests synaptic depression accounts for progressively less deviance detection signal, thus revealing a true prediction error mechanism that is more prominent as we go up in the hierarchy (using cascade or multi-standard controls; Parras, Nieto-Diego, Carbajal, Valdés-Baizabal, Escera and Malmierca, 2017; see Carbajal and Malmierca, 2018 –their Figure 1D-).

In our first study, the suggested progressively greater presence of a genuine prediction error mechanism along the auditory hierarchy, above simple adaptation, may help re-interpret the functional dissociation observed. We used an oddball location paradigm to elicit deviance detection responses, a very simple repetition-based regularity to which deviance detection signals were obtained at both lower and higher stages of the auditory hierarchy (as reflected by MLR and LLR). Instead of increasing the complexity of the rule, which would prevent deviance responses to appear at lower stages of the hierarchy (Althen, et al., 2013; see Escera and Malmierca, 2014), here the experimental manipulation was performed over the probability of the deviant tone, comparing evoked responses to deviant with those to reversed standard (the same physical sound from the same location but with standard probability). Such manipulation produced prediction error responses that were larger as the probability of the deviant was smaller (20%, 10% or 5%), but only at higher levels of auditory processing, as reflected in LLR. Notably, deviance detection signals were obtained by comparing evoked responses to each of the three deviants with the response to a unique

reversed standard, with had a fixed probability of 91.5%. This implies that, while deviance detection signals (difference between deviant and reversed standard) at both MLR and LLR levels could be explained by simple adaptation to the redundant standard stimulus, comparisons within different evoked responses to deviants were reflecting a true prediction error mechanism, as comparisons were not made between more and less suppressed responses. That is, for instance, the evoked response to the 5% deviant was not compared with a 95% standard, a more suppressed response, but directly with an evoked response to the 10% deviant, and that comparison yielded a significant difference only at higher levels of the hierarchy. While obviously the 5% deviant is preceded by more standards, the comparison made does not include responses to these standard stimuli and, thus, differences observed should not be influenced by adaptation, but rather by purely prediction error. Provided this interpretation is valid, the functional dissociation between MLR and LLR generators in their sensitivity to deviant probability manipulations may be explained by the mentioned findings on animal studies fitting predictive coding framework (Parras et al., 2017), in which deviance detection at higher levels of the hierarchy is better explained by true prediction error than by adaptation. Deviance detection at the level of the MLR may rely more on simple adaptation, and therefore comparisons between deviant responses would not yield significant differences, whereas this would occur at higher levels generating LLR.

An alternative interpretation for the dissociation observed between MLR and LLR levels in the first study, also fitting predictive coding theory, concerns the strength of the prediction. While, as mentioned above, the probability of our reversed standard condition was fixed at 91.5%, the amount of preceding standard stimuli to the different deviants tested was obviously different. To this regard, some authors have stated that when a train of standard stimuli is interrupted (in our case, by a deviant) a rebound of neuronal activity occurs due to the release of adaptation (May and Tiitinen, 2010). Therefore, the differences observed in the evoked responses to the different deviant probabilities may be due to the different contribution of this rebound of activity to them, which would vary depending on the amount of previous neuronal suppression explained by the number of preceding standard stimuli (80%, 90% or 95%). That being the case, the strength of the predictive model in our study would be greater as more repetitions of the standard stimuli occur, producing a stronger adaptation on the evoked response to them and, in turn, eliciting a larger deviance detection signal when the model is violated. From there, it could be argued that at higher levels of representation along the ascending auditory pathway the strength of the prediction is encoded, and thus reflected in the different deviance responses, while at lower levels of

representation it is not, and the system only elicits a common deviance response regardless of the strength of the prediction.

Moreover, yet another possible interpretation for our results comes from the consideration of stimulus probability as a feature whose extraction requires a more complex type of processing than simple stimulus repetition. As shown, a functional dissociation between different stages of the auditory hierarchy exists for simple (simple stimulus repetition) vs complex (e.g., Saarinen et al., 1992) acoustic regularities (Cornella, et al., 2012). In the same way that lower levels cannot encode complex regularities, they may not be able to encode for stimulus probability. Indeed, one key feature to define the complexity of a sound sequence is the length of the time-window required to integrate its interstimulus statistical relationships (Kiebel et al., 2008). To this regard, encoding deviant stimulus probability in our study (e.g., 20% deviants vs 80% standards) would imply extracting a rule over a whole sequence, and would require evidence accumulation over a larger period of time than that to detect solely deviations. Predictive models from lower levels generating MLR could therefore only encode for very local relationships within the sequence, and thus being sensitive to deviant stimuli but not to their probability within the sequence. This argument has a controversial implication, which is that, if interstimulus relationships across the whole sequence were to be extracted in order to account for the probability of the deviant stimuli, that would imply that the predictive model should also account for the deviant stimulus appearance within the sequence, and therefore no prediction error signal should be triggered at upper levels of the hierarchy, where deviant probability is encoded. While this interpretation may be valid, a possible explanation would be that, even if deviant probability would be encoded, the specific timing for the arrival of the deviant within the sequence of standards would not be included in the predictive model, and therefore the prediction error signal would still be triggered.

Some limitations to be considered in this first study are our focus on amplitude changes between probability conditions, disregarding the potential changes on the latency of the components. Although not with changes in deviant probability (Tiitinen, May, Reinikainen, Näätänen, 1994), latency effects are observed for MMN with deviance magnitude (Friston, 2010), so it would be worth to measure latency effects on the MLR. Moreover, we did not try to localize the sources of our scalp-recorded signals, so that we could better estimate the generators of the observed effects. Future studies should address these issues, trying to replicate our findings to confirm the lack of sensitivity of MLR to deviant probability, as well as trying to integrate these findings with animal studies of single unit recordings,

in which sensitivity to deviant probability has been found below the cortical level (e.g., Ulanovsky et al., 2003). Moreover, further research should try to determine deviance detection and probability encoding at the MLR level using control conditions that allow the separation of true prediction error from simple adaptation mechanisms (e.g., cascade or multi-standard paradigms), which we did not use in this study. Finally, a next step within predictive coding framework would be to study patterns of connectivity between the different stages of auditory processing (sources at cortical, thalamus or midbrain level), rather than studying them separately, which would allow of a more global and comprehensive understanding of deviance detection along the auditory hierarchy.

Neural generators of the FFR

In the second study of the thesis, our main question on the cortical contributions to the FFR with different stimulus frequencies could not be answered given the inconclusive results. Specifically, the null effects of cTBS on cortical potentials (LLR) left results on the FFR uninterpretable. As stated in the corresponding manuscript discussion, different potential reasons for this lack of effects include inter and intra subject variability in cTBS effectiveness, the depth of our target area of stimulation or compensatory mechanisms from contralateral areas. These could be informative for future studies targeting auditory cortical areas with cTBS, especially when recording auditory evoked potentials. Despite the impossibility to test our hypothesis given the results from the second study, new evidence on the FFR field emerged as this study was conducted, which may help clarify the neural underpinnings of this signal.

In a recent study from our laboratory (Gorina-Careta et al., in preparation), FFRs at different stimulus frequencies (low: 89 Hz; High: 333 Hz) were obtained with Magnetoencephalography (MEG). In comparison with Coffey et al., study (2016), the novelty of this work was the use of an additional frequency above the phase-locking capabilities of cortical neurons (~100 Hz). There, results revealed that, while FFR sources contained cortical contributions when using low-frequency stimuli (replicating findings from Coffey and colleagues), such contribution disappeared when using high-frequency ones. These findings support results from source reconstruction of FFR data using EEG (Bidelman, 2018), in which the same pattern of results was observed, with contributions from the auditory cortex being restricted to stimulus frequencies below 150 Hz. Moreover, going back to results with MEG, a recent research addressed the question on whether attention to auditory stimuli could modulate FFR at the source level (Hartmann and Weisz,

2019). Using stimulus frequencies of 114 Hz, these authors found contributions to the MEG recorded FFR from the right auditory cortex, again replicating findings from Coffey et al. (2016), where attentional effects were found. To sum up, combined evidence from both EEG and MEG source reconstruction analyses suggest that FFR to low stimulus frequencies contain cortical contributions, while FFR to high stimulus frequencies does not, thus supporting the hypothesis of our second study.

Notably, most findings on FFR research showing a modulation of this signal by factors such as bilingualism (Krizman et al., 2012), musical training (Parbery-Clark et al., 2011), auditory aging (Anderson, White-Schwoch, Choi and Kraus, 2013) or deviance detection (Slabu et al., 2012), used low-frequency stimuli (around 100 Hz), and could therefore be re-interpreted in the light of the recent source evidence. While these modulatory effects were originally associated with subcortical activity, it could be argued that they may also, or rather, reflect plasticity phenomena at the cortical level. Indeed, neural phase-locking to external stimulus occurs across the entire auditory pathway (Joris et al., 2004), and some of the mentioned factors modulating FFR, such as musical training, are known to induce cortical plasticity (Pantev et al., 1998). A third possibility is that FFR was the result of neural phase-locking at subcortical structures (as demonstrated for high stimulus frequencies) but in turn was modulated by cortical areas through top-down mechanisms, which, as some authors suggest (Wong, Skoe, Russo, Dees and Kraus, 2007), could have their anatomical underpinnings in the corticofugal pathway (Suga, Gao, Zhang, Ma and Olsen, 2000). Of particular interest for this matter are FFR experiments studying endogenous auditory attention, a cognitive process requiring cortical resources which can trigger top-down mechanisms, modulating neural processes at multiple levels (see Posner, 2004). To this regard, several studies have observed modulation of the FFR by attention using stimulus frequencies above the phase-locking capabilities of the cortex (Galbraith, Olfman and Huffman, 2003; Lehmann and Schönwiesner, 2014). In a study conducted in our laboratory (Bedford, Costa-Faidella and Escera, unpublished data), the attentional reorganization of an ambiguous sound sequence modulated the scalp-recorded FFR at 394 Hz. In this experiment, perception of specific rhythms within the sound sequence required the active mobilization of attentional resources in the context of competing sound organizations, a process previously shown to be dependent on cortical audio-motor networks (Costa-Faidella, Sussman and Escera, 2017). Source reconstruction of the FFR revealed a main contribution from IC, although the attentional effects could not be replicated at the source level. Overall, it is inconclusive from these experiments whether the modulatory effects

observed in the scalp-recorded FFR are the result of neural-plasticity at the subcortical level (as originally postulated), cortical plasticity, or a mix of both.

In addition to the several reasons discussed in the manuscript which may partially explain or negative results, an important limitation in this second study is the fact that we performed the experiment without any prior evidence on the feasibility of the method for the particular use we pursued. That is, we would have required to previously develop a proof-of-concept research for the use of cTBS protocols in auditory cortex to modulate auditory evoked potentials, which defined details such as the ideal intensity threshold for our stimulation target (here we used a very conservative one), or the type and orientation of the TMS coil. This would have provided us with an effective methodological approach which could guarantee the transient inactivation of the targeted area and, at least, the expected modulatory effects on our control condition (LLR). Future studies should take these limitations into consideration and try to develop effective methodologies for the transient and effective inactivation of the auditory cortex with cTBS. Beyond this, possible next steps in the FFR field should aim to determine the neurophysiological bases of FFR modulations by factors such as musical or language experience observed in the literature, in order to better understand what kind of mechanisms can be inferred from the signal, and taking special consideration to the stimulus frequency to elicit the signal, the neural generators and the connectivity patterns between them. To this regard, the already mentioned MEG study from Hartmann and Weisz (2019) was the first one to effectively find attentional effects on the FFR at the source level, restricted to cortical areas.

Brain rhythms: induced activity with binaural beats

In contrast to the previous two studies, in this third study we moved from the measurement of different evoked potentials generated in the auditory pathway to the analysis of induced oscillatory activity in the brain with acoustic stimulation, still with the aim to contribute to the further characterization of the biological principles that govern auditory perception. In the context of contradictory findings in the literature (see Herrmann et al., 2016), here, negative results were interpreted as a null effect of binaural beats to induce brain rhythms, using a design that controls for possible confounds such as stimulation with acoustic beats.

The study of binaural beat effects on ongoing neural oscillations has its rationale in the assumption that stimulation with these acoustic input elicits entrainment effects in the EEG which would, in turn, enhance certain brain rhythms ultimately leading to subjective states of relaxation and/or the improvement of certain cognitive functions (see Vernon, 2009). However, little consistent evidence exists supporting the effects of binaural beats neither for the synchronization of brain activity nor for its effects of behavioral performance or emotional arousal. Regarding the first element of that assumption (brainwave entrainment), electrophysiological responses to binaural beats have indeed been found with single-unit recordings in animals (Wernick and Starr, 1968; Spitzer and Semple, 1998), as well as in humans by means of the Auditory Steady-State Response (ASSR; Schwarz and Taylor, 2005; Draganova et al., 2007), a sustained potential reflecting phase-locked activity to external stimulation. Further understanding the neurophysiological bases of binaural beat perception, these combined evidences from human and animal research suggested that the first source of neural activity corresponding to the beat frequency (not present in the acoustic signal) starts in the superior olivary complex (SOC). Interestingly, SOC is a crucial structure for sound localization which, according to Jeffress model (1948), contains neurons activated by convergent neural activity from bilateral CN (Moore, 1997). Therefore, as Draganova et al. (2007) proposed, these interaction of bilateral input at the SOC could generate ASSR in the following way: given a frequency difference between the two original dichotically-presented tones of 40 Hz, convergent input in the SOC for both inputs (equal phase) would occur 40 times per second. Neurons in that structure would thus display maximum activity at that frequency, generating a sustained evoked response following the frequency of the beat. That neural activity could then travel along the auditory hierarchy to be further processed at the cortical level, where binaural beat evoked responses have also been source-localized with both EEG (Pratt et al., 2010) and MEG (Draganova et al., 2007).

Despite the findings on entrainment effects with binaural beats, demonstrating brain phase-locked activity related with the processing of these sounds, the next assumption on whether these evoked responses would indirectly modulate ongoing neuronal oscillations has not been proven, and our study failed to find any evidence supporting it. The idea is that rhythmic stimulation processed in the auditory system can effectively induce changes in ongoing brain rhythms, for instance, enhancing the amplitude of a particular frequency band related with cognitive functions, such as gamma (Tallon-Baudry and Bertrand, 1999). Since that brain activity would not be the direct response to a stimulus, but rather the consequence of the system resonating at the stimulus frequency, the modulation

of brain rhythms could have long lasting effects exceeding the presentation of the stimuli (Halbleib et al., 2012). However, in our study no power enhancement of any of the frequencies studied during or after binaural beats presentation was found relative to baseline, in contrast with studies using other types of rhythmic stimulation (e.g., audiovisual; Roberts, Clarke, Addante and Ranganath, 2018). Several reasons discussed for these null effects include the short duration of the exposure to binaural beats or attention to the sounds (Vernon, Peryer, Louch and Shaw, 2014), although different experiments manipulating these variables in different ways found no consistent results. Therefore, it could be that binaural beat stimulation altogether is not effective to induce brain oscillations.

Possible ways to improve this third study would be to increase the sample size, as well as to further explore the evoked effects of binaural beats, instead of just focusing on induced activity. Since previous research found steady-state responses with this type of stimulation, we could have aimed to replicate them by analyzing phase-locking effects during the three minutes of stimulation. Moreover, we calculated the frequency content of our data averaging epochs of 1 minute, while we could have performed a more fine-grained analysis of the power variations over the three minutes of stimulation with time-frequency analyses. It is also worth noting that in a follow-up study (unpublished data) we confirmed no effects of binaural beats of gamma frequency in brain oscillations as well as in cognitive functions of visual attention and working memory. Future studies on the enhancement of ongoing neural oscillations with binaural beats should focus on measuring EEG along the behavioral effects classically reported in the literature, to truly demonstrate changes in neural activity related with its presentation. Moreover, studies making effective comparisons between different techniques to induce brain oscillations, such as binaural beats, transcranial direct current stimulation, repetitive TMS, EEG neurofeedback or audiovisual stimulation, would help clarify which are the differential mechanisms that explain its effectiveness, contributing to further understand the neural mechanisms behind this phenomenon.

Conclusions

In the first study we demonstrated a functional dissociation between MLR and LLR evoked potentials in their sensitivity to deviant probability in a classical oddball paradigm, which is coherent with previous literature showing different modulatory effects at these AEPs to progressively more complex types of regularity violations. Within predictive coding framework, this suggests that prediction error signals to violations with different probabilities would only differ at higher levels of the auditory hierarchy than those reflected by MLR.

From the second study, we concluded cTBS, as used in the present research, is ineffective to produce a transient inactivation at the auditory cortex, as reflected in long latency evoked potentials, and yield several aspects to consider for its use in future studies to achieve inhibitory effects, including possible contralateral compensatory mechanisms, and sub-threshold TMS pulse intensities. Moreover, recent evidence from other studies supports the hypothesis initially raised on the cortical contributions to the FFR dependent on the frequency of stimulation.

Finally, with the third study we contributed to the understanding on the potential usefulness of binaural beats to induce oscillatory activity measured with EEG. We found no evidence of binaural beats with frequencies within the classical EEG bands of theta, alpha, beta or gamma to modulate these brain rhythms. Given the inconclusive evidence in the literature and our use of strict controls, including treatment versus "placebo", and baseline-treatment-washout sessions, we consider our results informative, and conclude the lack of induced oscillatory activity on the brain with binaural beat stimulation.

Overall, our results contribute to the further characterization of deviance detection hierarchical organization, yield some interesting highlights about the use cTBS protocols in auditory cortical areas and its relationship with EEG evoked potentials, and provide a thorough research on the potential effects of binaural-beat stimulation on enhancing EEG activity of specific frequency bands.

References

Aghamolaei, S., Farhadi, M., & Zarrabi-Zadeh, H. (2015, August). Diversity maximization via composable coresets. In *27th Canadian Conference on Computational Geometry (CCCG)* (p. 43).

Althen, H., Grimm, S., & Escera, C. (2013). Simple and complex acoustic regularities are encoded at different levels of the auditory hierarchy. *European Journal of Neuroscience*, *38*(10), 3448-3455.

Aminoff, M. J., Boller, F., & Swaab, D. F. (2015). It is curious how little attention most neurologists direct at hearing. Introduction.

Anderson, S., White-Schwoch, T., Choi, H. J., & Kraus, N. (2013). Training changes processing of speech cues in older adults with hearing loss. *Frontiers in systems neuroscience*, *7*, 97.

Antunes, F. M., & Malmierca, M. S. (2011). Effect of auditory cortex deactivation on stimulus-specific adaptation in the medial geniculate body. *Journal of Neuroscience*, *31*(47), 17306-17316.

Barlow, H. B. (1961). Possible principles underlying the transformation of sensory messages. *Sensory communication*, *1*, 217-234.

Bartlett, E. L. (2013). The organization and physiology of the auditory thalamus and its role in processing acoustic features important for speech perception. *Brain and language*, *126*(1), 29-48.

Bastos, A. M., Usrey, W. M., Adams, R. A., Mangun, G. R., Fries, P., & Friston, K. J. (2012). Canonical microcircuits for predictive coding. *Neuron*, *76*(4), 695-711.

Bidelman, G. M. (2013). The role of the auditory brainstem in processing musically relevant pitch. *Frontiers in psychology*, *4*, 264.

Bidelman, G. M. (2015). Multichannel recordings of the human brainstem frequency-following response: scalp topography, source generators, and distinctions from the transient ABR. *Hearing research*, *323*, 68-80.

Bidelman, G. M. (2018). Subcortical sources dominate the neuroelectric auditory frequency-following response to speech. *Neuroimage*, *175*, 56-69.

Cacciaglia, R., Escera, C., Slabu, L., Grimm, S., Sanjuán, A., Ventura-Campos, N., & Ávila, C. (2015). Involvement of the human midbrain and thalamus in auditory deviance detection. *Neuropsychologia*, *68*, 51-58.

Carbajal, G. V., & Malmierca, M. S. (2018). The neuronal basis of predictive coding along the auditory pathway: From the subcortical roots to cortical deviance detection. *Trends in hearing*, *22*, 2331216518784822.

Chennu, S., Noreika, V., Gueorguiev, D., Shtyrov, Y., Bekinschtein, T. A., & Henson, R. (2016). Silent expectations: dynamic causal modeling of cortical prediction and attention to sounds that weren't. *Journal of Neuroscience*, *36*(32), 8305-8316.

Coffey, E. B., Herholz, S. C., Chepesiuk, A. M., Baillet, S., & Zatorre, R. J. (2016). Cortical contributions to the auditory frequency-following response revealed by MEG. *Nature communications*, *7*, 11070.

Cornella, M., Bendixen, A., Grimm, S., Leung, S., Schröger, E., & Escera, C. (2015). Spatial auditory regularity encoding and prediction: Human middle-latency and long-latency auditory evoked potentials. *Brain research*, *1626*, 21-30.

Cornella, M., Leung, S., Grimm, S., & Escera, C. (2012). Detection of simple and pattern regularity violations occurs at different levels of the auditory hierarchy. *PLoS One*, *7*(8), e43604.

Costa-Faidella, J., Sussman, E. S., & Escera, C. (2017). Selective entrainment of brain oscillations drives auditory perceptual organization. *NeuroImage*, *159*, 195-206.

Culler, E., Coakley, J. D., Lowy, K., & Gross, N. (1943). A revised frequency-map of the guinea-pig cochlea. *The American Journal of Psychology*, *56*(4), 475-500.

David, O., Kilner, J. M., & Friston, K. J. (2006). Mechanisms of evoked and induced responses in MEG/EEG. *Neuroimage*, *31*(4), 1580-1591.

Davis, H., Mast, T., Yoshie, N., & Zerlin, S. (1966). The slow response of the human cortex to auditory stimuli: recovery process. *Electroencephalography and clinical neurophysiology*, *21*(2), 105-113.

Dove, H. W. (1841). Über die Combination der Eindrücke beider Ohren und beider Augen zu einem Eindruck. *Monatsberichte der Berliner preussische Akademie der Wissenschaften*, *41*, 251-252.

Draganova, R., Ross, B., Wollbrink, A., & Pantev, C. (2007). Cortical steady-state responses to central and peripheral auditory beats. *Cerebral Cortex*, *18*(5), 1193-1200.

Escera, C., & Malmierca, M. S. (2014). The auditory novelty system: an attempt to integrate human and animal research. *Psychophysiology*, *51*(2), 111-123.

Escera, C., Leung, S., & Grimm, S. (2014). Deviance detection based on regularity encoding along the auditory hierarchy: electrophysiological evidence in humans. *Brain Topography*, *27*(4), 527-538.

Fries, P., Reynolds, J. H., Rorie, A. E., & Desimone, R. (2001). Modulation of oscillatory neuronal synchronization by selective visual attention. *Science*, *291*(5508), 1560-1563.

Friston, K. (2005). A theory of cortical responses. *Philosophical transactions of the Royal Society B: Biological sciences*, *360*(1456), 815-836.

Friston, K. (2010). The free-energy principle: a unified brain theory?. *Nature reviews neuroscience*, *11*(2), 127.

Fruhstorfer, H., Soveri, P., & Järvilehto, T. (1970). Short-term habituation of the auditory evoked response in man. *Electroencephalography and clinical Neurophysiology*, *28*(2), 153-161.

Galambos, R. (1992). A comparison of certain gamma band (40-Hz) brain rhythms in cat and man. In *Induced rhythms in the brain* (pp. 201-216). Birkhäuser, Boston, MA.

Galbraith, G. C., Olfman, D. M., & Huffman, T. M. (2003). Selective attention affects human brain stem frequency-following response. *Neuroreport*, *14*(5), 735-738.

Goldstein, E. B. (2009). Sensation and perception. 8th. *Belmont: Wadsworth, Cengage Learning*, 496.

Gorina-Careta, N., Kurkela, J., Hämälainen, J., Astikainen, P., & Escera, C. (2018). Understanding the Frequency-Following Response and its generators to sounds of different frequencies: an MEG study. (In preparation)

Grimm, S., Escera, C., Slabu, L., & Costa-Faidella, J. (2011). Electrophysiological evidence for the hierarchical organization of auditory change detection in the human brain. *Psychophysiology*, *48*(3), 377-384.

Halbleib, A., Gratkowski, M., Schwab, K., Ligges, C., Witte, H., & Haueisen, J. (2012). Topographic analysis of engagement and disengagement of neural oscillators in photic driving: a combined electroencephalogram/magnetoencephalogram study. *Journal of Clinical Neurophysiology*, *29*(1), 33-41.

Hartmann, T., & Weisz, N. (2019). Auditory cortical generators of the Frequency Following Response are modulated by intermodal attention. *bioRxiv*, 633834.

Heffner, R. S., & Heffner, H. E. (1990). Hearing in domestic pigs (Sus scrofa) and goats (Capra hircus). *Hearing Research*, *48*(3), 231-240.

Heilbron, M., & Chait, M. (2017). Great expectations: is there evidence for predictive coding in auditory cortex?. *Neuroscience*.

Herrmann, C. S., Strüber, D., Helfrich, R. F., & Engel, A. K. (2016). EEG oscillations: from correlation to causality. *International Journal of Psychophysiology*, *103*, 12-21.

Jeffress, L. A. (1948). A place theory of sound localization. *Journal of comparative and physiological psychology*, *41*(1), 35.

Jewett, D. L., & WILLISTON, J. S. (1971). Auditory-evoked far fields averaged from the scalp of humans. *Brain*, *94*(4), 681-696.

Joris, P. X., Schreiner, C. E., & Rees, A. (2004). Neural processing of amplitude-modulated sounds. *Physiological reviews*, *84*(2), 541-577.

Kamiński, J., Brzezicka, A., Gola, M., & Wróbel, A. (2012). Beta band oscillations engagement in human alertness process. *International Journal of Psychophysiology*, *85*(1), 125-128.

Kiebel, S. J., Daunizeau, J., & Friston, K. J. (2008). A hierarchy of time-scales and the brain. *PLoS computational biology*, *4*(11), e1000209.

Kraus, N., Anderson, S., & White-Schwoch, T. (2017). The frequency-following response: A window into human communication. In *The frequency-following response* (pp. 1-15). Springer, Cham.

Krishnan, A., Xu, Y., Gandour, J. T., & Cariani, P. A. (2004). Human frequency-following response: representation of pitch contours in Chinese tones. *Hearing research*, *189*(1-2), 1-12.

Krizman, J., Marian, V., Shook, A., Skoe, E., & Kraus, N. (2012). Subcortical encoding of sound is enhanced in bilinguals and relates to executive function advantages. *Proceedings of the National Academy of Sciences*, *109*(20), 7877-7881.

Langner, G. (1992). Periodicity coding in the auditory system. *Hearing research*, *60*(2), 115-142.

Lehmann, A., & Schönwiesner, M. (2014). Selective attention modulates human auditory brainstem responses: relative contributions of frequency and spatial cues. *PloS one*, *9*(1), e85442.
Litovsky, R. (2015). Development of the auditory system. In Handbook of clinical neurology (Vol. 129, pp. 55-72). Elsevier.
Long, P., Wan, G., Roberts, M. T., & Corfas, G. (2018). Myelin development, plasticity, and pathology in the auditory system. *Developmental neurobiology*, *78*(2), 80-92.
Long, Y., Liu, H., Li, Y., Jin, X., Zhou, Y., Li, J., ... & Zhang, J. (2018). Early auditory skills development in Mandarin speaking children after bilateral cochlear implantation. *International journal of pediatric otorhinolaryngology*.
López-Caballero, F., & Escera, C. (2017). Binaural beat: A failure to enhance EEG power and emotional arousal. *Frontiers in human neuroscience*, *11*, 557.
López-Caballero, F., Martín-Trias, P. Ribas-Prats, T., Gorina-Careta, N., Bartrés-Faz, D & Escera, C. (2019). The effects of cTBS on the Frequency-Following Response and other auditory evoked potentials. (In preparation)
López-Caballero, F., Zarnowiec, K., & Escera, C. (2016). Differential deviant probability effects on two hierarchical levels of the auditory novelty system. *Biological psychology*, *120*, 1-9.
Luck, S. J. (2012). Event-related potentials. *APA handbook of research methods in psychology*, *1*, 523-546.
Machado, M. S., Teixeira, A. R., & Costa, S. S. D. (2018). Correlation between cognitive functions and central auditory processing in adolescents with non-cholesteatomatous chronic otitis media. *Dementia & neuropsychologia*, *12*(3), 314-320.
Mai, J. K., & Paxinos, G. (Eds.). (2011). *The human nervous system*. Academic Press.
Malmierca, M. S. (2003). The structure and physiology of the rat auditory system: an overview.
Malmierca, M. S., Sanchez-Vives, M. V., Escera, C., & Bendixen, A. (2014). Neuronal adaptation, novelty detection and regularity encoding in audition. *Frontiers in systems neuroscience*, *8*, 111.
Marsh, J. T., Brown, W. S., & Smith, J. C. (1974). Differential brainstem pathways for the conduction of auditory frequency-following responses. *Electroencephalography and clinical neurophysiology*, *36*, 415-424.
Mathewson, K. E., Gratton, G., Fabiani, M., Beck, D. M., & Ro, T. (2009). To see or not to see: prestimulus α phase predicts visual awareness. *Journal of Neuroscience*, *29*(9), 2725-2732.
May, P. J., & Tiitinen, H. (2010). Mismatch negativity (MMN), the deviance-elicited auditory deflection, explained. *Psychophysiology*, *47*(1), 66-122.
May, P., Tiitinen, H., Ilmoniemi, R. J., Nyman, G., Taylor, J. G., & Näätänen, R. (1999). Frequency change detection in human auditory cortex. *Journal of computational neuroscience*, *6*(2), 99-120.
Moore, B. C. J. (1997). *An Introduction to the Psychology of Hearing*. San Diego, CA: Academic Press.

Moran, R. J., Campo, P., Maestu, F., Reilly, R. B., Dolan, R. J., & Strange, B. A. (2010). Peak frequency in the theta and alpha bands correlates with human working memory capacity. *Frontiers in human neuroscience*, *4*, 200.

Näätänen, R., Gaillard, A. W., & Mäntysalo, S. (1978). Early selective-attention effect on evoked potential reinterpreted. *Acta psychologica*, *42*(4), 313-329.

Näätänen, R., Paavilainen, P., Rinne, T., & Alho, K. (2007). The mismatch negativity (MMN) in basic research of central auditory processing: a review. *Clinical neurophysiology*, *118*(12), 2544-2590.

Näätänen, R., Pakarinen, S., Rinne, T., & Takegata, R. (2004). The mismatch negativity (MMN): towards the optimal paradigm. *Clinical Neurophysiology*, *115*(1), 140-144.

Nelken, I. (2004). Processing of complex stimuli and natural scenes in the auditory cortex. *Current opinion in neurobiology*, *14*(4), 474-480.

Opitz, B., Schröger, E., & Von Cramon, D. Y. (2005). Sensory and cognitive mechanisms for preattentive change detection in auditory cortex. *European Journal of Neuroscience*, *21*(2), 531-535.

Paavilainen, P. (2013). The mismatch-negativity (MMN) component of the auditory event-related potential to violations of abstract regularities: a review. *International journal of psychophysiology*, *88*(2), 109-123.

Pantev, C., Oostenveld, R., Engelien, A., Ross, B., Roberts, L. E., & Hoke, M. (1998). Increased auditory cortical representation in musicians. *Nature*, *392*(6678), 811.

Parbery-Clark, A., Strait, D. L., Anderson, S., Hittner, E., & Kraus, N. (2011). Musical experience and the aging auditory system: implications for cognitive abilities and hearing speech in noise. *PloS one*, *6*(5), e18082.

Parras, G. G., Nieto-Diego, J., Carbajal, G. V., Valdés-Baizabal, C., Escera, C., & Malmierca, M. S. (2017). Neurons along the auditory pathway exhibit a hierarchical organization of prediction error. *Nature communications*, *8*(1), 2148.

Pérez-González, D., Malmierca, M. S., & Covey, E. (2005). Novelty detector neurons in the mammalian auditory midbrain. *European Journal of Neuroscience*, *22*(11), 2879-2885.

Picton, T. W. (2010). *Human auditory evoked potentials*. Plural Publishing.

Picton, T. W., Hillyard, S. A., Krausz, H. I., & Galambos, R. (1974). Human auditory evoked potentials. I: Evaluation of components. *Electroencephalography and clinical neurophysiology*, *36*, 179-190.

Posner, M. I., Snyder, C. R., & Solso, R. (2004). Attention and cognitive control. *Cognitive psychology: Key readings*, *205*.

Pratt, H., Starr, A., Michalewski, H. J., Dimitrijevic, A., Bleich, N., & Mittelman, N. (2010). A comparison of auditory evoked potentials to acoustic beats and to binaural beats. *Hearing Research*, *262*(1-2), 34-44.

Purves, Augustine, Fitzpatrick, Hall, LaMantia, McNamara & Williams (2004). Neuroscience. 3rd edition. *Sinauear Associates, Inc.*

Recanzone, G. H., & Sutter, M. L. (2008). The biological basis of audition. *Annu. Rev. Psychol.*, *59*, 119-142.

Roberts, B. M., Clarke, A., Addante, R. J., & Ranganath, C. (2018). Entrainment enhances theta oscillations and improves episodic memory. *Cognitive neuroscience*, *9*(3-4), 181-193.

Rocha-Muniz, C. N., Befi-Lopes, D. M., & Schochat, E. (2012). Investigation of auditory processing disorder and language impairment using the speech-evoked auditory brainstem response. *Hearing research*, *294*(1-2), 143-152.

Ruhnau, P., Herrmann, B., & Schröger, E. (2012). Finding the right control: the mismatch negativity under investigation. *Clinical Neurophysiology*, *123*(3), 507-512.

Rummell, B. P., Klee, J. L., & Sigurdsson, T. (2016). Attenuation of responses to self-generated sounds in auditory cortical neurons. *Journal of Neuroscience*, *36*(47), 12010-12026.

Saarinen, J., Paavilainen, P., Schöger, E., Tervaniemi, M., & Näätänen, R. (1992). Representation of abstract attributes of auditory stimuli in the human brain. *NeuroReport*, *3*(12), 1149-1151.

Schnupp, J., Nelken, I., & King, A. (2011). *Auditory neuroscience: Making sense of sound*. MIT press.

Schonwiesner, M., Novitski, N., Pakarinen, S., Carlson, S., Tervaniemi, M., & Naatanen, R. (2007). Heschl's gyrus, posterior superior temporal gyrus, and mid-ventrolateral prefrontal cortex have different roles in the detection of acoustic changes. *Journal of Neurophysiology*, *97*(3), 2075-2082.

Schreiner, C. E., & Langner, G. E. R. A. L. D. (1988). Periodicity coding in the inferior colliculus of the cat. II. Topographical organization. *Journal of neurophysiology*, *60*(6), 1823-1840.

Schröger, E., & Wolff, C. (1996). Mismatch response of the human brain to changes in sound location. *Neuroreport*, *7*(18), 3005-3008.

Schwarz, D. W., & Taylor, P. (2005). Human auditory steady state responses to binaural and monaural beats. *Clinical Neurophysiology*, *116*(3), 658-668.

Seebeck, A. (1841). Beobachtungen über einige Bedingungen der Entstehung von Tönen. *Annalen der Physik*, *129*(7), 417-436.

Shiga, T., Althen, H., Cornella, M., Zarnowiec, K., Yabe, H., & Escera, C. (2015). Deviance-related responses along the auditory hierarchy: Combined FFR, MLR and MMN evidence. *PloS one*, *10*(9), e0136794.

Shipp, S. (2016). Neural elements for predictive coding. *Frontiers in psychology*, *7*, 1792.

Singer, W., & Gray, C. M. (1995). Visual feature integration and the temporal correlation hypothesis. *Annual review of neuroscience*, *18*(1), 555-586.

Skoe, E., & Kraus, N. (2010). Auditory brainstem response to complex sounds: a tutorial. *Ear and hearing*, *31*(3), 302.

Skoe, E., Chandrasekaran, B., Spitzer, E. R., Wong, P. C., & Kraus, N. (2014). Human brainstem plasticity: the interaction of stimulus probability and auditory learning. *Neurobiology of learning and memory*, *109*, 82-93.

Slabu, L., Grimm, S., & Escera, C. (2012). Novelty detection in the human auditory brainstem. *Journal of Neuroscience*, *32*(4), 1447-1452.

Smith, J. C., Marsh, J. T., & Brown, W. S. (1975). Far-field recorded frequency-following responses: evidence for the locus of brainstem sources. *Electroencephalography and clinical neurophysiology*, *39*(5), 465-472.

Sohmer, H., Pratt, H., & Kinarti, R. (1977). Sources of frequency following responses (FFR) in man. *Electroencephalography and clinical neurophysiology*, *42*(5), 656-664.

Spitzer, M. W., & Semple, M. N. (1998). Transformation of binaural response properties in the ascending auditory pathway: influence of time-varying interaural phase disparity. *Journal of neurophysiology*, *80*(6), 3062-3076.

Suga, N., Gao, E., Zhang, Y., Ma, X., & Olsen, J. F. (2000). The corticofugal system for hearing: recent progress. *Proceedings of the National Academy of Sciences*, *97*(22), 11807-11814.

Tallon-Baudry, C., & Bertrand, O. (1999). Oscillatory gamma activity in humans and its role in object representation. *Trends in cognitive sciences*, *3*(4), 151-162.

Tiitinen, H., May, P., Reinikainen, K., & Näätänen, R. (1994). Attentive novelty detection in humans is governed by pre-attentive sensory memory. *Nature*, *372*(6501), 90.

Ulanovsky, N., Las, L., & Nelken, I. (2003). Processing of low-probability sounds by cortical neurons. *Nature neuroscience*, *6*(4), 391.

Varela, F. J. (1995). Resonant cell assemblies: a new approach to cognitive functions and neuronal synchrony. *Biological research*, *28*(1), 81-95.

Vernon, D. (2009). *Human potential: Exploring techniques used to enhance human performance*. Routledge.

Vernon, D., Peryer, G., Louch, J., & Shaw, M. (2014). Tracking EEG changes in response to alpha and beta binaural beats. *International Journal of Psychophysiology*, *93*(1), 134-139.

Walter, W. G. (1953). The living brain. SpringerLink.

Wernick, J. S., & Starr, A. (1968). Binaural interaction in the superior olivary complex of the cat: an analysis of field potentials evoked by binaural-beat stimuli. *Journal of neurophysiology*, *31*(3), 428-441.

Winer, J. A., & Schreiner, C. E. (Eds.). (2010). *The auditory cortex*. Springer Science & Business Media.

Wong, P. C., Skoe, E., Russo, N. M., Dees, T., & Kraus, N. (2007). Musical experience shapes human brainstem encoding of linguistic pitch patterns. *Nature neuroscience*, *10*(4), 420.

Yvert, B., Fischer, C., Bertrand, O., & Pernier, J. (2005). Localization of human supratemporal auditory areas from intracerebral auditory evoked potentials using distributed source models. *Neuroimage*, *28*(1), 140-153.

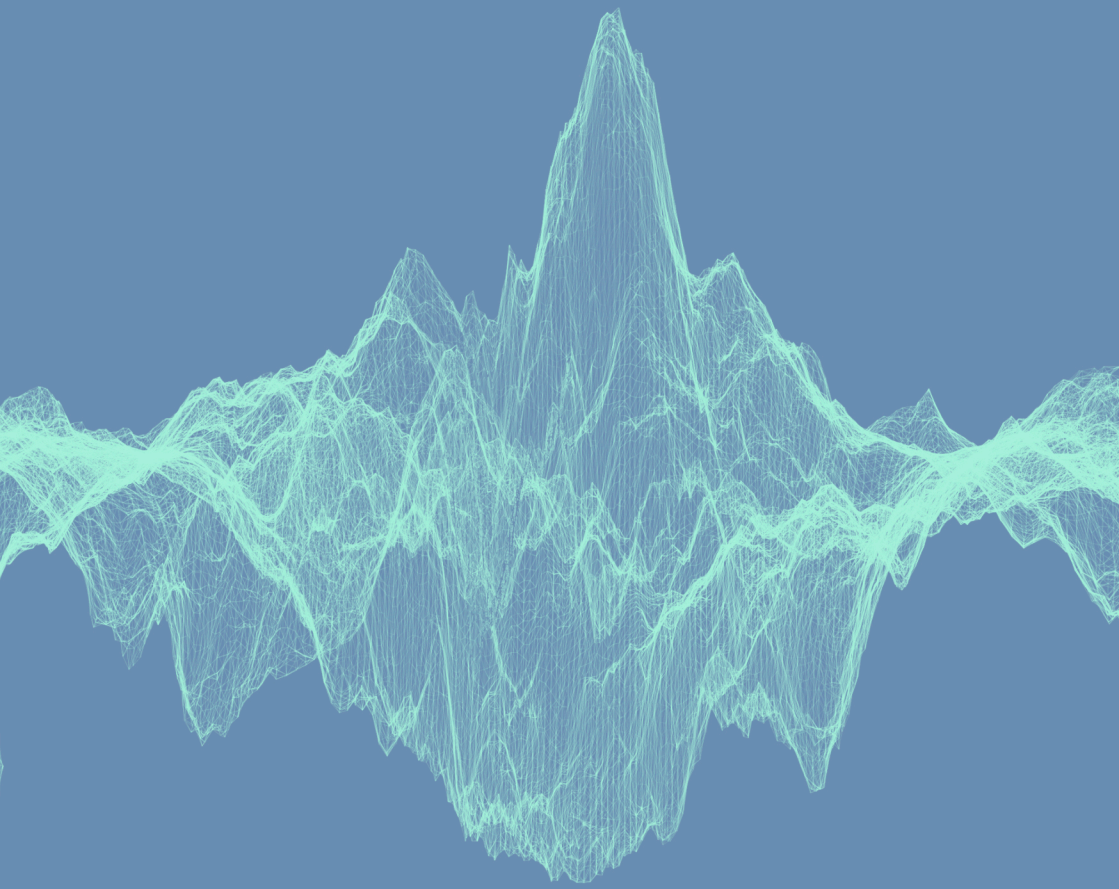

BrainLab - Grup de Recerca en Neurociència Cognitiva
Departament de Psicologia Clínica i Psicobiologia
Facultat de Psicologia

UNIVERSITAT DE BARCELONA